SANDIA REPORT

SAND2017-4612

Unlimited Release
Printed May 2017

DE-FOA-EE0005502

Advanced Percussive Drilling Technology for Geothermal Exploration and Development

Phase II Report

Jiann-Cherng Su, David W. Raymond, Somuri V. Prasad
Sandia National Laboratories

Dale R. Wolfer
Atlas-Copco Secoroc LLC

Prepared by
Sandia National Laboratories
Albuquerque, New Mexico 87185 and Livermore, California 94550

Sandia National Laboratories is a multimission laboratory managed and operated by National Technology & Engineering Solutions of Sandia, LLC., a wholly owned subsidiary of Honeywell International, Inc., for the U.S. Department of Energy's National Nuclear Security Administration under contract DE-NA0003525.

Sandia National Laboratories

Atlas Copco

Atlas Copco Secoroc

Issued by Sandia National Laboratories, operated for the United States Department of Energy by National Technology and Engineering Solutions of Sandia, LLC.

Available to DOE and DOE contractors from

U.S. Department of Energy
Office of Scientific and Technical Information
P.O. Box 62
Oak Ridge, TN 37831

Telephone: (865) 576-8401
Facsimile: (865) 576-5728
E-Mail: reports@osti.gov
Online ordering: http://www.osti.gov/scitech

Available to the public from

U.S. Department of Commerce
National Technical Information Service
5301 Shawnee Rd
Alexandria, VA 22312

Telephone: (800) 553-6847
Facsimile: (703) 605-6900
E-Mail: orders@ntis.gov
Online order: http://www.ntis.gov/search

SAND2017-4612
Printed April 2017
Unlimited Release

Advanced Percussive Drilling Technology Phase II Report

Jiann-Cherng Su
Geothermal Research

David W. Raymond
Geothermal Research

Somuri V. Prasad
Materials Mechanics & Tribology

Sandia National Laboratories
P.O. Box 5800
Albuquerque, New Mexico 87185-MS1033

Dale Wolfer

Atlas-Copco Secoroc, LLC
7500 Shadwell Drive
Roanoke, Virginia 24019

Abstract

Percussive hammers are a promising advance in drilling technology for geothermal since they rely upon rock reduction mechanisms that are well-suited for use in the hard, brittle rock characteristic of geothermal formations. The project research approach and work plan includes a critical path to development of a high-temperature (HT) percussive hammer using a two-phase approach. The work completed in Phase I of the project demonstrated the viability of percussive hammers and that solutions to technical challenges in design, material technology, and performance are likely to be resolved. Work completed in Phase II focused on testing the findings from Phase I and evaluating performance of the materials and designs at high-operating temperatures. A high-operating temperature (HOT) drilling facility was designed, built, and used to test the performance of the DTH under extreme conditions. Results from the testing indicate that a high-temperature capable hammer can be developed and is a viable alternative for user in the driller's toolbox.

ACKNOWLEDGMENTS

Atlas-Copco Secoroc, LLC

Michael White - R&D Manager

Paul Campbell - Senior Development Engineer

Ron Boyd - Project Manager Oil & Gas and EDGE

Kelly Ferguson - Laboratory Technician

Trevor Jones – Test Engineer

Sandia National Laboratories

Doug Blankenship - Manager, Geothermal Research

Jeff Greving - Geothermal Research

Elton Wright - Geothermal Research

Dennis King – Geothermal Research

Anirban Mazumdar – Robotics R&D

Steve Buerger – Robotics R&D

Rand Garfield - Materials Science R&D

Lisa Deibler – Materials Characterization & Performance

Carlos Medrano – Sandia Facilities

CONTENTS

FIGURES

TABLES

NOMENCLATURE

DOE	United States Department of Energy
SNL	Sandia National Laboratories
AC	Atlas-Copco Secoroc
ROP	Rate of penetration
BHA	Bottom hole assembly
DTHH	Down the hole hammer
HT	High-temperature
LT	Low-temperature
HOT	High-operating temperature
TRL	Technology readiness level
scfm	Standard cubic feet per minute
α	rock volume fraction
γ	gas heat capacity ratio
ρ	density
μ	viscosity
C_D	drag coefficient
c_p	heat capacity
d	rock particle diameter
g	gravitational acceleration
h	heat transfer coefficient
P	pressure
T	temperature
U	velocity
W	wall friction
z	elevation

Subscripts

d	gas downward flow
g	gas upward flow
p	rock particles
w	formation
i	interchange between downward and upward gas flows

1. INTRODUCTION

1.1 Background

Geothermal drilling is hampered by the challenges of hard/abrasive/ fractured rock formations, high temperatures, and the frequent loss of circulated drilling fluids to the formation. Rock reduction in conventional geothermal well construction is dominated by roller cone bits. While this technology has served the industry well with capability of drilling the varied rock types typical of geothermal formations, roller cones are subject to slow penetration rates (10-20 ft/hr) and limited bit life (< 40 hours) under the rigors of hard-rock, high-temperature, abrasive rock drilling. Since cone rotation is required for rock crushing, cone seizure will render the entire bit inoperative. Seal failure usually precipitates bearing failure as the seals protect bearings that can fail when exposed to the abrasive cuttings in geothermal formations. Even with properly functioning bearings and seals, roller cone bits have thrust load limits imposed by bearing designs that inhibit the energy that can be imparted to the rock interface. Roller cone technology is mature and few major improvements are likely.

More generally, other bit technology types can be considered that rely upon advanced material formulations within the cutting structure. However, these solutions typically offer promise for significantly extending bit life with modest improvements in penetration rate. As geothermal drilling continues into deeper and hotter formations for development of both conventional and enhanced geothermal systems, advanced penetration rate drilling technologies must be realized to keep well construction costs manageable.

Drilling costs contribute substantially to geothermal electricity production costs. Industry norms suggest geothermal well construction costs can generally approximate one-half of the overall geothermal project cost [1]. A recent geothermal well construction technology evaluation study sponsored by the Department of Energy Office of Geothermal Technologies has shown that drilling services and consumables can exceed 50% of total construction costs for deep geothermal wells [2]. Since drill rig time dominates well drilling costs, technology is needed that improves rate of penetration (ROP) and is capable of drilling exploration and production wells to depth.

Percussive hammers are a promising advanced exploratory drilling technology for geothermal since they rely upon rock reduction mechanisms that are well-suited for use in the hard, brittle rock characteristic of geothermal formations. Down hole hammers are also compatible with low-density fluids that are often used for geothermal drilling. Experience in mining and oil and gas drilling has demonstrated their utility for penetrating hard rock. Percussive hammers have the potential to reduce overall well construction costs by significantly improving the penetration rate capability of geothermal drilling in the hot, hard, abrasive environment typical of geothermal drilling.

1.2 Technical Approach

Application of pneumatic hammers to geothermal drilling is innovative. Although existing pneumatic hammer product lines may be able to penetrate typical geothermal formations, the

down hole temperatures of geothermal wells (100 – 300 C) can challenge the elastomeric and polymer-based components that presently comprise conventional percussive hammer componentry. Hence, they are unable to survive the "soak temperatures" encountered in a geothermal well. Additionally, the metal alloy components comprising a percussive hammer may potentially be compromised with reduced strength and fatigue life at elevated temperatures. Development of a geothermal-specific high temperature hammer is required for application to geothermal drilling and will be the primary intent of this project.

The project approach is scientifically innovative in that advanced drilling technology producing deep hole access is being realized through down hole energy augmentation. Conventional geothermal drilling relies upon the mechanical energy delivered from the surface rig through the drill pipe to the bit. Similarly percussive hammers rely upon down hole thrust and surface rotation to maintain rock contact and incremental bit rotation during operation, respectively. Yet percussive drilling additionally relies upon the drill stem to deliver high pressure air to the bit face to augment the rock reduction process. From an energy balance perspective, application of increased power at the bit face gives rise to increased bit penetration advances per revolution contributing to an increase in drilling penetration rates. Percussive hammers offer this benefit in that energy is stored in the compressed air stream that powers the hammer.

The project research approach and work plan include a critical path to development of a HT percussive hammer using a two-phase approach.

1.3 Phase I Overview

Phase I of the Advanced Percussive Drilling Technology was focused on demonstrating the feasibility of a high-temperature hammer [3]. The primary goal of Phase I activities was to develop a proof of concept hammer validating a technology readiness level (TRL) 2/3 level. The tasks associated with the development were specifically to:

- Establish a preliminary design for a HT DTHH that is elastomer-less, polymer-less
- Computationally model the requisite power delivery to drill geothermal formations
- Demonstrate material formulations that constitute the Proof of Concept design backed by significant laboratory testing validating the material formulations under representative operational conditions (temperatures, impact loads & cycling)
- Environmentally test of high temperature bits (bit heads, buttons, retention designs)

The results from Phase I activities proved to be quite promising. An elastomer-free, polymer-free hammer was designed and built from standard materials. Computational modeling of the hammer performance was used to define the timing ports for the hammer. Leak paths and other issues were identified and resolved, and the prototype was tested in the Atlas-Copco test cell. Performance levels were comparable to conventional hammers.

Uncertainty regarding bit button retention, potentially a concern at high temperature, was resolved. A test was designed and conducted to determine whether conventional assembly techniques would be sufficient under high temperature operation. Results from the tests showed that in the temperatures of interest for geothermal drilling, the standard methods used to retain buttons at low temperature are also suitable for high-temperature bits.

Coupon level tests showed that high-temperature capable materials are available to replace standard materials. Baseline properties were derived from tests of conventional hammer components. Bulk properties as well as fatigue and impact toughness tests were conducted to assess adequacy. Additional tests are being performed to assess the wear characteristics of the lubricious and wear-resistant coatings. Reporting the results of these tests continued into Phase II due to the nature of the tests.

1.4 Phase II Approach and Activities

Phase II activities are focused on component and system-level testing and are intended to advance the technology readiness level (TRL) of the Phase I proof-of-concept demonstration. Based on information gathered in Phase I, prototype high-temperature hammers were built and tested. Prototype components were built with the candidate materials and coatings selected from Phase I. Testing was conducted in at the Atlas-Copco Roanoke facility and at the Sandia high-temperature test facility. The tasks required for executing the Phase 2 technical approach included the following:

- Establish baseline prototype hammer performance at the Atlas Copco Roanoke test facility
- Provide Proof-of-Concept (POC) validation via laboratory testing of representative design features.
- Build full-scale prototype hammers based on design and material selection from Phase 1
- Test and characterize prototype hammers under ambient conditions at the Atlas Copco Roanoke test facility
- Identify options and test requirements for high-temperature test facility
- Design, build and test high-temperature test facility
- Validate performance of prototype HT hammer at temperatures up to 300°C (572°F) on the high-temperature facility

The current work is the continuation of Phase I activities from DE-FOA-0000522 Advanced Percussive Drilling Technology. The work completed in Phase I of the project demonstrated the viability of percussive hammers as a means to significantly reduce development costs of hot, deep geothermal wells, and that solutions to technical challenges in design, material technology, and performance are likely to be resolved. Portions of the Phase I report are repeated in the current report for completeness.

This page intentionally left blank.

2. MATERIALS DEVELOPMENT FOR THE HIGH TEMPERATURE HAMMER

2.1 Limitations of the Baseline Design

An exploded view of a typical down the hole hammer is shown in Figure 1. Air or foam is used to cycle an internal piston which in turn strikes the bit to generate rock reduction. The repeated impact between the piston and the bit produces cyclic loading on the various components in the system. Sliding contact exists between the piston and internal hammer components. Beyond conventional operation, material properties are compromised at the operating temperatures seen in geothermal environments.

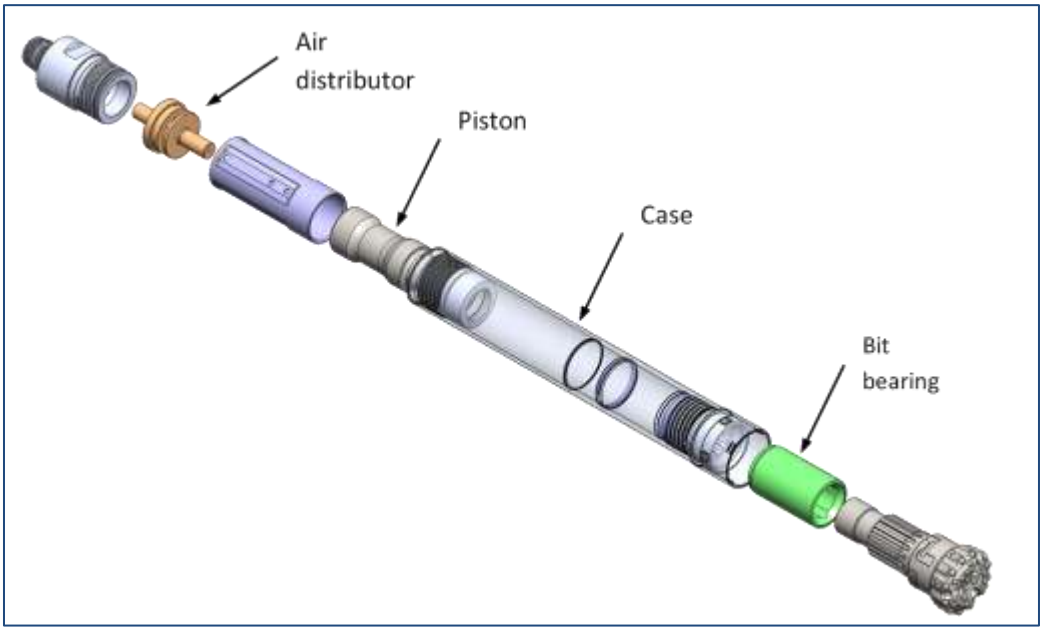

Figure 1. Down-the-hole hammer illustration

2.2 Complete Coupon-Level Coatings Testing

Test facilities available in the Sandia Materials R&D Department were used for the coupon-level testing of the solid lubricants. A high temperature tribometer capable of making friction and wear measurements up to 300°C was been designed and fabricated (Figure 2). Tests were conducted under atmospheric conditions. The counter-face was a 440C steel ball.

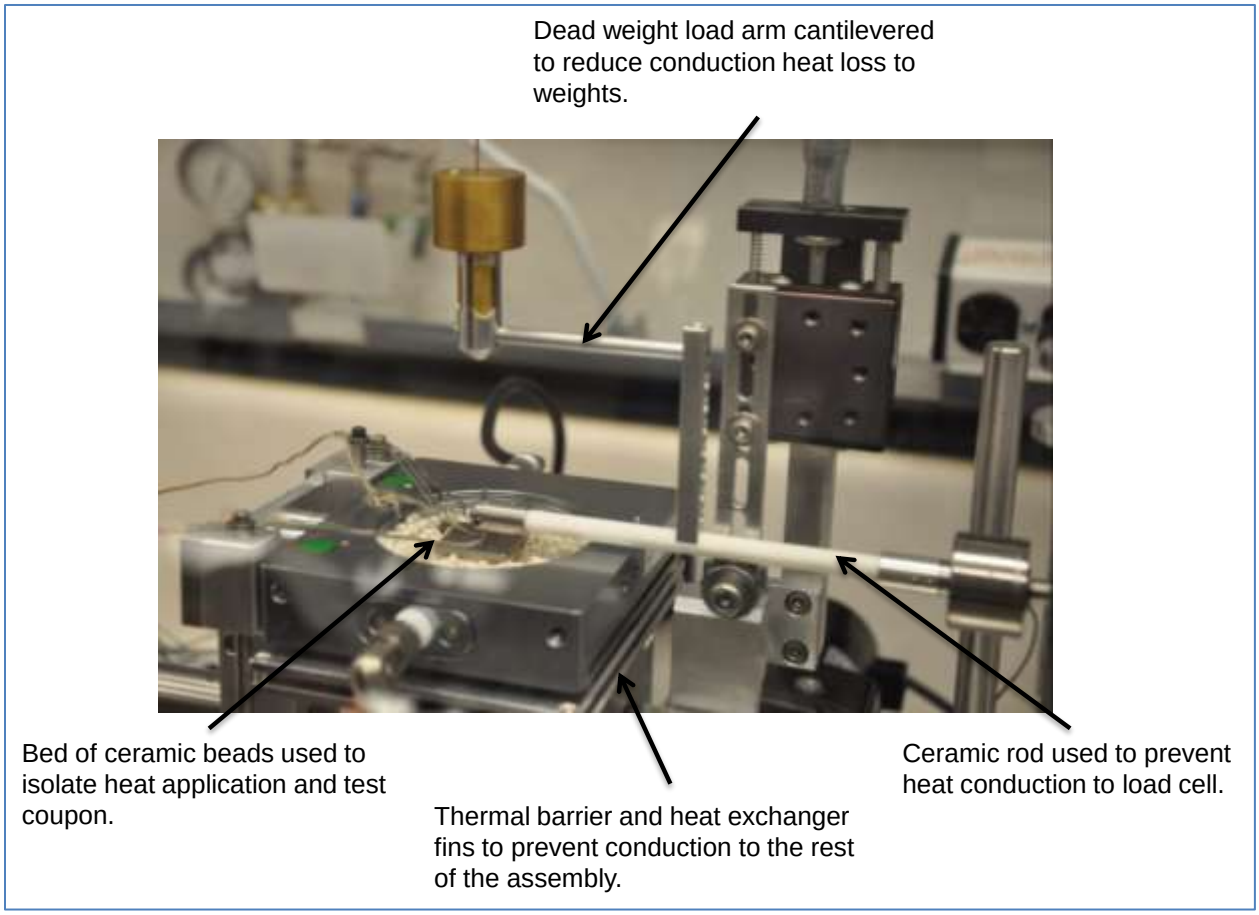

Figure 2. High-temperature tribometer for friction and wear

First, an uncoated H-13 steel was tested at 300°C. Friction was high with coefficient of friction (CoF) around 0.6. A cross section of the wear scar suitable for transmission electron microscopy (TEM) was prepared by focused ion beam microscopy (FIB). The FIB cut was made in the center of the wear surface along the direction of sliding. Results show that the surface was heavily oxidized. The depth of the oxidized layer can be gaged from the TEM micrograph (Figure 3). The phenomenon is called tribo-oxidation.

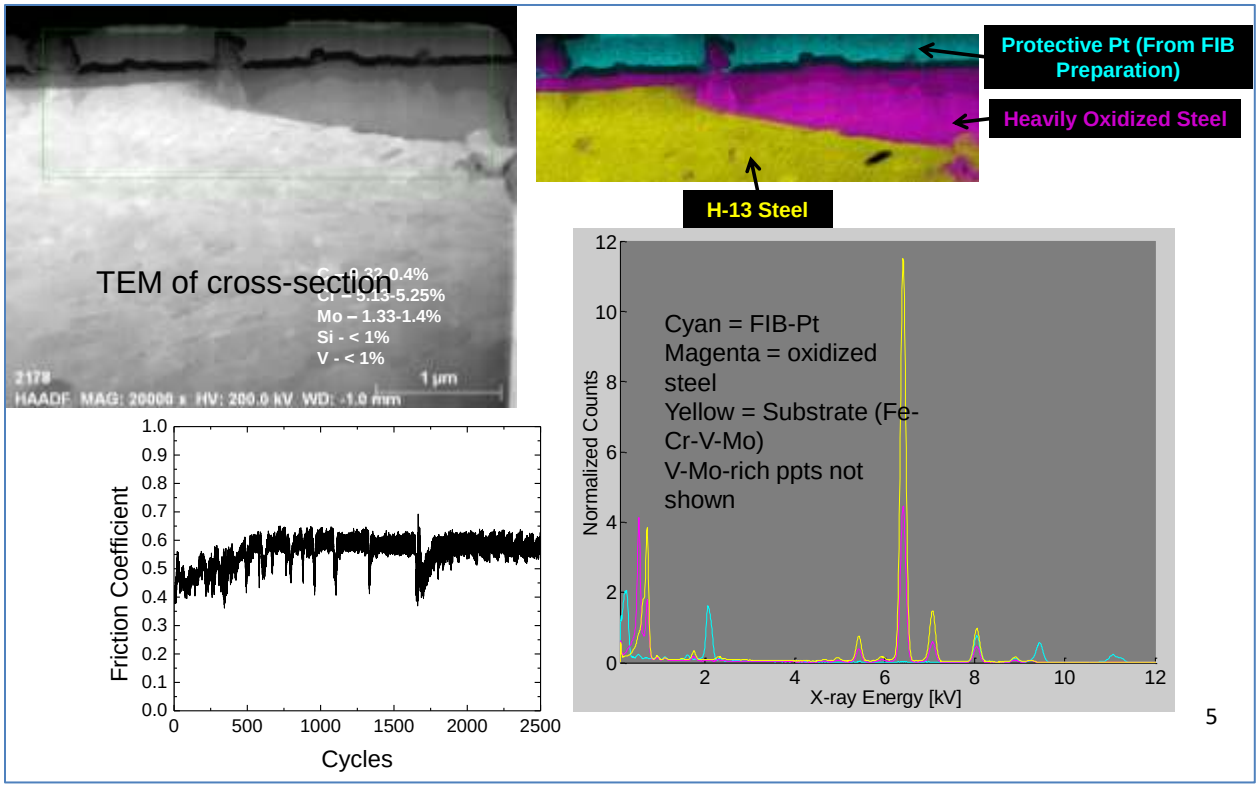

Figure 3. Uncoated H-13 tested at 300°C

Figure 4 shows the friction and cross-sectional TEM data on the diamond-like carbon (DLC) solid lubricant. The DLC is an amorphous mix of diamond-like and quartz like networks, essentially a nanocomposite. A ceramic barrier layer was introduced between the steel substrate and the DLC. Note that the friction reduced progressively with cycles of sliding, reaching very low values of the order of 0.05 to 0.1.

The sample, after the first test, was cooled to room temperature and reheated to 300°C before starting the second test. The friction behavior, i.e., decreasing CoF with cycles, is repeatable.

Raman analysis was being carried out to confirm whether frictional contact had introduced chemical changes to DLC that were indeed beneficial. The CoF is changing with time, but is decreasing not increasing as one might expect. The top two images of Figure 4 correspond to TEM of a typical cross-section with corresponding spectral image map. Tribo-oxidation was significantly reduced. There was practically no plastic deformation in the steel substrate. There also was no apparent loss (wear) of thickness in DLC.

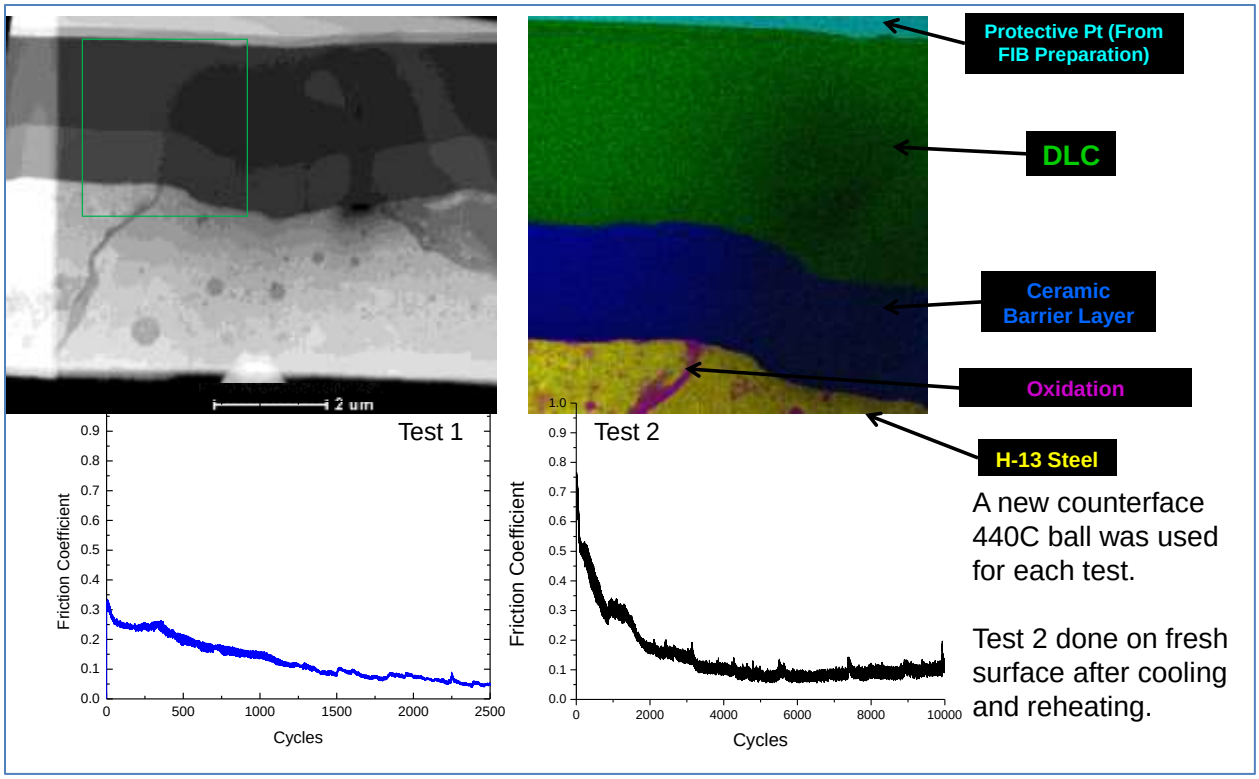

Figure 4. DLC nanocomposite on ceramic layer

Scanning electron microscope (SEM) and spectral images of wear surfaces (left) and transfer films on steel balls (right) are shown in Figure 5. Again, there was no observable loss of material seen on the wear surfaces. It is interesting to note that the wear scars appear smoother than the unworn regions on the coating. Spectral images reveal the enrichment of SiO fragments on the wear surfaces. There is also transfer of DLC material onto the steel counter-face, but no significant damage to the ball.

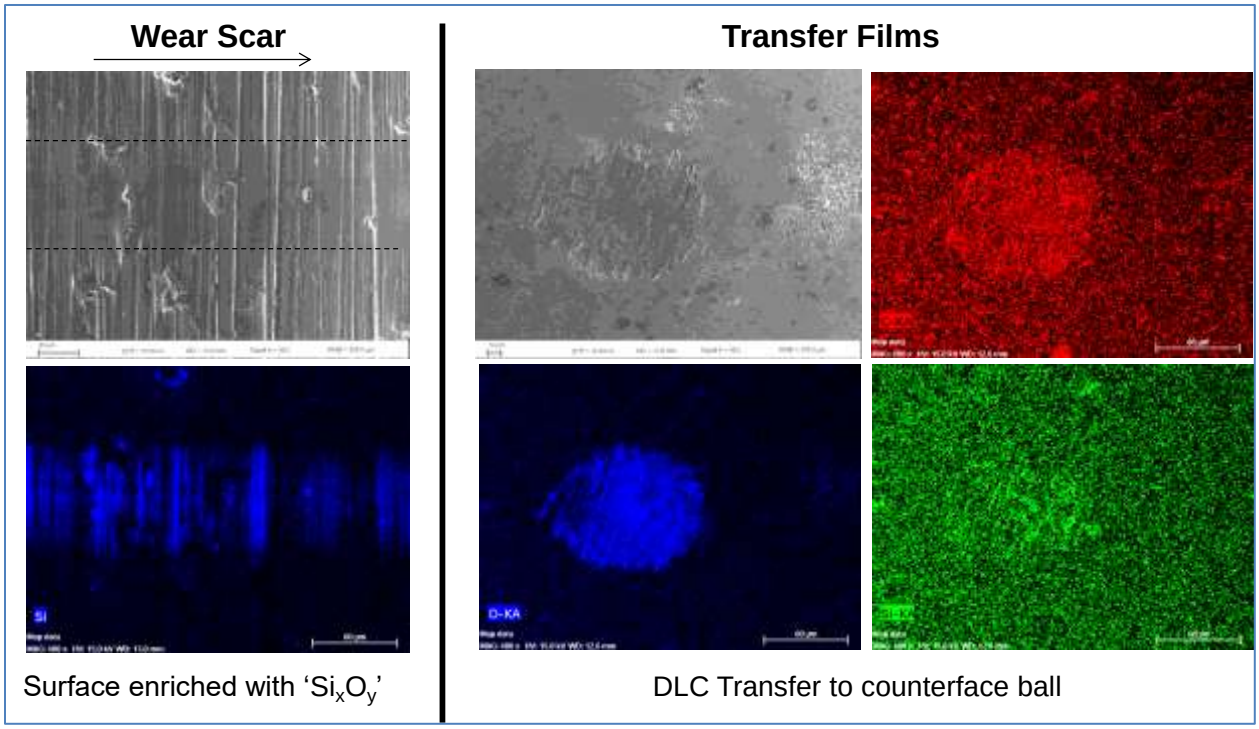

Figure 5. Wear surfaces & transfer films

A typical cross-section of DLC coating with multiple barrier coating (a ceramic layer in blue and TiCN nanolamiante in red is shown in Figure 6. Either the residual stresses in the TiCN nanolaminate or friction induced shear stresses begin to induce delamination of the nanolamiante.

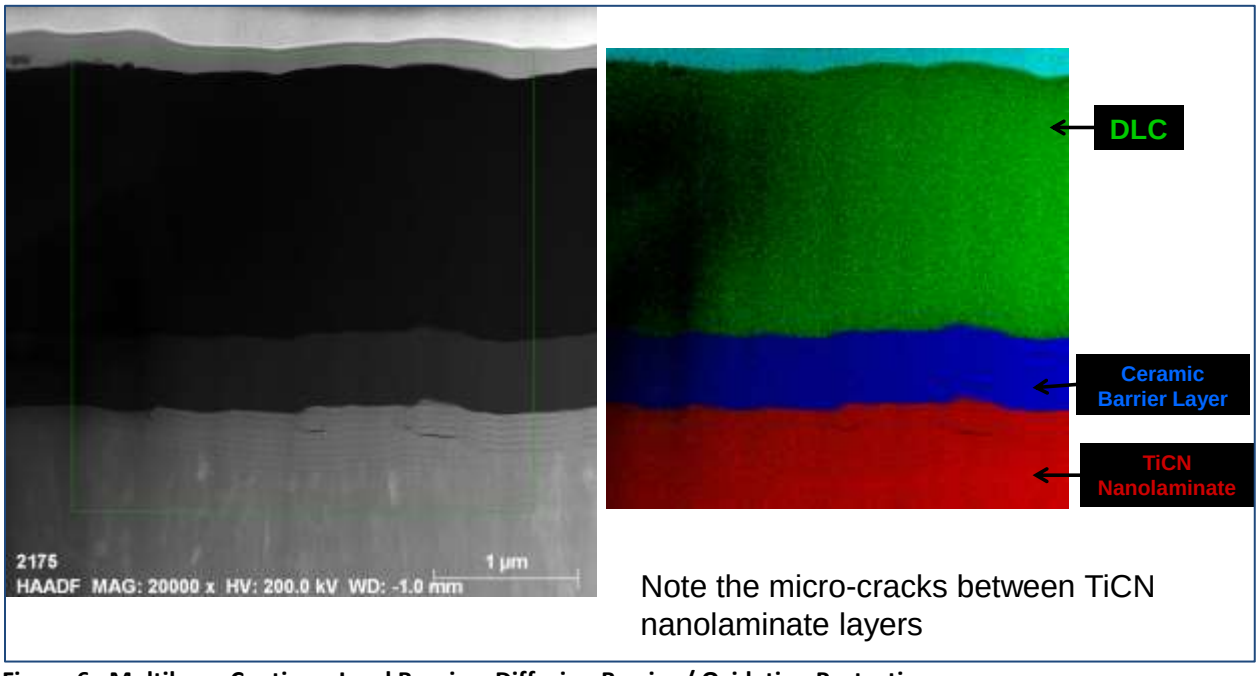

Figure 6. Multilayer Coatings: Load Bearing, Diffusion Barrier / Oxidation Protection

Based on the test coupon-level test results, a DLC-Si_xO_y nanocomposite DLC with a single ceramic barrier coating was selected as the preferred solid lubricant to mitigate high temperature friction and wear.

3. HIGH-TEMPERATURE HAMMER BUILD AND TESTING

3.1 Build High-Temperature Prototypes

High-temperature prototype 5 inch diameter hammers were built and tested using the materials selected from the Phase I recommendations. The hammers were built to the same geometry of the proof-of-concept hammer. Figure 7 shows a cross sectional drawing view of the assembled hammer. Note the bit head is not shown. The dimensions shown describe the relevant timing points of the pneumatic cycle.

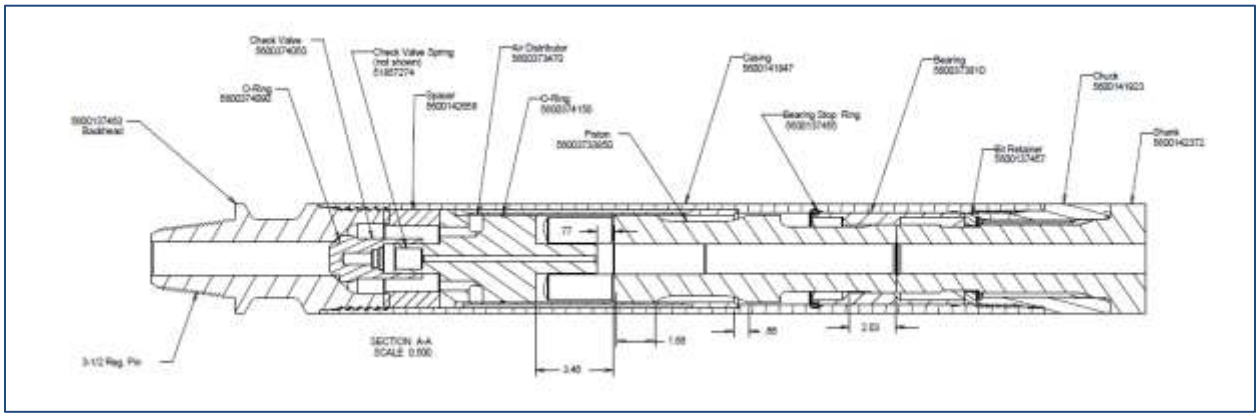

Figure 7. Hammer timing points

The cycle chosen for the POC hammer is unlike any currently sold by Secoroc, but represents a combination of elements aimed at survivability in high temperatures, efficiency without conventional lubrication, and consistent performance in deep holes without the use of elastomers. These elements include:

- Fixed porting. Flows into and out of chambers is controlled only by piston position. Active valve operation is difficult to achieve without the use of elastomers.
- Constant piloting of the piston in cylinder and bearing. Unlike other piston stem bearing hammer designs, the piston is always supported by two removable internal parts.
- No piston/casing contact. Unlike most hammers, the piston is not piloted inside the casing and in fact never makes contact. This eliminates any need for lubricious treatment of the casing.
- Absence of constant downward piston bias. Most hammer designs feed the return chamber by connecting a portion of the piston area to line pressure. This produces a constant downward force that must be overcome during the return stroke and increases required return area. Absence of this bias allows a smaller return area (and larger/stronger piston stem) to be used.

Movement of return chamber inlet timing upward to the cylinder, increasing chamber volume; this improves performance against backpressure and increases air consumption.

Testing of the low temperature prototype during Phase I showed a significant drop in ROP against expected values due to internal leakage between the Air Distributor and Cylinder. For low ambient temperature operation, a common, 70 Durometer Buna N o-ring was found to effect a sufficient seal such that hammer performance met target values. Since this solution was not viable for high temperature operation, a suitable sealing method was required. Tests were conducted using high temperature, graphite filled valve packing in lieu of the o-ring. The results are shown graphically below.

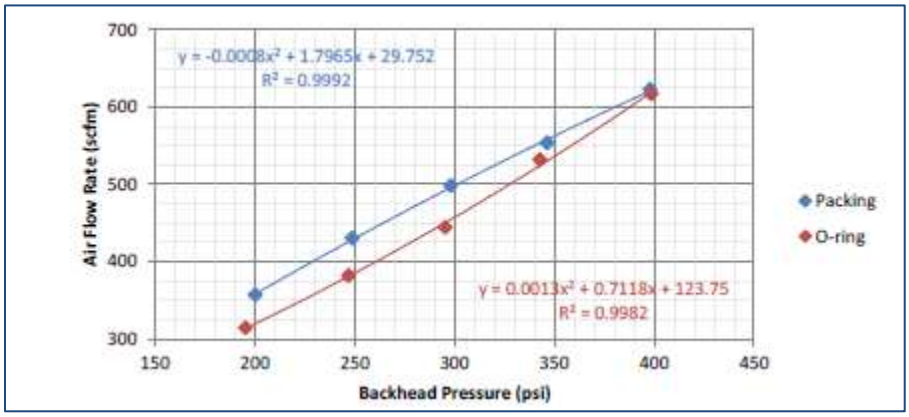

Figure 8. Flow rate vs. backhead pressure

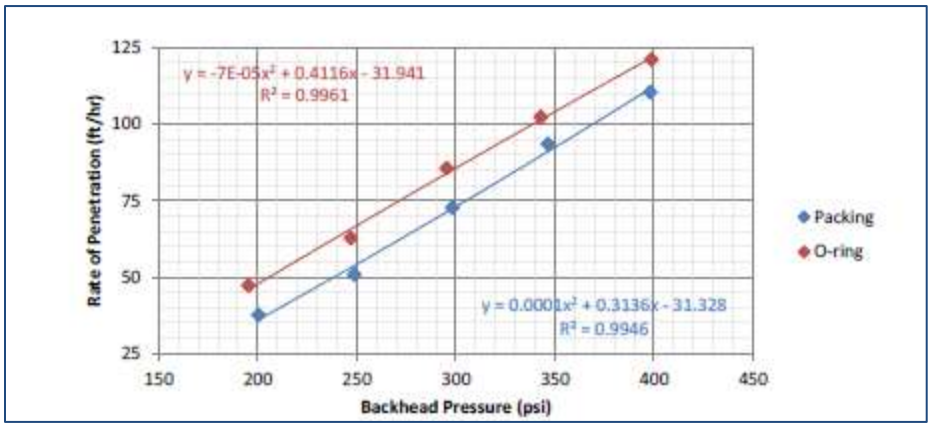

Figure 9. Rate of penetration vs. backhead pressure

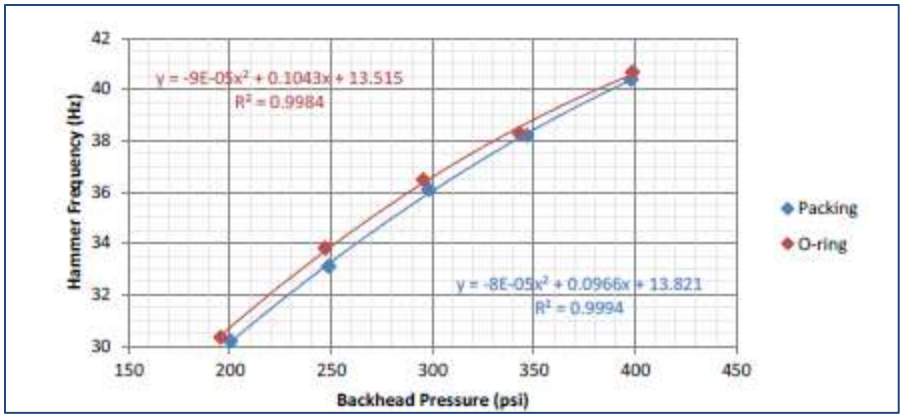

Figure 10. Hammer frequency vs. backhead pressure

These results showed an average increase in air flow of 7.9% and an average decrease in ROP of 39.54% versus a conventional o-ring. About the time these tests were done, a perfluoroelastomer material, Marketed by DuPont as Kalrez® was identified as a good candidate for a sealing element, with a maximum operating temperature of 325 C (617 F). Since this material is a drop-in replacement for the low temperature o-ring, this option was adopted and further work on the valve packing seal was abandoned. It is believed that modifications to the valve packing seal arrangement could achieve better results than observed, but that these results would be unlikely to exhibit any advantageous performance versus the high temperature o-ring.

Pistons, Air Distributors, and Bearings were produced using the materials and heat treatment conditions identified in the material selection, testing and evaluation portion of the project. Since it had been determined that the material and heat treatment condition of the remaining hammer components were suitable for operation at the target temperature, existing parts from the low temperature prototype were used for the assembly of the high temperature prototype.

3.2 Baseline Performance Testing at Atlas Copco Test Cell

Baseline testing of the high temperature prototype was conducted at the test facility at Atlas Copco Secoroc, USA in Roanoke, VA. The test stand is a purpose built, computer controlled drill tower (see Figure 11 and Figure 12). All tests were conducted at ambient temperature. Drilling was conducted in Barre Granite blocks with an unconfined compressive strength of 22ksi (151 MPa). Feed force was maintained constant at 5500 lbf (24.46 kN). Rotation speed was maintained at 40 rpm. A standard, 5.5 inch (140 mm bit fitted with spherical tungsten carbide inserts was used for testing. Testing of the high temperature prototype was conducted using the low temperature prototype as a control.

Figure 11. Drill Tower, Showing Basement Access for Rock Sample

Figure 12. Control Room

Feed force is determined by the hydraulic pressures, hold down and hold back, in a feed cylinder in combination with a constant test stand weight. Hold down pressure is the hydraulic pressure on the top side of the feed cylinder while hold back pressure is the hydraulic pressure on the bottom side of the feed cylinder. In combination, these two measurements determine the feed force. The hydraulic pressures are set and maintained with valves controlled by automated regulators. These pressures are monitored and recorded during each test run to ensure consistency.

Each performance test is started by setting a rotation speed along with holddown and holdback pressures appropriate for the desired feed force. Once these values are set, a desired supply pressure is dictated to the automated regulator and initiated. As air flow begins, the drill is slowly lowered to the rock specimen and the automated feed control is allowed to take over. The air pressure is monitored for stabilization. Once the system is stable, data collection is initiated and carried out for the desired test time (10 seconds in this case). Collected data includes: air flow, hammer frequency, and hammer advancement along with the controlled variables previously described. Controlled variable data and air flow data is collected at a rate of 2 Hz while hammer vibrations are acquired at 10kHz. Hammer advancement is measured using a linear displacement transducer at 50kHz.

Each hammer was run three times at five pressure steps from 200 psi to 400 psi (1379 to 2758 kPa) in 50 psi (345 kPa) intervals. At each pressure step, data was recorded for 10 seconds. After each of the three runs on the high temperature hammer, it was disassembled to monitor wear and other types of damage on the internal components. The control hammer was not disassembled because pervious laboratory testing had shown that wear and mechanical damage was not likely. The low temperature prototype hammer was lubricated with ISO 220 Rock Drill Oil injected into the air stream at a rate of 12 cc per minute. The high temperature prototype was not lubricated during the test runs. It should be noted that small amounts of oil may have been in the air system from oil clinging to the drill pipe and bypassed compressor oil.

Results are plotted below:

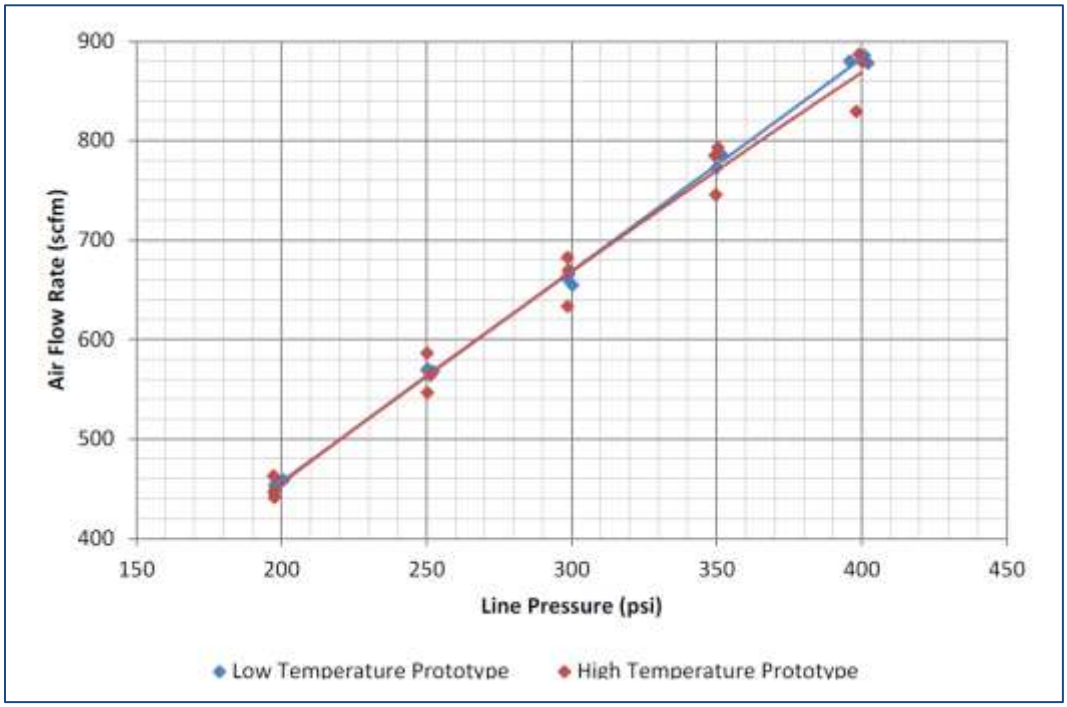

Figure 13. Flow rate vs. backhead pressure comparison for LT and HT prototype

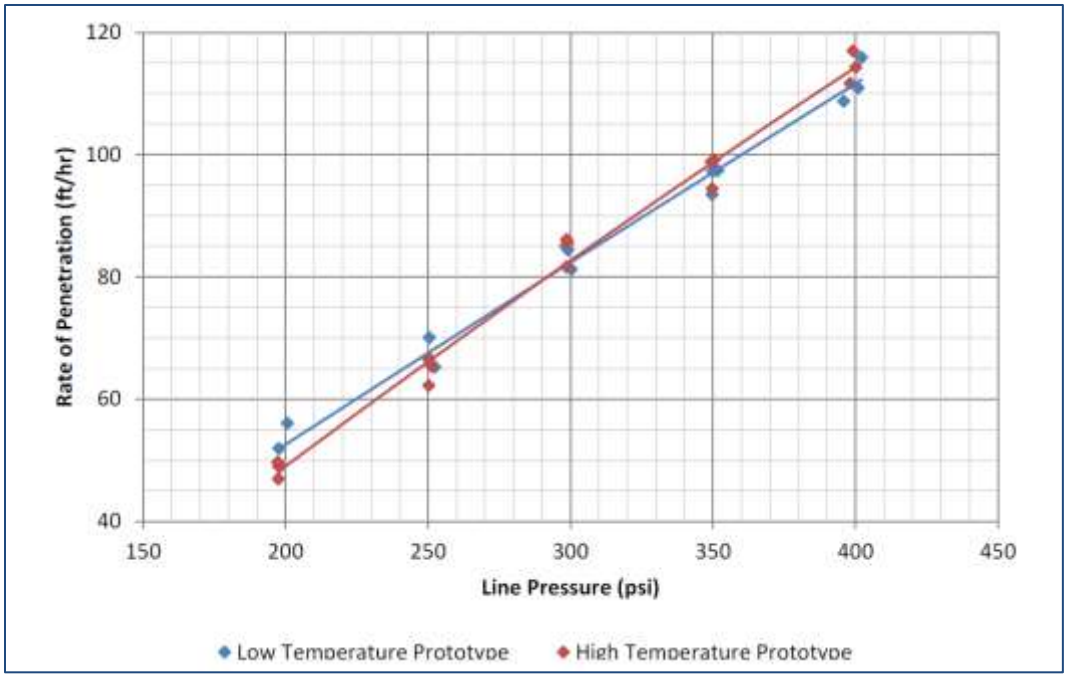

Figure 14. Rate of penetration vs. backhead pressure comparison for LT and HT prototype

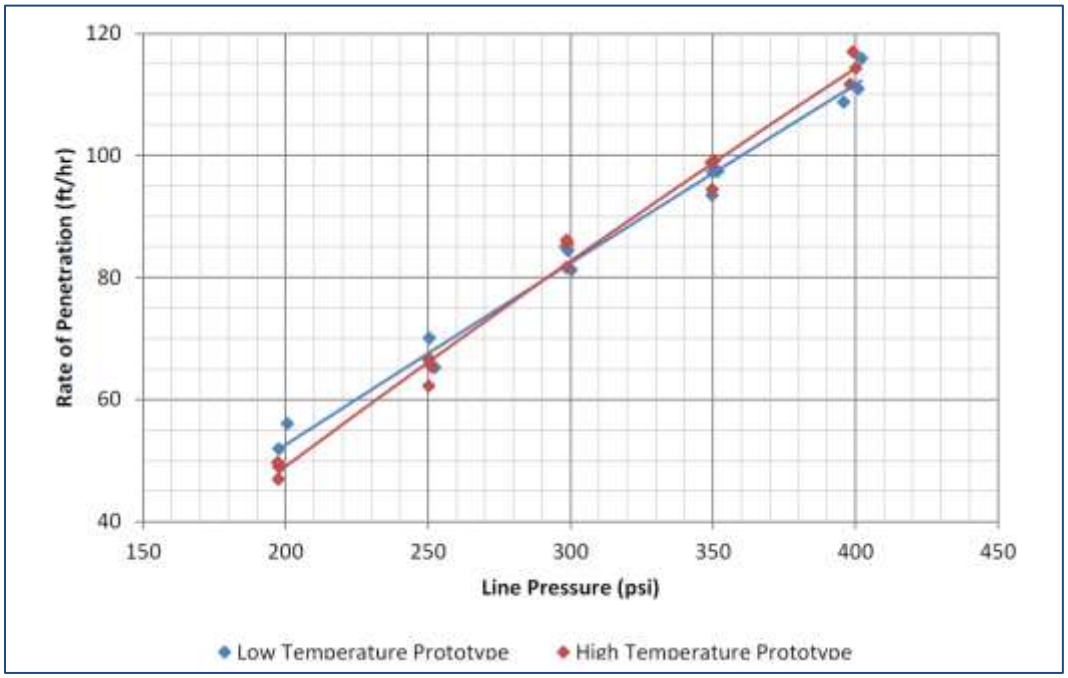

Figure 15. Frequency vs. backhead pressure comparison for LT and HT prototype

The performance of the high temperature prototype compares very favorably with that of the low temperature prototype. The slight differences observed are well within normal test variation.

The appearance of the high temperature prototype piston and air distributor are shown in the photos below:

Figure 16. High-temperature prototype after first run

Figure 17. High-temperature prototype after second run

Figure 18. High-temperature prototype after third run

The photos clearly show a developing wear pattern in the lubricious coating on the piston OD, adjacent to the striking end. Barely visible after the first test, this wear pattern progressed into a wear band approximately .125” (3 mm) wide. A very faint wear ring was visible in the middle piston land after the third run. The top piston land and Air Distributor stem showed no visible wear or damage.

After the third run, an embossed wear pattern was visible on the piston striking face corresponding to the impact surface of the bit. It is believed the relatively soft surface hardness of the stainless steel piston contributed to this deformation, shown below.

Figure 19. Striking face of piston

This testing having validated the performance of the high temperature prototype to be consistent with that of the low temperature prototype, and that no catastrophic failure of parts or the lubricious and wear resistant coating was observed. The high temperature prototype was sent to SNL for both low and high temperature testing at the HOT facility.

3.3 Low-Temperature Testing at Sandia HOT Facility

Baseline performance tests were conducted at the HOT facility validate the data acquisition system and to establish a baseline for hammer performance at various temperatures. The low-temperature prototype was used in the early tests.

Tests were conducted on Sierra White granite blocks sourced from Coldspring quarry in Raymond, California. The published unconfined compressive strength of the rock is 23.8 ksi.[1]

Three tests were run at a target pressure of 300 psi to determine flow, frequency, and rate of penetration (ROP). The rotation rate was set to 40 rpm with the WOB at 4000 lbf. The hammer temperature was set to 400°F with process air temperature values of 200°F, 300°F, and 500°F. Approximately 10 seconds of data was collected for each run. The temperature of the hammer is measured with a thermocouple located within the heating chamber.

Data was collected with National Instruments based hardware and software. Data was sampled at 2048 Hz. Flow is calculated from the differential pressure output in the orifice plate flow

[1] http://www.coldspringusa.com/Building-Materials/Products-Colors-and-Finishes/Granite/Sierra-White/

meter along with the measured process gas pressure using Equation 3-22 from Crane Technical Paper No. 410.

$$Q_{scfm} = 412 \frac{Y \cdot d_{orifice}^2 \cdot C}{S_g} \sqrt{\Delta P \cdot \rho_{gas}} \quad (1)$$

Hammering frequency is computed from the acceleration data collected on an accelerometer mounted on the swivel. Rate of penetration is calculated by taking the derivative of the drill head position with respect to time and converting to the desired units.

Post-processing of the data using a tdms read program is used to plot the data points. Results are shown below.

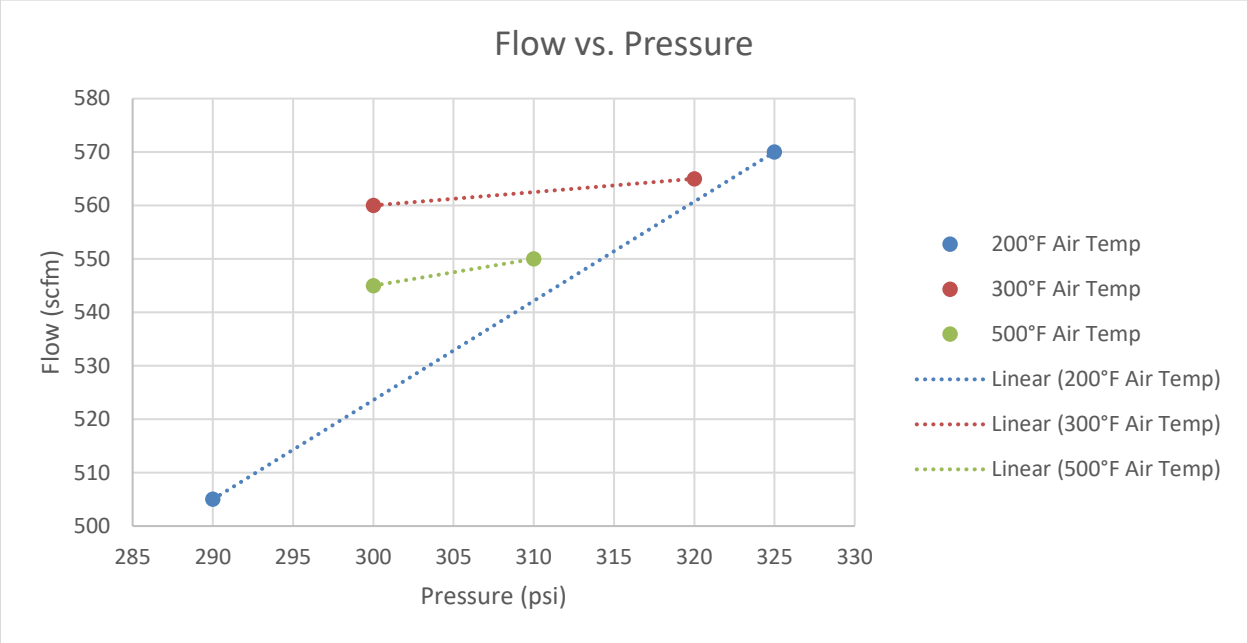

Figure 20. Flow vs. pressure test results for HOT facility characterization

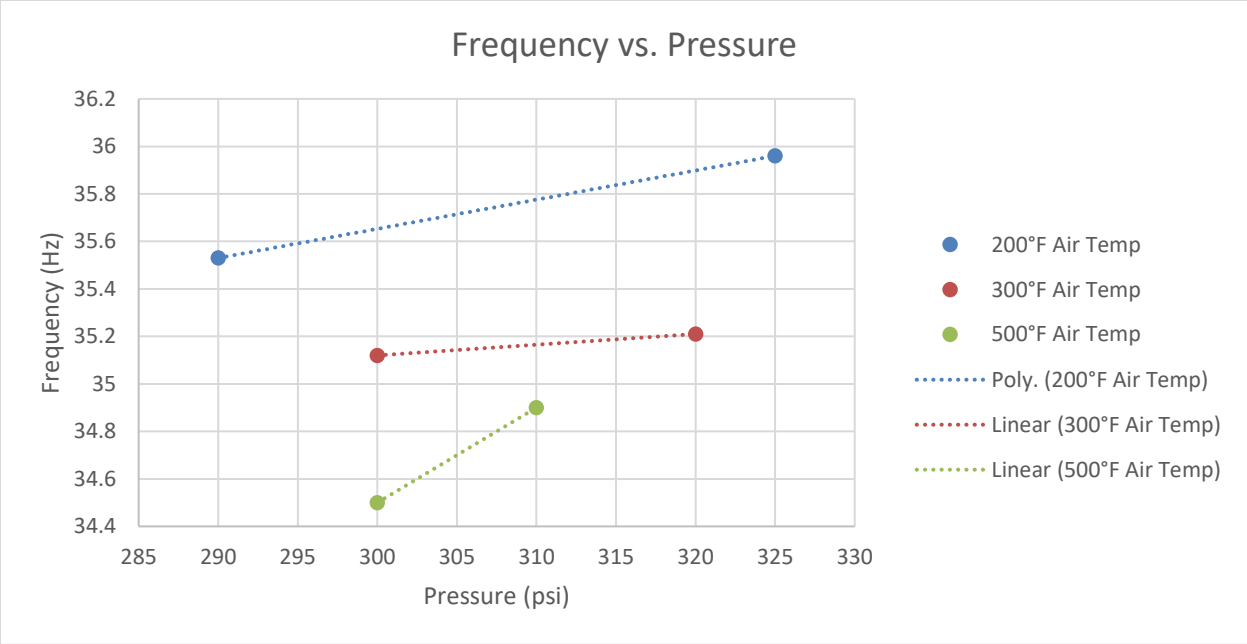

Figure 21. Frequency vs. pressure test results for HOT facility characterization

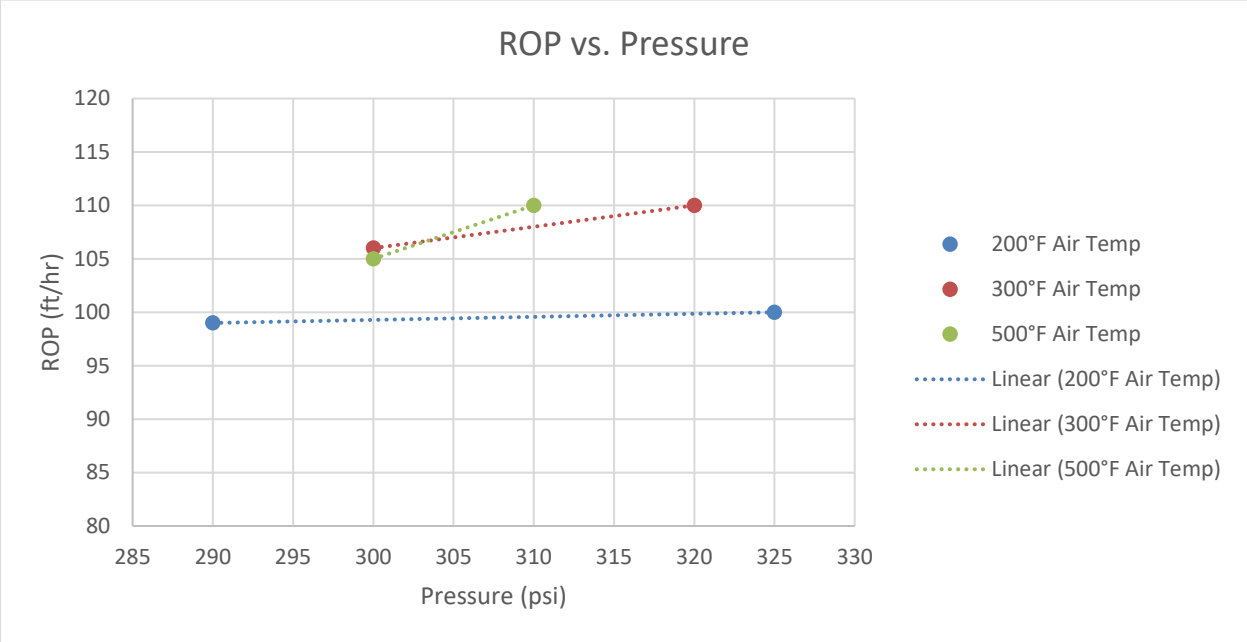

Figure 22. ROP vs. pressure test results for HOT facility characterization

These tests were conducted early in the development of the HOT facility. At the time the data was collected, pressure, RPM, and WOB were in open-loop control. There is some drift from test to test in the actual pressure values. Overall, the trends and values of performance are consistent with the results collected in the Atlas Copco test cell.

After the initial tests were conducted, the hammer was disassembled and visually inspected. Figure 23-Figure 25 show the effect of elevated temperatures on conventional lubricants and

the hammer components. Residual lubricants from the initial assembly become solid and leave a solid film on the hammer air cylinder and piston.

Figure 23. Piston sleeve assembly after operating at 400°F

Figure 24. Piston sleeve inner diameter after operating at 400°F

Figure 25. Piston with no lubrication at 400°F

3.4 High-Temperature Testing at Sandia HOT Facility

3.4.1 HT piston with coating testing at temperature

After verifying the performance of the HOT facility control and DAQ system, tests on the high-temperature prototype were started. Based on these preliminary test results from the low-temperature prototype testing, elevated-temperature testing was conducted with the high-temperature prototype.

The goal of the testing was to determine hammer performance as well as the durability of the piston material and coating. The test matrix, sorted by increasing hammer temperature, is shown in Table 1.

Table 1. High-temperature prototype test matrix (inconclusive data for empty rows)

RPM	Actual Pressure (psi)	Hammer Temp (°F)	Air Temp (°F)	Flow (scfm)	Frequency (Hz)	ROP (ft/hr)
40	300	400	150	560	34.6	92
40	315	400	150	566	35.0	95
40	300	400	150			
40	300	400	300	590	34.0	85
40	310	400	300	590	34.7	81
40	300	400	300			
40	310	400	550	578	34.6	88
40	313	400	550	563	35.1	85
40	315	400	550	560	34.7	92
40	300	450	500	550	34.5	99

40	310	450	500	550	34.9	95
40	310	450	500	545	34.9	90
40	300	450	500	535	34.5	90
40	300	450	500	540	34.4	98
40	300	450	500	560	34.4	88
40	230	450	150	425	31.0	60
40	200	450	250	350	32.0	45
40	200	450	300	350	32.4	46

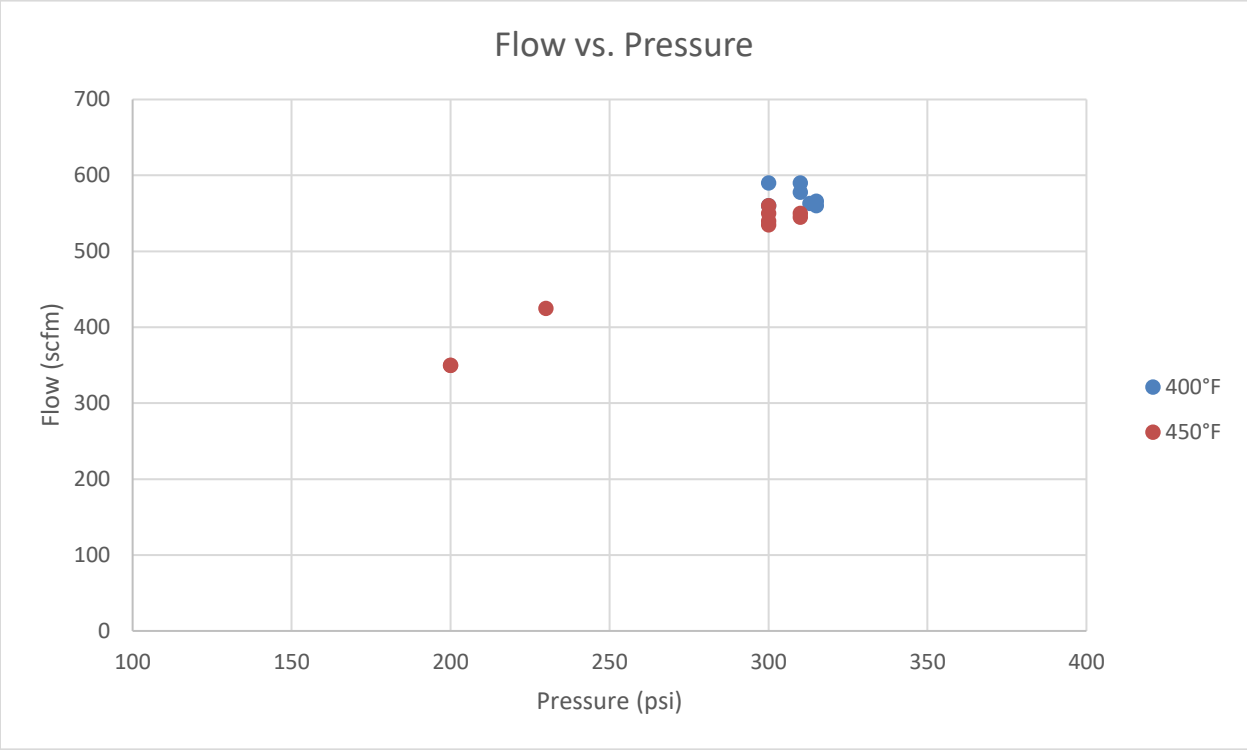

Figure 26. Flow vs. pressure for HT piston

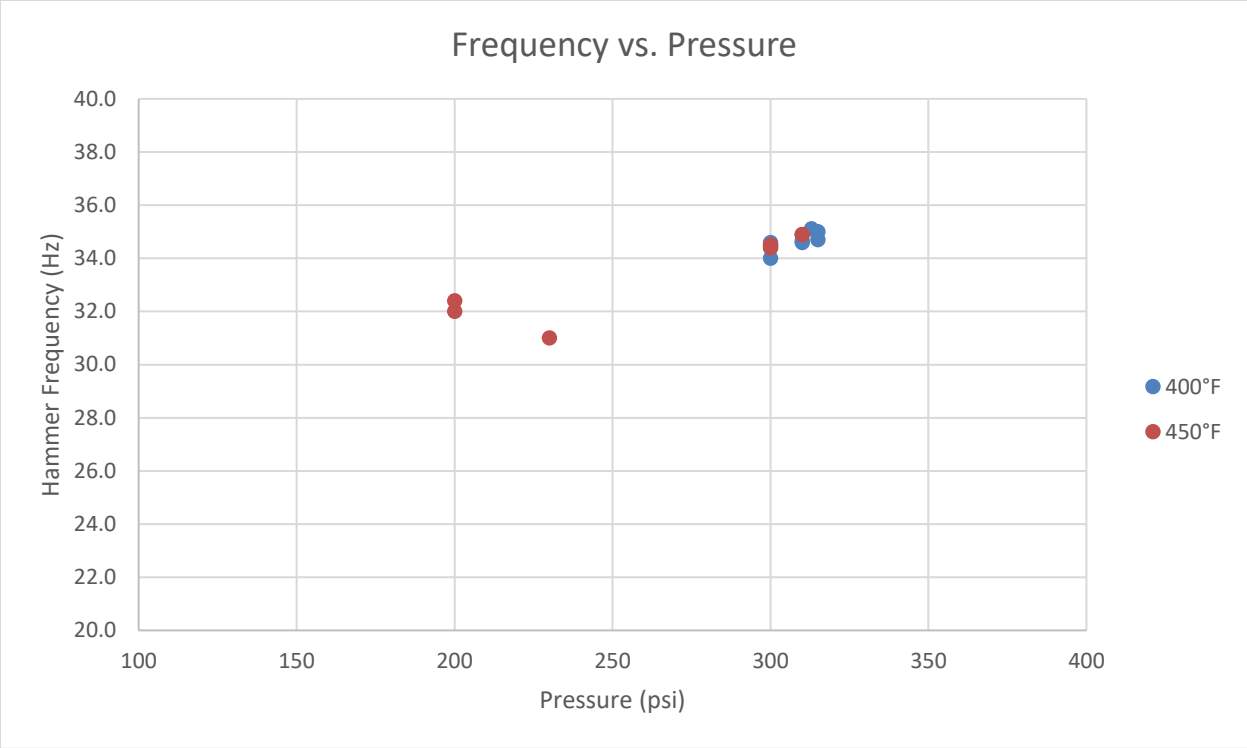

Figure 27. Frequency vs. pressure for HT piston

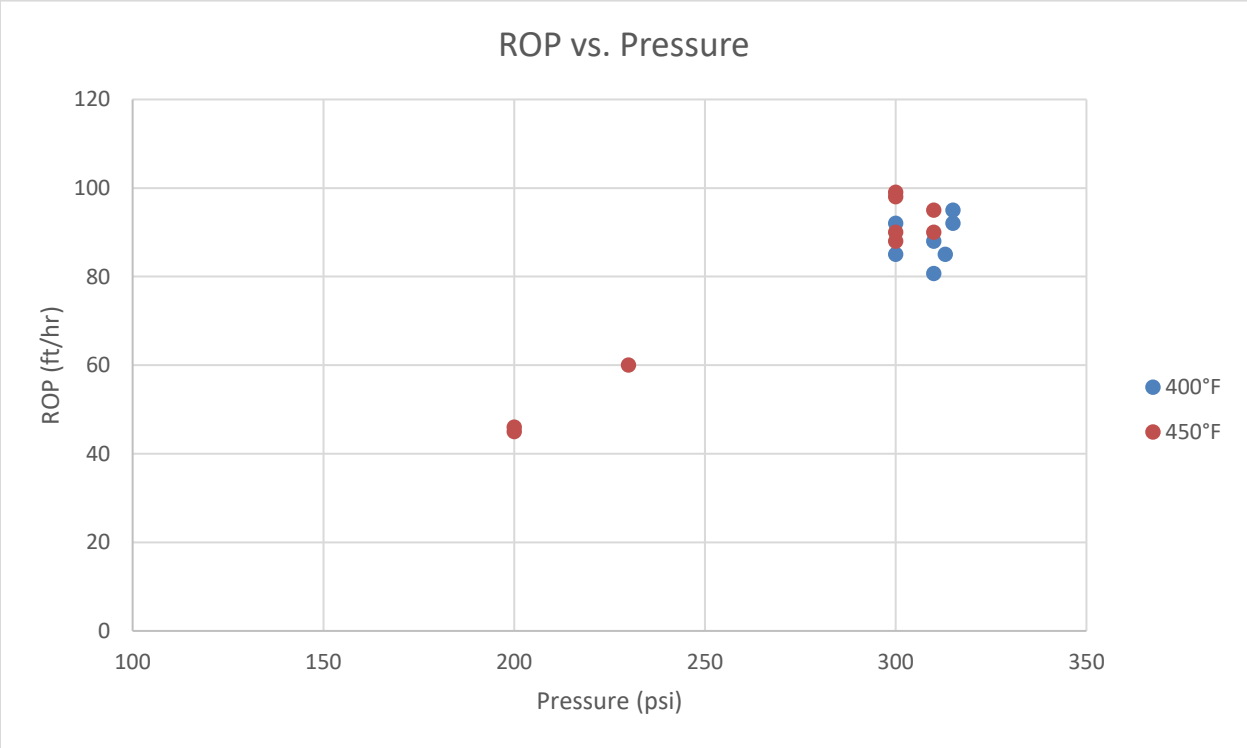

Figure 28. ROP vs. pressure for HT piston

The progression of wear on the HT piston is illustrated in Figure 29 - Figure 34. Through the early tests, the hammer was disassembled frequently to assess the wear rate of the coating. The first inspection was performed after 36” of drilling at 400°F. The inspection revealed

dramatic wear of the coating and base material at the stem end of the piston. The other rubbing sections of the piston showed no signs of wear.

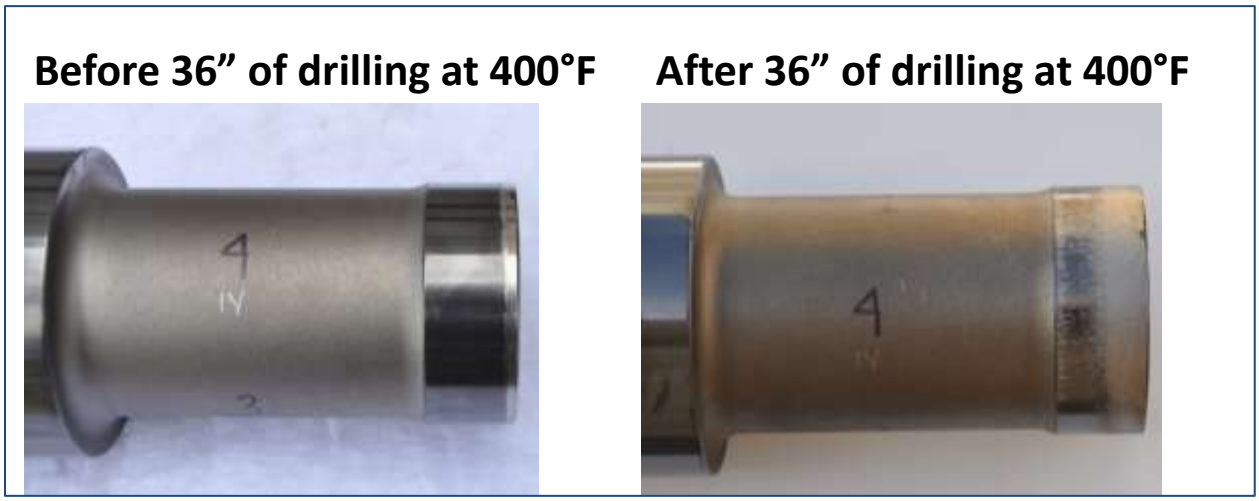

Figure 29. Stem end of HT piston with solid lubricant

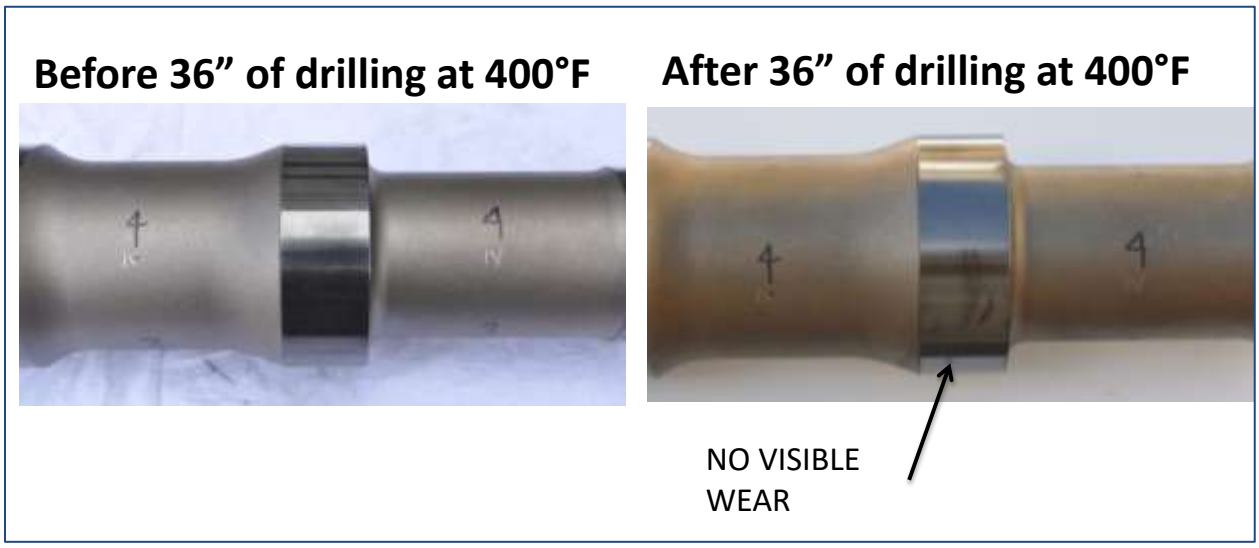

Figure 30. Middle section of HT piston with solid lubricant

Subsequent inspections were conducted at longer intervals after the initial inspection to allow more footage to be drilled. The coating on the stem was completely worn away after 27 feet. Additional wear patterns began to develop on the mid-section of the piston.

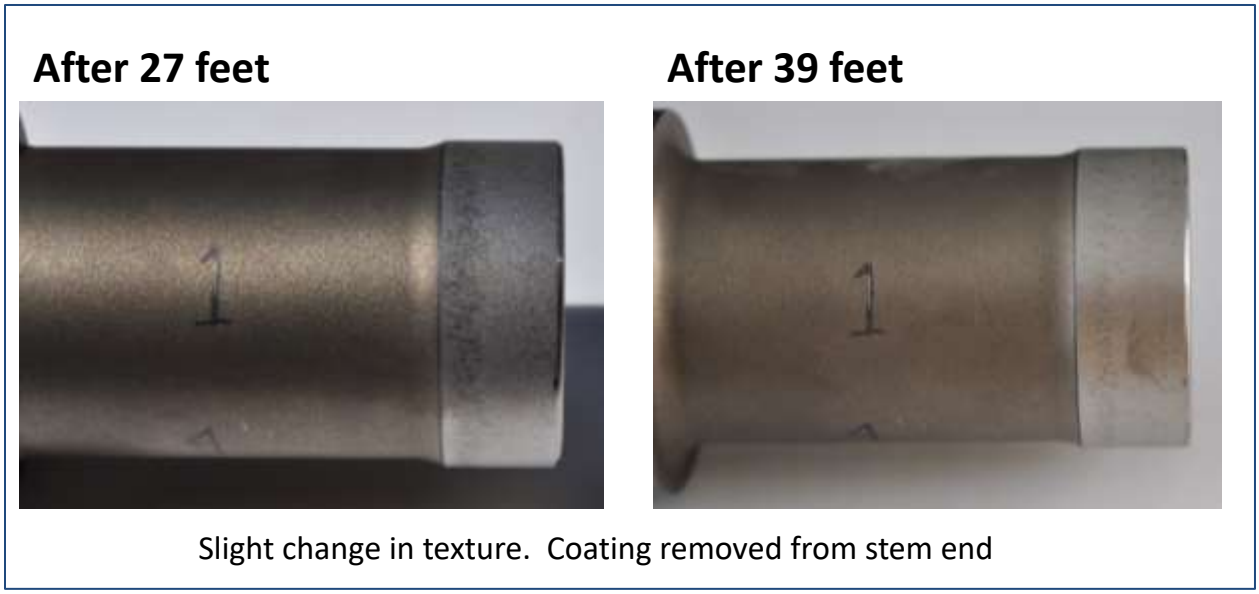

Figure 31. HT piston wear progression (stem end)

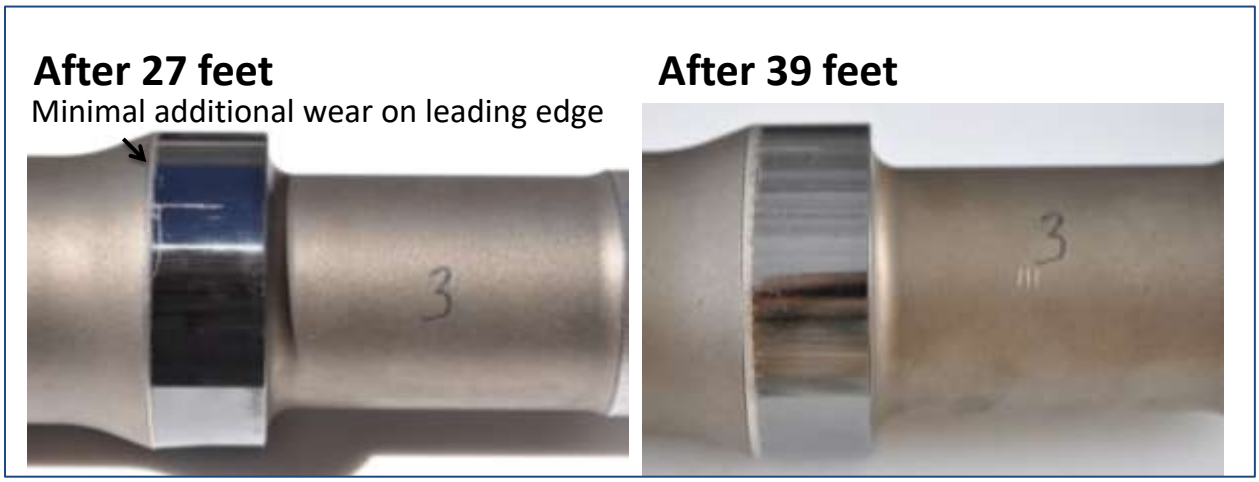

Figure 32. HT piston wear progression (mid-section)

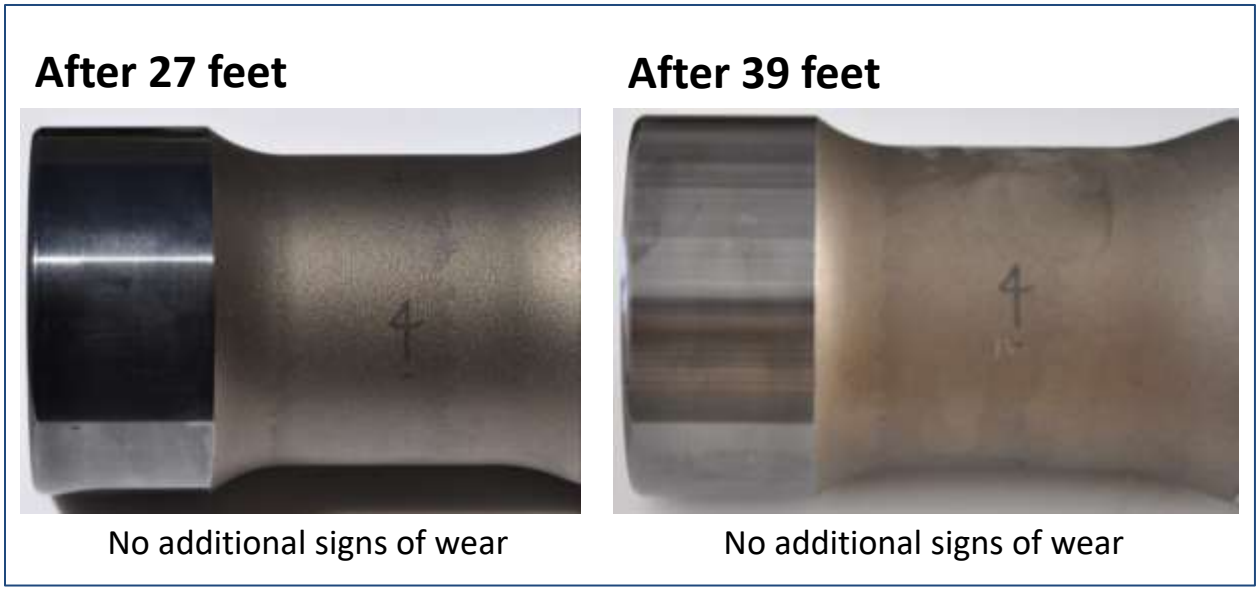

Figure 33. HT piston wear progression (far end)

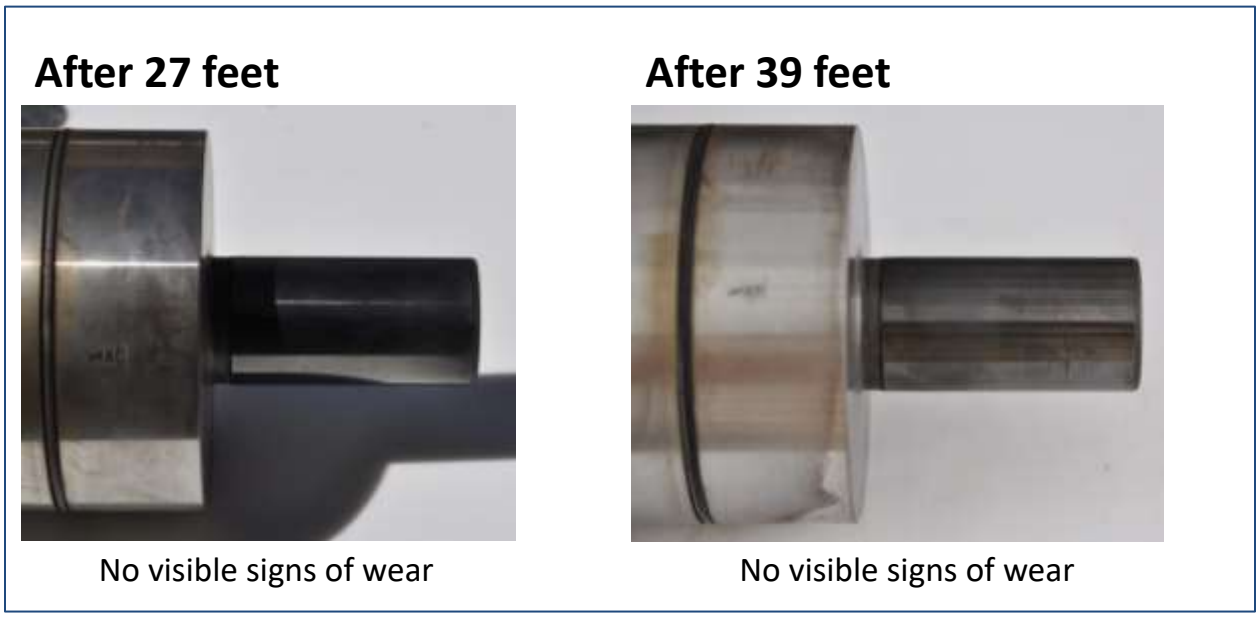

Figure 34. HT distributor wear progression

As the previous figures illustrate, the high-temperature piston showed signs of galling and excessive wear early on. The lower hardness of the material (~HRC 46) compared to the conventional material selection was the cause of the high levels of wear. Test of the high-temperature piston was abandoned in favor of coating the low-temperature piston with the same coating.

The distributor showed no visible signs of wear throughout the tests with the high-temperature piston. Because of its performance in those tests, it was used in subsequent tests with the alternative piston.

3.4.2 LT piston with coating testing at temperature

Previous coupon-level material tests indicated that a carburized surface would provide a solid substrate for the DLC and barrier layer. Although the tempering temperature of the standard piston material was a possible concern, the known hardness of the low-temperature material made it a good candidate for testing the coating at temperature.

In addition to addressing the material hardness, several geometric changes were made to the piston to reduce contact stresses along sliding surfaces. A chamfer was added to the leading edge of the piston. A radius was added to the leading edge of the mid-section of the piston where it enters the air cylinder. The same hammer components were used from the previous tests. A picture of the coated LT piston is shown in Figure 35.

Figure 35. LT piston with DLC coating applied

The test conditions for the low-temperature piston are shown in Table 2. The conditions are sorted by increasing hammer temperature. At least three runs were made at were made at pressure set points to evaluate the performance. Additional runs were made to reach total footage of 200 ft.

Table 2. Low-temperature piston material with coating test matrix

Actual Pressure (psi)	Hammer Temp (°F)	Air Temp (°F)	Flow (scfm)	Frequency (Hz)	ROP (ft/hr)
230	400	200	435	32.0	65
325	400	200	640	35.9	100

310	400	200	600	35.0	85
330	450	200	630	35.7	105
300	450	200	560	35.0	
270	450	200	500	34.0	80
200	550	200	275	30.0	
275	550	200	470	34.0	
280	550	200	523	34.6	72
350	550	200	650	36.3	110
300	550	300			
350	550	300	630	35.9	110
300	550	300	575	35.1	86
350	550	300	625	36.3	110
300	572	120			
300	572	120	550	34.4	82
292	572	150	520	34.6	88
300	572	150	530	34.8	85
310	572	200	585	35.4	100
208	572	200	336	33.2	45
286	572	200	532	34.2	72
210	572	250	370	34.5	52
277	572	250	528	34.2	73
350	572	300	615	36.1	100
325	572	300	590	35.5	105
310	572	300	570	34.6	95
300	572	300	560	34.7	92
290	572	300	530	34.4	83
300	572	300	550	34.9	88
300	572	300	530	34.6	85
250	572	300	500	32.7	70
295	572	350	540	35.1	90
300	572	400	550	35.4	90
300	572	400	530	34.5	88
290	572	400	530	34.8	84
313	572	400	582	35.2	80
250	572	400	420	32.4	72
306	572	400	550	35.3	96
310	572	400	550	34.9	88
275	572	400	490	33.8	90
300	572	400			
300	572	400	550	35.5	88
300	572	400	520	35.5	85

285	572	400	470	34.5	80
275	572	400	485	34.8	79
310	572	400	555	35.4	89
310	572	450	550	35.8	90
307	572	450	545	35.5	92
307	572	450	550	35.5	88
300	572	450	520	35.8	83
300	572	450	545	35.7	80
295	572	450	513	35.6	87
300	572	500	540	35.5	99
214	572	500	360	30.6	68
250	572	500	420	32.5	55
300	572	500			
330	572	500	540	36.5	110
300	572	500			
300	572	500	524	35.4	88
305	572	500	542	35.1	88
325	572	500	580	36.0	95
300	572	500	530	35.7	88
300	572	500	510	35.5	92
250	572	500	475	32.1	58
300	572	500	520	35.8	79
300	572	500			
294	572	500	470	34.9	79
310	572	500	532	35.1	85
300	572	500	514	35.6	86
300	572	500	517	35.4	80
300	572	500	530	35.5	80
300	572	500			
213	572	500	418	33.1	60
267	572	500	490	33.7	64
244	572	500	443	34.0	56
305	572	500	537	34.0	80
294	572	500	502	35.4	84
225	572	500	385	33.0	54
300	572	550	509	35.2	83
225	572	550			
300	572	550	526	34.4	80
305	572	550	542	35.3	80
306	572	550	542	35.1	84
300	572	550			

300	572	550			
307	572	550	528	35.7	80
300	572	600	500	35.4	88
300	572	600	503	35.1	80

Hammer performance results are captured in Figure 36-Figure 38. The plots include data from all the runs at the various soak and process gas temperatures. The overall performance of the hammer at temperature is consistent with the measured performance at the Atlas Copco test cell.

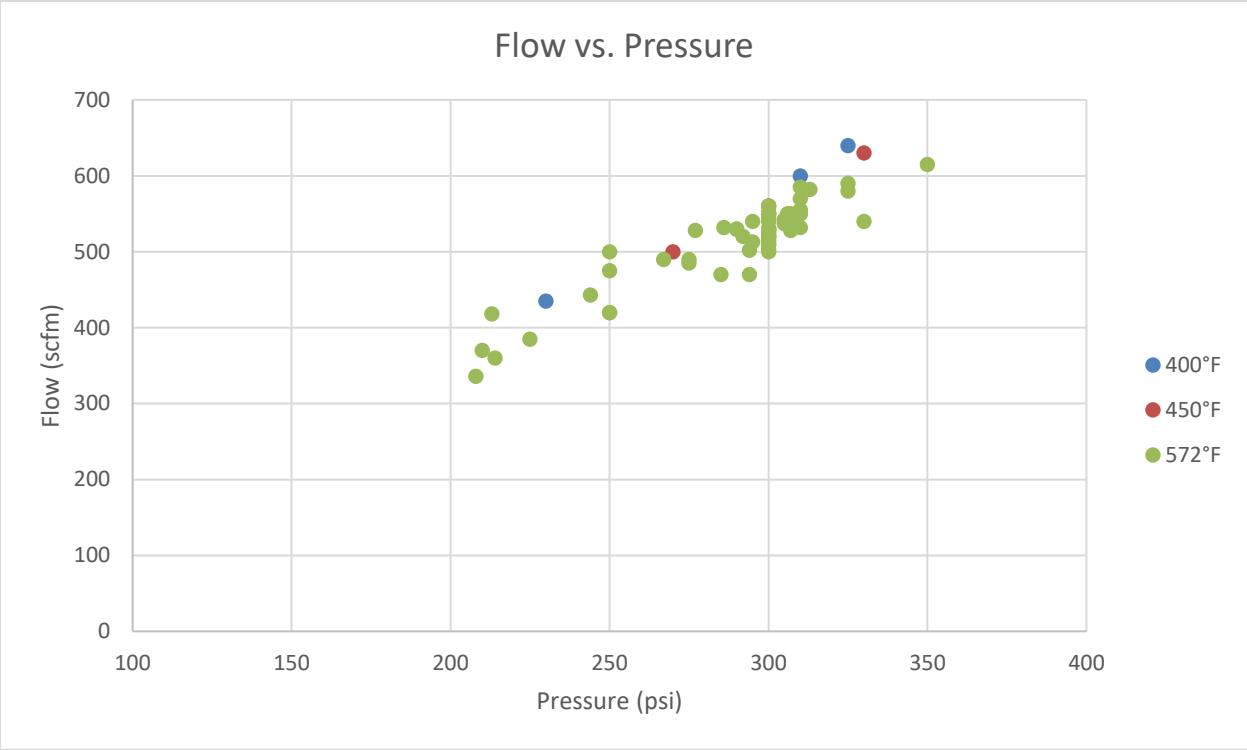

Figure 36. Flow vs. pressure for all LT piston tests

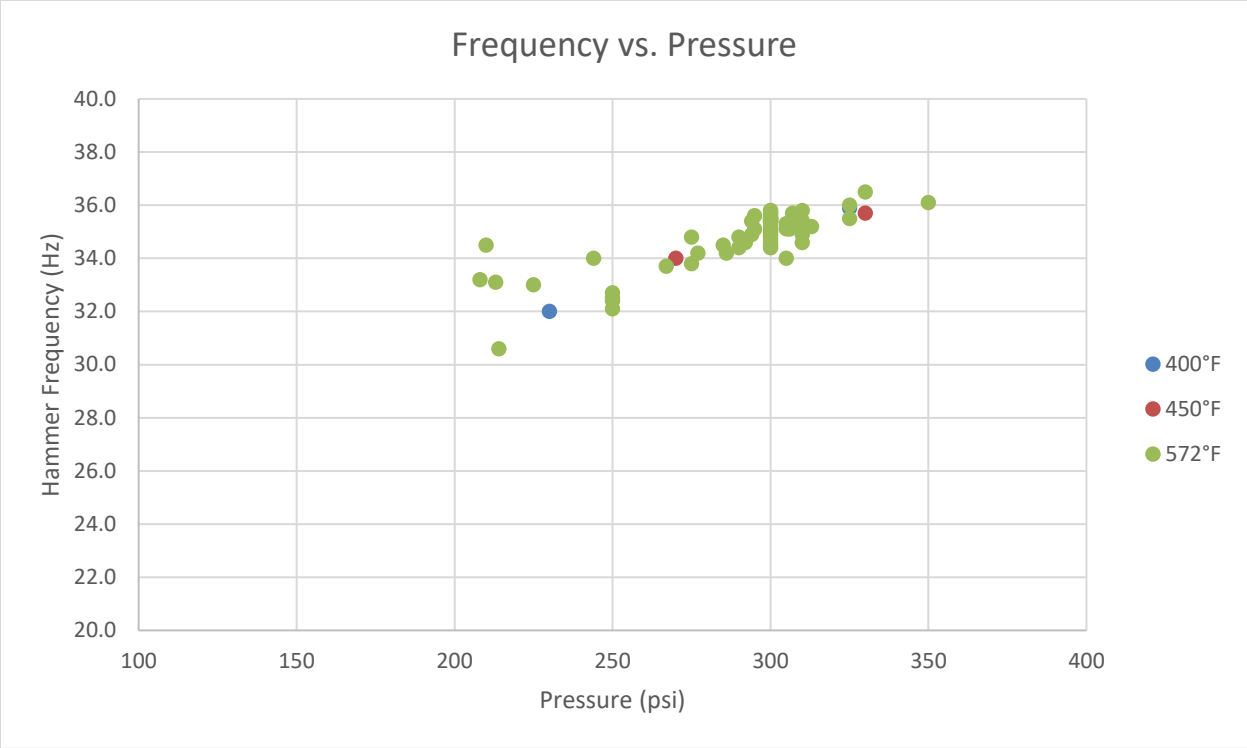

Figure 37. Hammer frequency vs. pressure for all LT piston tests

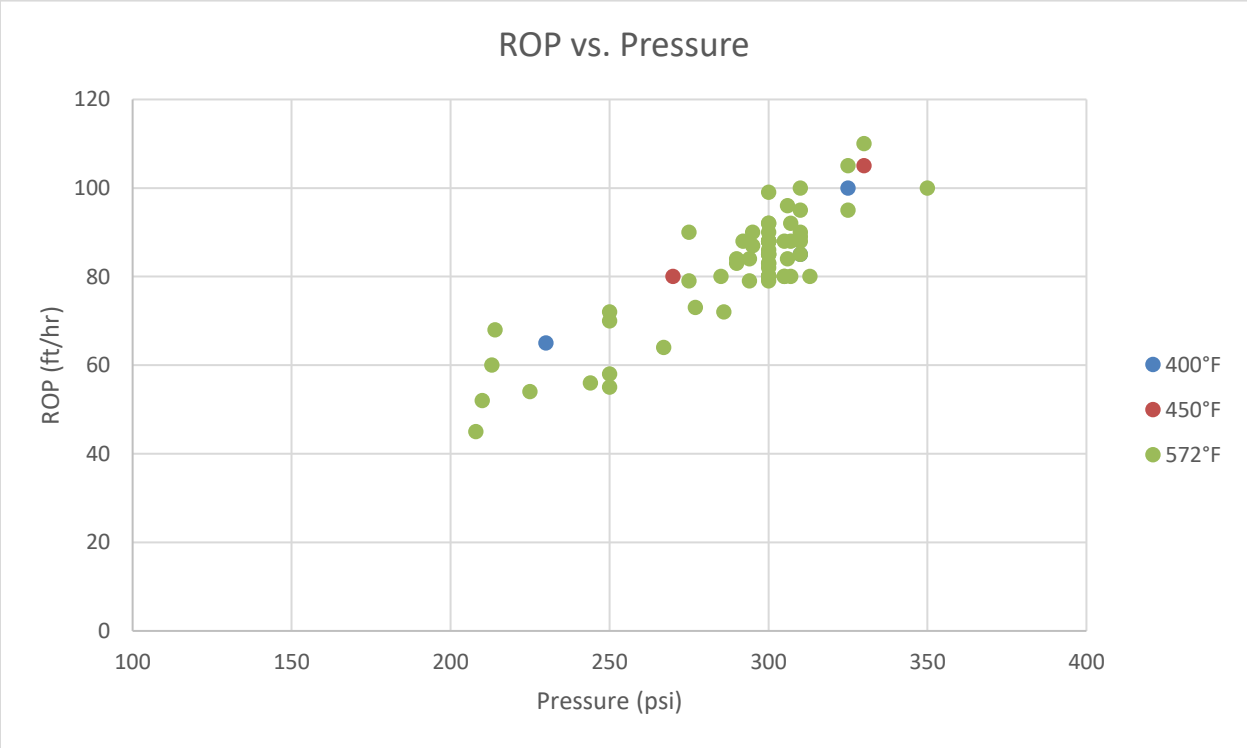

Figure 38. ROP vs. pressure for all LT piston tests

3.4.3 Progression of coatings wear

Similar to the tests with the high-temperature piston, the low-temperature piston hammer was disassembled and inspected at specified intervals. The intervals at the start of the tests were shorter due to uncertainty in how the piston would behave. The results from first test interval are shown in Figure 39. The distributor is shown in Figure 40.

No visible signs of wear were apparent after the initial test interval. This early performance allowed inspection intervals to be extended. Those intervals varied throughout testing due to timing and coordination of the rock samples being drilled.

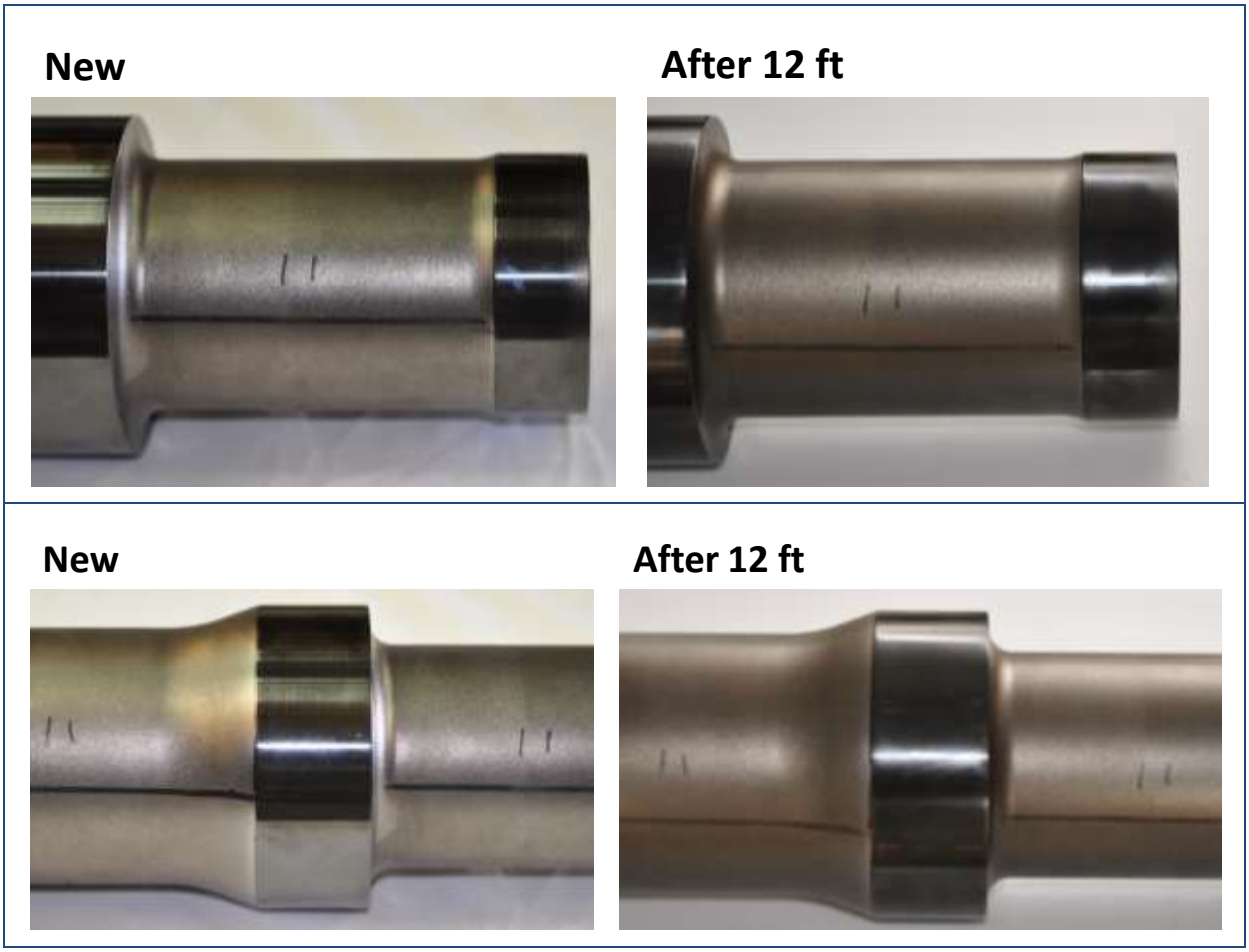

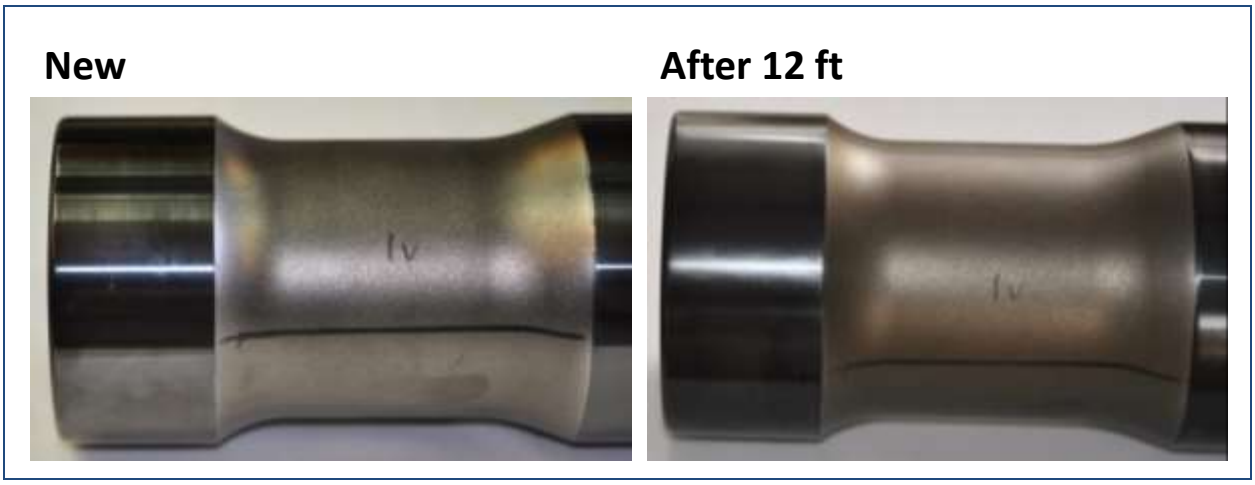

Figure 39. LT piston with DLC coating applied

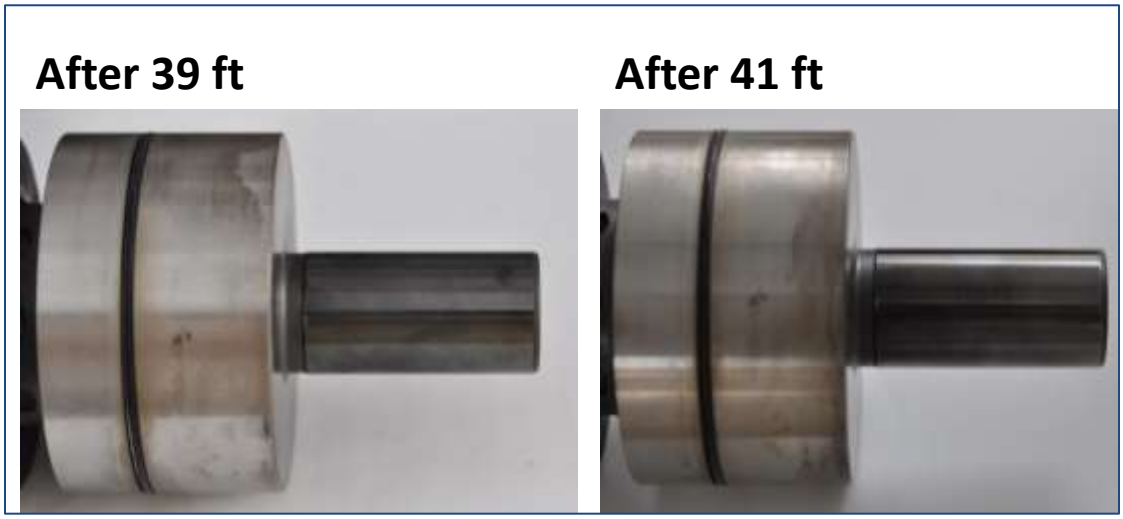

Figure 40. HT distributor performance continued from previous tests

In the second interval, hammer soak temperatures were increased to 550°F. This result of the increased temperatures is evident in Figure 41. The exposed piston material has turned blue indicating tempering temperatures of approximately 550°F.

Two visible wear patterns started to develop on the piston at the struck end.

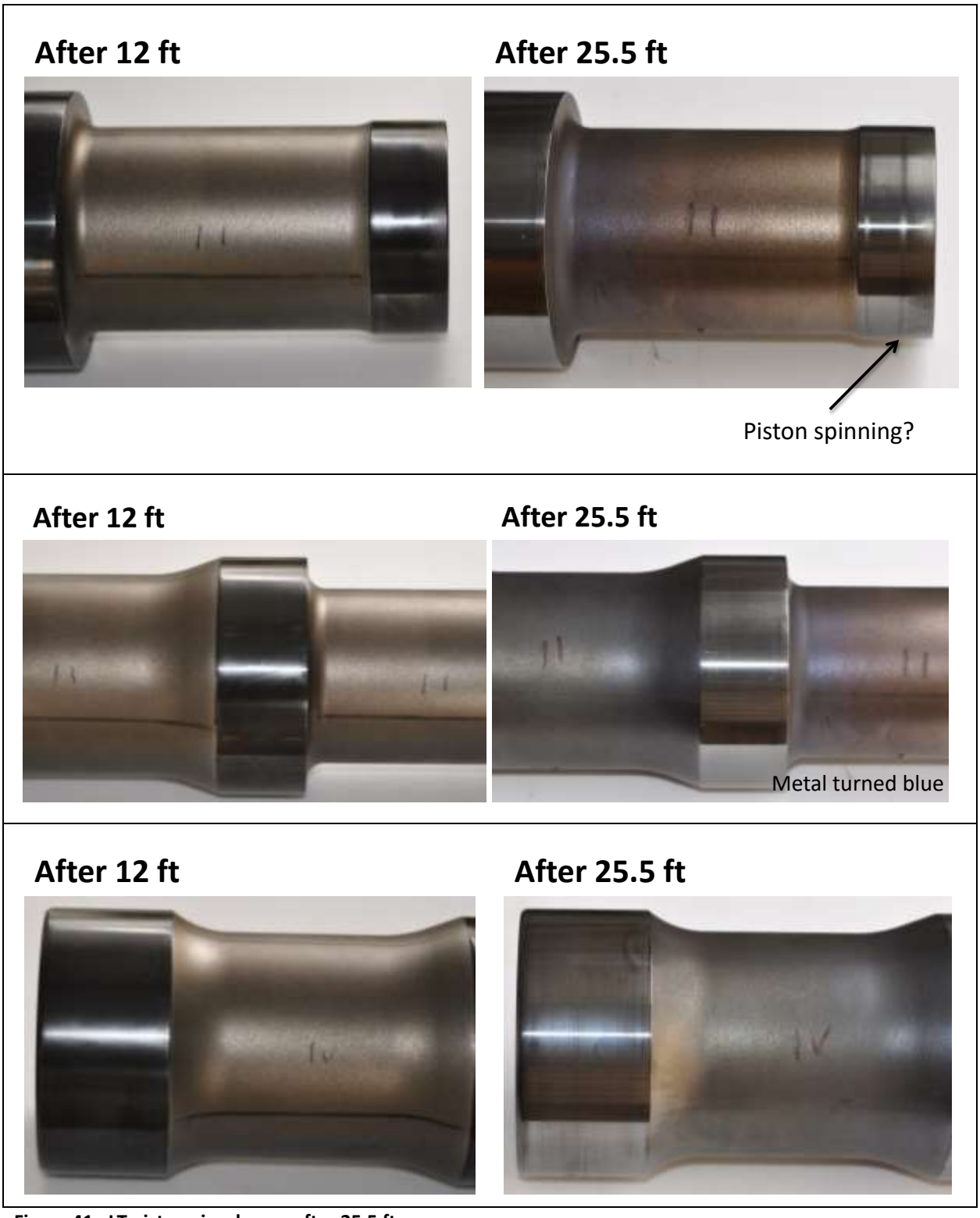

Figure 41. LT piston visual wear after 25.5 ft

There is no visible wear on the distributor.

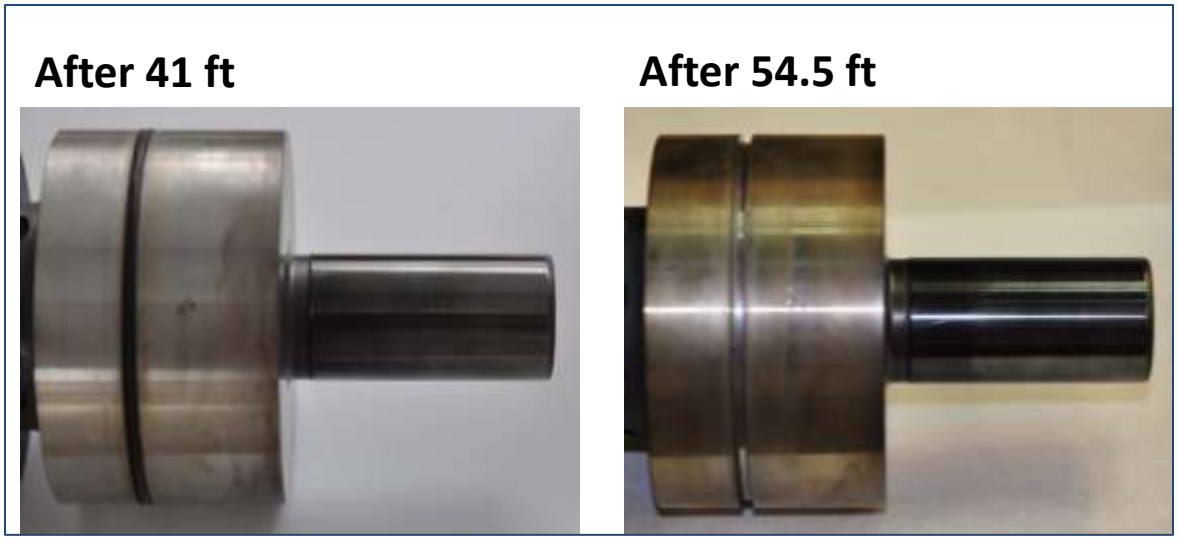

Figure 42. HT distributor performance after 54.5 cumulative feet

The next internal inspection was conducted after 79.5 ft of total footage as shown Figure 43. The wear ring on the struck end has grown. There are also visible wear patterns developing on the mid-section and far-end of the piston.

After 79.5 ft

- Additional bluing
- 2 wear rings developing
- Due to piston rotation?

After 79.5 ft

Visible ring near end

Figure 43. LT piston with DLC performance after 79.5 ft

A small chip on the distributor stem was visible during this inspection interval.

Figure 44. HT distributor performance with 108.5 feet cumulative

The wear patterns that developed in the previous intervals are more prominent after the 119 ft interval inspection. The tempered region has expanded towards the struck end of the piston. On the struck end, bare metal is visible in Figure 45. The wear pattern is non-uniform around the circumference.

The wear patterns were inspected under a microscope to provide a better understanding of the phenomenon. On the fare end of the piston, the wear marks are perpendicular to the axis of the piston. This indicates that the wear is due to the piston sliding within the air cylinder. This is to be expected since this is the normal motion of the piston.

In the mid-section and struck end, source of the wear is not as clear. The magnified images show the original machining marks being burnished away. This process could be the result of a combination of the piston rotating and sliding within the hammer case.

After 119 ft

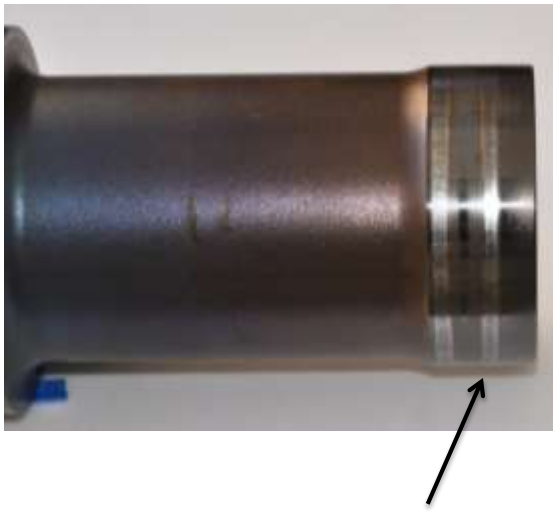

Additional wear

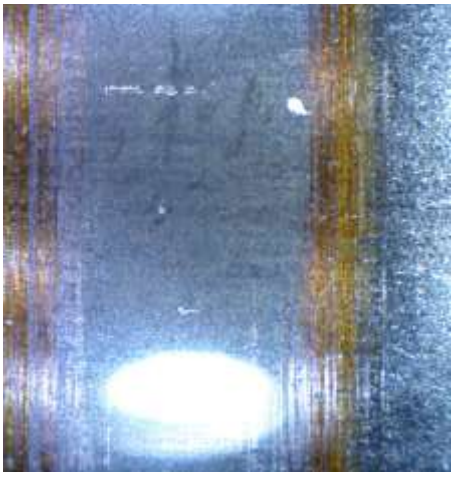

50x zoom of stem end

After 119 ft

- Wear locations consistent with 40-58

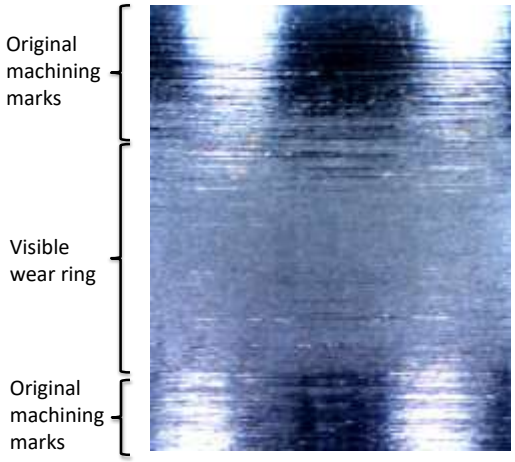

50x zoom of wear ring on mid-section of piston

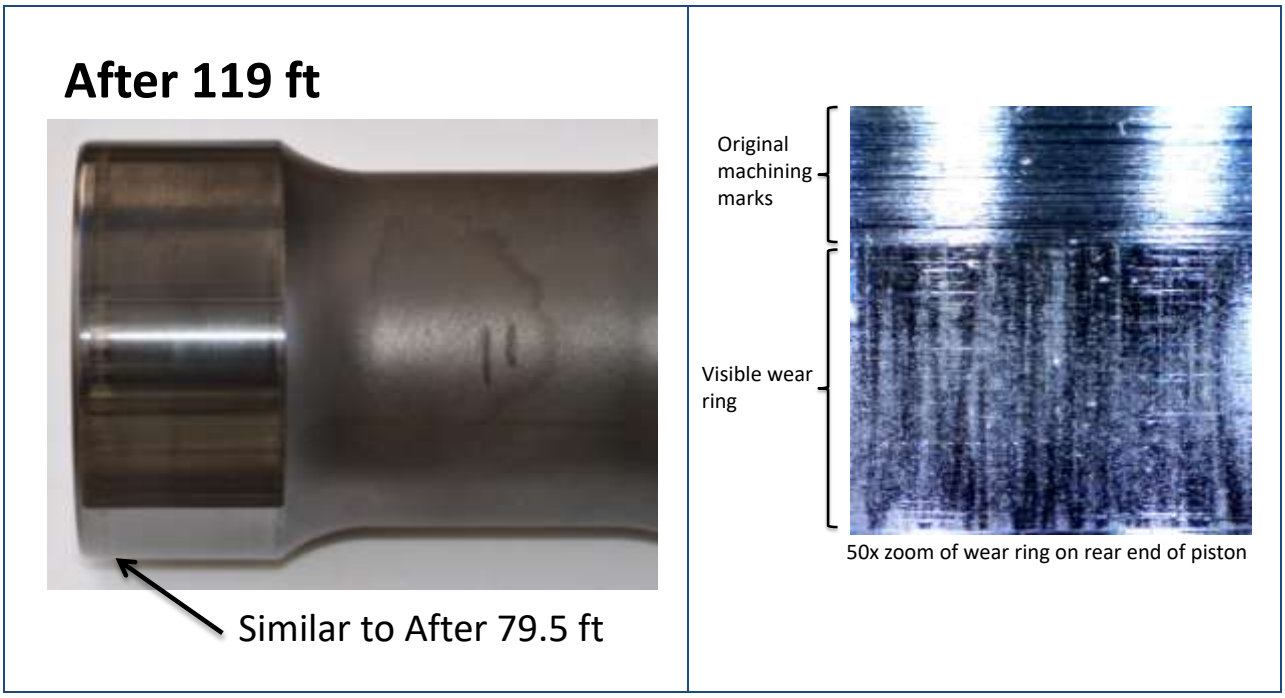

Figure 45. LT piston with DLC after 119 ft.

Additional pits can be seen in the distributor. These are clearly visible in the magnified image in Figure 46. The body of the distributor is also showing discoloration due to the thermal cycles. The brownish color indicate temperatures around 500°F.

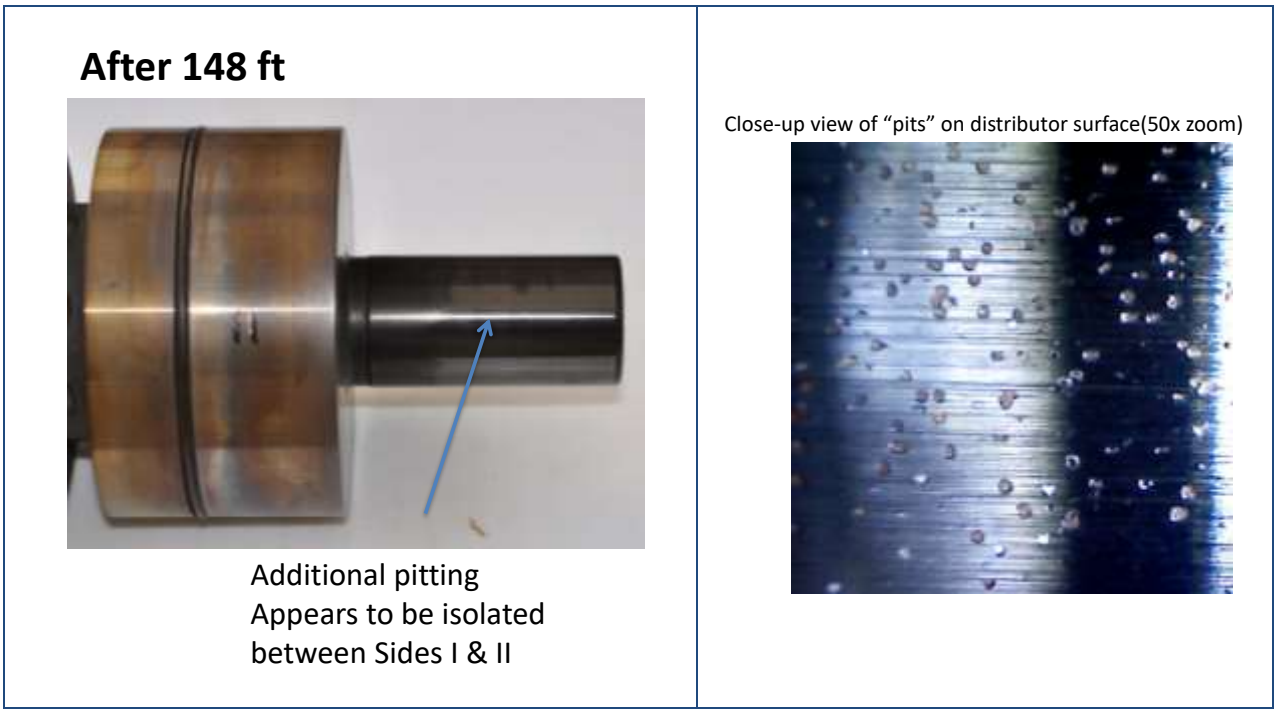

Figure 46. HT distributor with DLC after 148 feet cumulative.

The check valve is shown in Figure 47 to illustrate the elevated temperatures seen within the hammer. The check valve is located within the hammer and sees direct heat from the process

gas air. The deep blue color indicates sustained temperatures in the range of approximately 550°F-600°F.

Figure 47. Check valve tempering temperature color change

The next inspection shows a steady progression of wear that was seen in the previous interval. The tempered region continued to expand towards the struck end. The wear bands on the stem appear more polished. The transverse wear pattern visible on the far end in the previous interval is now visible in the mid-section.

After 167.25 ft

50x zoom of stem end

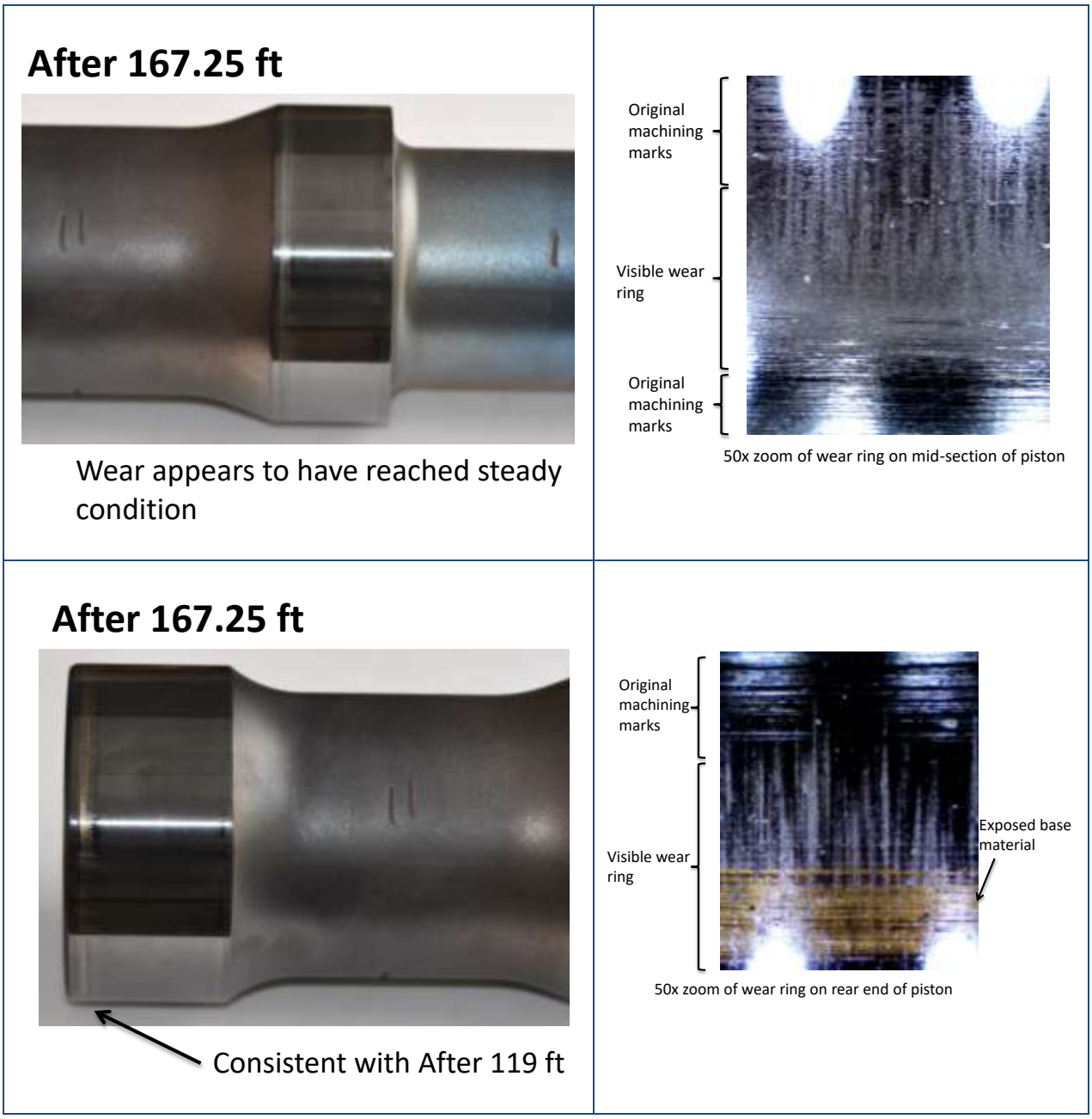

Figure 48. LT piston with DLC after 167.25 ft.

Pitting in the distributor stem has expanded, but is isolated to the same side. There is visible exposed substrate in both the magnified and regular view.

After 196.25 ft

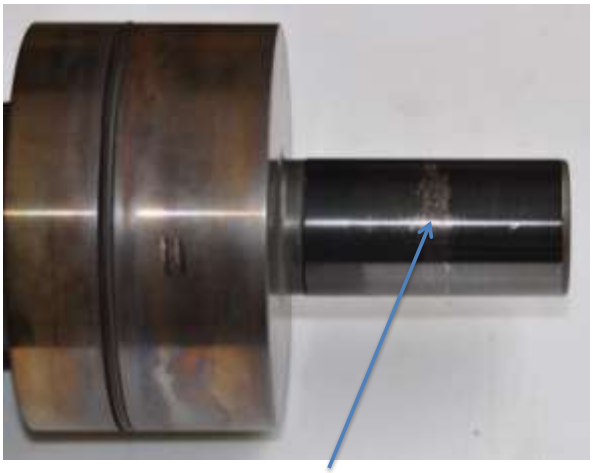

Additional pitting
Exposed barrier layer

Close-up view of “pits” on distributor surface(50x zoom)

Figure 49. HT distributor with DLC after 196.25 feet cumulative.

The final inspection revealed additional wear on the stem end. The two wear rings have nearly coalesced. A band of the original coating remains in place. The transverse wear patterns in the mid-section and the far end have expanded. There is a visible ring on the far end of the piston indicating material transfer between the air cylinder and piston.

After 201.75 ft

After 201.75 ft

Wear appears to have reached steady condition

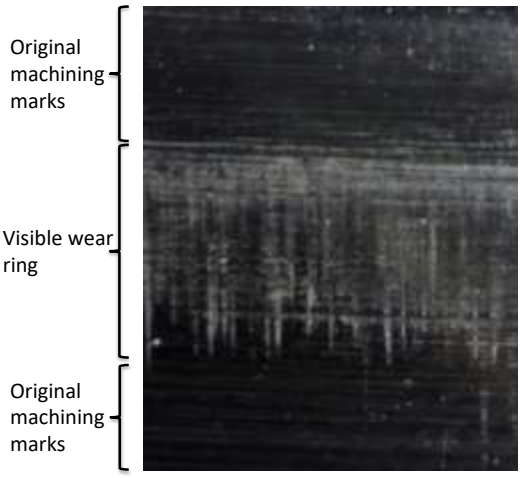

After 201.75 ft

Wear ring has more metallic look after this run due to metal transfer

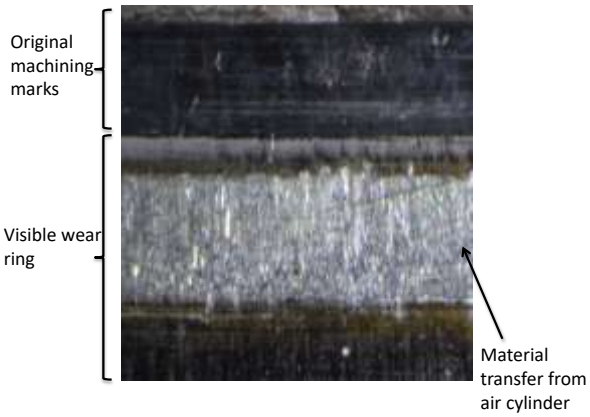

Figure 50. LT piston with DLC after 201.75 ft.

Additional pitting and discoloration is visible in the distributor stem.

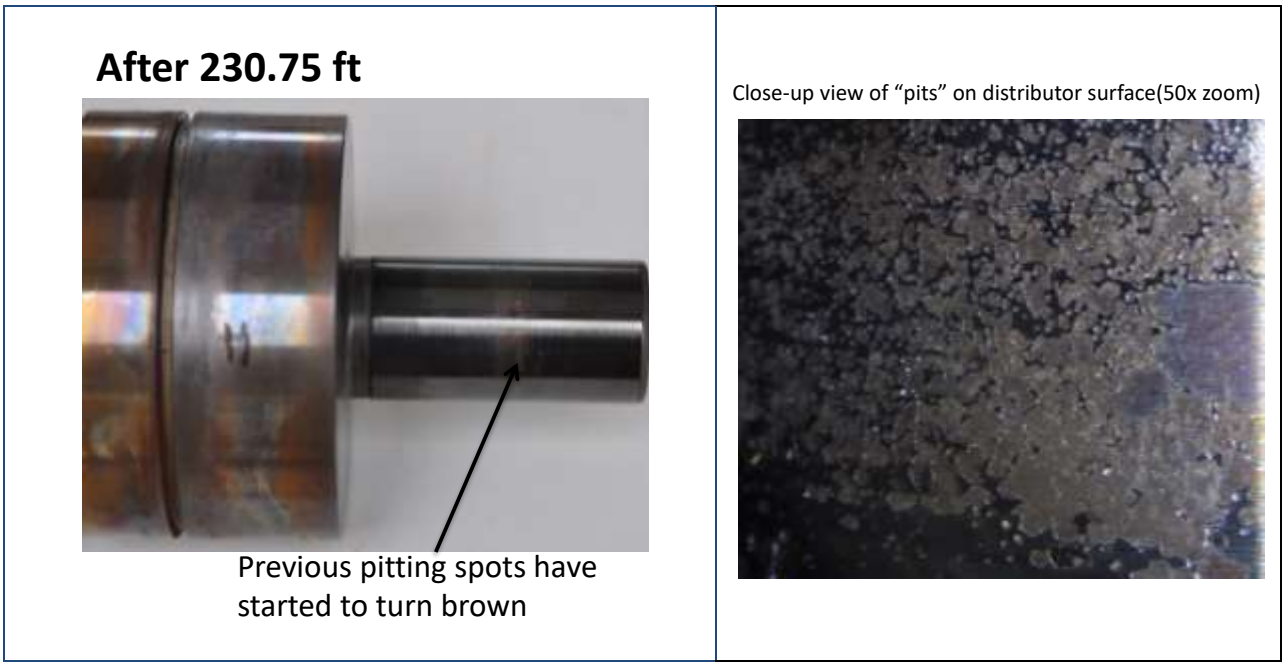

Figure 51. HT distributor with DLC after 230.75 feet cumulative.

Overall, the hammer configuration with the LT material piston and HT material distributor drilled more than 200 ft. in 24 ksi Sierra White granite at temperatures up to 572°F without liquid lubricants. During this time, it went through multiple thermal cycles and was able to maintain performance with rates of penetration exceeding 100 ft/hr. Although wear patterns developed on the moving parts, the performance of the hammer was quite remarkable when considering the operating environment.

4. HIGH-OPERATING TEMPERATURE (HOT) TEST FACILITY DEVELOPMENT

Designing and building a DTH capable of operating at temperature was a challenge. Developing the capability to test the hammer under high-temperature conditions posed an entirely different set of challenges.

Typical drilling rigs or test cells are operated and actuated with hydraulic equipment. Pressurized oil in hydraulic systems present a fire hazard, especially in the vicinity of a heat source. Following a conventional design for those systems would result in a combination of hydraulics and heat sources that would have potentially serious hazards to both property and operators. Additional challenges included implementing remote operation to minimize operator hazards as well as developing the infrastructure to support the testing.

In order to address the challenges, the high-operating temperature (HOT) facility development was divided into three main sub-systems. The first was *Facility* and infrastructure-related needs. The second sub-system was the *Hot Cell.* This sub-system included the hardware and various control elements required to simulate elevated-temperature drilling conditions. The *Drill* sub-system captures the components and controls necessary to operate the percussive down-the-hole hammer for drilling.

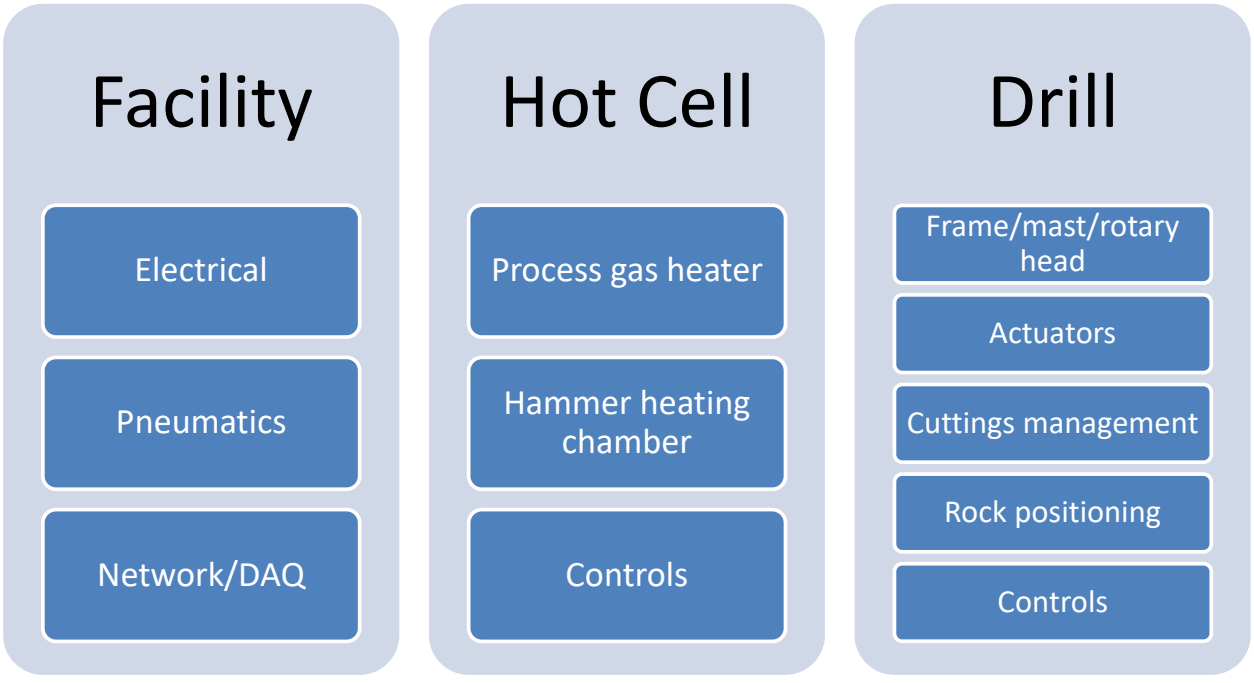

Figure 52. HOT test facility sub-systems

4.1 Operating requirements

Operating requirements for the overall system were developed in Phase I. The key requirements driving the test facility development are summarized below.

4.1.1 Temperature requirements

Formation temperatures can be expected to reach 300°C/572°F at total depth (although hotter geothermal wells are known to exist). DTH Hammers developed within this specification are categorized as follows:

Conventional	135 °C / 275 °F
Moderate Temperature	200 °C / 392 °F
High Temperature	250 °C / 482 °F
Extreme Temperature	300 °C / 572 °F

Based on wellbore hydraulics modeling from Phase I, the expected downhole process air temperature at 3000 m is approximately 230°C. This assumes a temperature gradient of 100°C/1000m and counter-flow heat exchange as the process gas moves from the surface to the hammer.

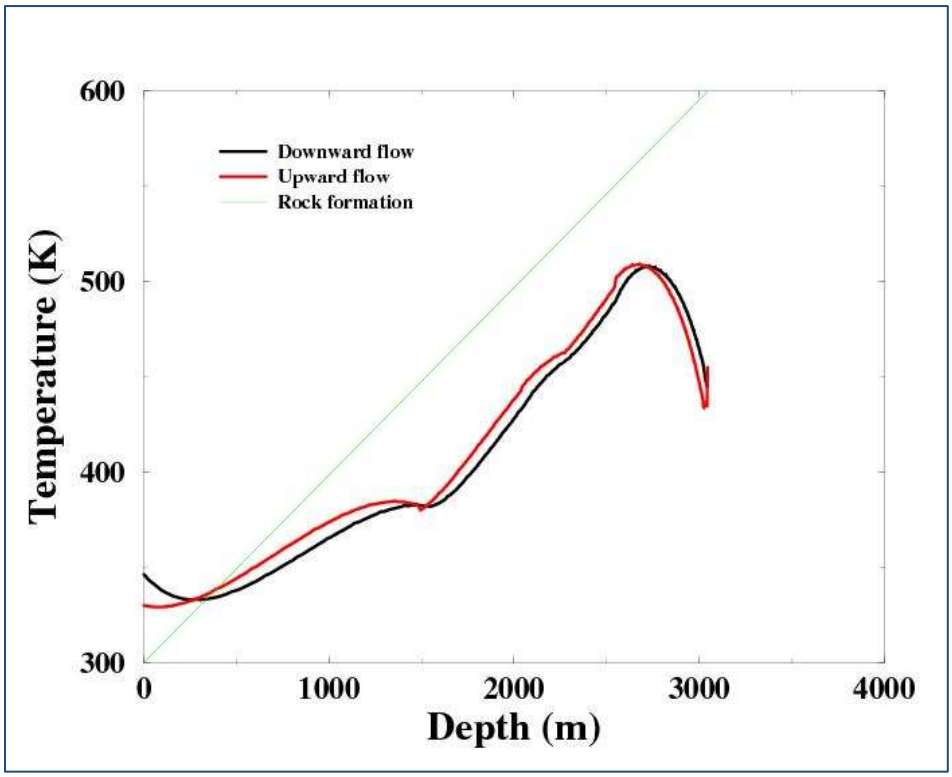

Figure 53. Temperature profiles in the two flow streams and the geologic medium during a drilling operation. [3]

4.1.2 Pressure requirements

Hammer operating pressure is up to 500 psi with flow rates up to 1000 scfm.

4.2 Facilities

4.2.1 Electrical

The planned location for the test facility is in a remote location on Sandia property. Electrical power will need to be supplied either via generators or a new permanent electrical installation.

A list of components required to meet testing and project objectives was compiled in order to establish an electrical budget for the test facility. Those components are shown in Table 3 .

Table 3. HOT facility electrical budget and key components

Test Facility Component	Power (kW)	Voltage (V)	Current (A)	Qty	Total Power (kW)
Process gas heater	190	480	229	1	190
Hammer heater	1.5	240	6	7	9
Lighting	0.4	120	3	10	4
DAQ/Computers	2	120	17	1	2
Process controllers	6	120	50	1	6
Process controller air compressor	3.7	480	4	2	7.4
Water pump	2.2	230	6	1	2.2

4.2.2 Pneumatics

In order to mitigate the hazards associated with hydraulics and heat sources, a decision was made early in the design process use pneumatics for actuation throughout the facility. In addition to eliminating a hazard, the selection of pneumatics reduced the number of power sources required to operate the facility. The primary system components identified in the design process are listed in Table 4.

Table 4. HOT facility pneumatic budget and key components

Component	Pressure (psi)	Max Flow (scfm)	Cv
Air Motor	90-115	420	8.9
DTHH	300-500	1000	19.2
WOB	90-115	110	2.3
Rock downforce	90-115	20	0.3
X-position	90-115	4	0.47
Y-position	90-115	4	0.47
Air pallet	45	85	2.55

The overall system is designed to allow the testing of down-the-hole-hammers (DTHH) or other drilling tools at elevated temperatures up to and including 300°C and at pressures up to and including 500 psig. The system consists of seven interconnected pressure sub-systems each with a different Maximum Allowable Working Pressure (MAWP). Each of the systems is discussed individually below.

4.2.2.1 CTRL-145

The CTRL-145 sub-system is primarily used for pneumatic control of the MOTOR-150 and AC-500 sub-systems. There is also a check valved cross over to the MOTOR-150 system which will be used for intermittent motor operation and testing purposes. The air source for this system is the PowerEx compressor (Figure 54). Compressed air flows from the output of the compressor through a filter and a pressure regulator. The compressed is then valved and piped to the 240 gallon air receiver. The system is designed to allow the future addition of another air receiver (Figure 55). From here the air travels in 2" Sch-40 pipe to the test structure (Figure 56). After entering the test structure, compressed air is piped to the control box (Figure 57). The control box houses a Parker modular pneumatic control system which controls the drilling system. A set of Parker 4MA cylinders control the actions of the drilling rig. The pressure relief valve for the CTRL-145 subsystem is shown in Figure 55 and is set at 145 psi.

The MAWP of the subsystem will be limited by the valve components and is limited to 145 psi by the PRV on the air receiver.

4.2.2.2 AIR-120

An air pallet is used to assist in the controlled movement of the rock samples. It consists of air bladders inflated within a metal housing. The air from the bladders creates a bearing surface between the frame and the floor making the rock easier to maneuver beneath the drill head. The air pallet is fed and controlled from the CTRL-145 sub-system.

This portion of the air system has a MAWP of 120 psi as recommended by the manufacturer. Although air pressure in the pallet is controlled via a regulator attached to the manifold, the MAWP of the circuit is limited with a dedicated pressure relief valve set to 120 psi.

4.2.2.3 MOTOR-150

The MOTOR-150 is intended provide air to the drilling motor. The compressor used to source air for this subsystem will be a rental unit, normally intended for use with a jackhammer. These compressors are of various makes and models so it will be important that the maximum available pressure of the compressor be determined before it is connected to the subsystem.

The MAWP for this subsystem is 226 psi. The compressor used for this subsystem is capable of generating pressure up to 150 psi. The output pressure is controlled via an onboard regulator and is limited by an internal pressure relief valve. An additional redundant PRV set at 150 psi has been installed in this part of the circuit.

4.2.2.4 AC-500

This system provides compressed air to the down-the-hole hammer under test. This subsystem utilizes 2" Sch-80 pipe and fittings. Air from the compressor is supplied via a 2" hose with hammer fittings. The air then passes through a two-stage Parker filter (coalescing and absorption) to remove oil residue. It then travels through the Rosemont DP flow meter into the Durex process gas heater where the outlet temperature is set as part of the test matrix. The compressed air continues through a 2" stainless steel flex hose into the ball joint and into the swivel. From there, it goes through the DTHH and out the exhaust. The majority of the flow path can be seen in Figure 60.

Based on system components, the MAWP for this subsystem is 750 psi. The compressor used to supply air to this subsystem is a large air drilling unit equivalent to the Sullair model 900XHH/1150XH capable of delivering 900 cfm at 500 psi or 1150 scfm at 350 psi. The output pressure of the compressor is controlled via an onboard regulator and normally-closed inlet valve and is limited with a pressure relief valve set at 600 psi in the internal air receiver. The inlet valve fails in a closed position in case of regulator malfunction. This cuts the air supply to the compressor and prevents additional pressurization. These two sub-systems are redundant and limit the maximum output pressure of the compressor. An additional redundant PRV set at 550 psi has been installed in this part of the circuit.

4.2.2.5 CYCLONE

The cyclone subsystem handles the exhaust of the down-the-hole hammer test article described in the AC-500 subsystem. The cyclone particle separator is an Imperial Systems ISC-42 designed to handle a volume flow rate from 1200-3000 scfm. The maximum generated flow rate of the air compressor is within the operating range of the cyclone separator. Figure 61 shows the components in the cyclone sub system. The water subsystem is used to suppress dust from the exhaust of the cyclone.

The MAWP of the cyclone is +/- 20 in H_2O or 1200-3000 scfm.

4.2.2.6 WATER WASHDOWN

The purpose of the water system is to aid in suppressing dust from the cyclone. The high pressure pump takes water from the supply tank and pumps the water through a set of spray nozzles to suppress dust. The sump subsystem is responsible for returning water to the supply tank to minimize water use. The water subsystem is divided into upstream and downstream of the Goulds water pump.

The MAWP for components downstream of the Goulds pump is 300 psi. Since the pump has a maximum pressure of 186 psi, no PRV is required in this subsystem.

4.2.2.7 WATER SUMP

The sump system consists of a sump pump capable of 9 PSI and a hose and PVC plumbing returning water to the tank. The sump pump transfers water for reuse from the open tank at the bottom of the water system to the supply tank.

The sump pump subsystem is only capable of 9 psi, and the hose and piping system which return to the open water storage tank is rated well above this pressure. No PRV is needed in this subsystem.

Figure 54. CTRL-145 Compressor and Output

Figure 55. 240 gallon air receiver with auto drain and pressure relief valve

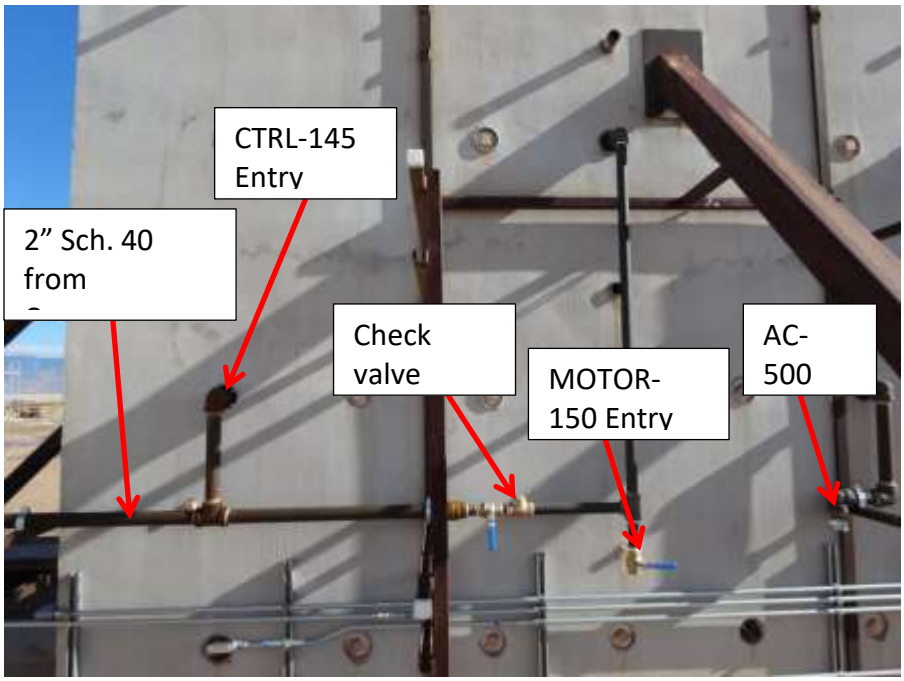

Figure 56. West wall piping to test cell and supply entries

Figure 57. Control Box Entry (2” pipe to 1 ½” reduction)

Figure 58. Pneumatic control box

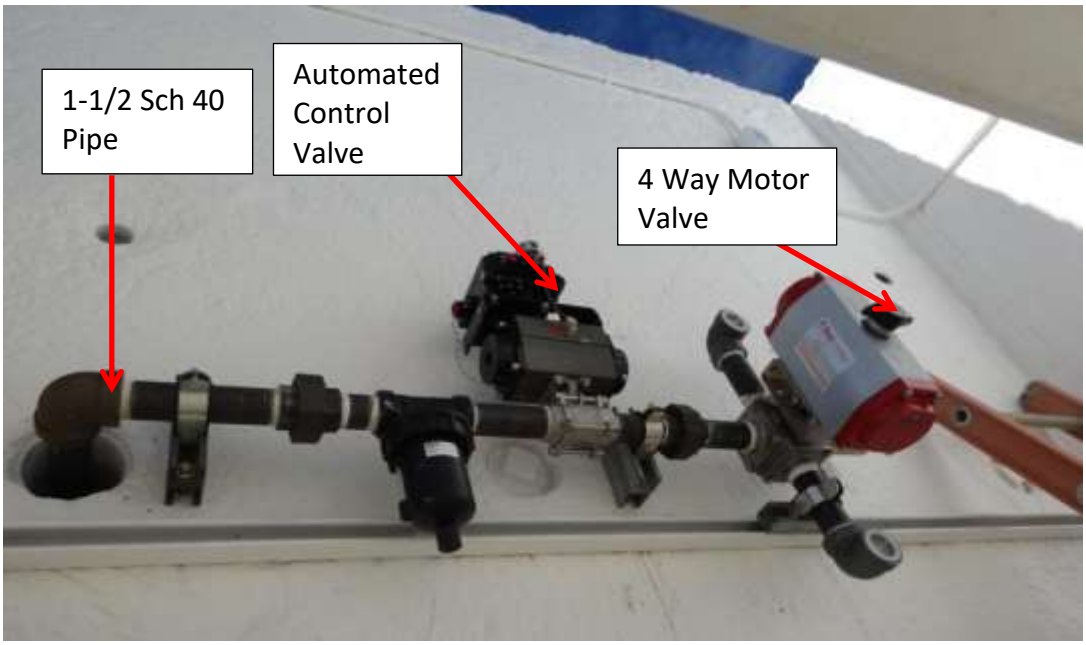

Figure 59. Motor-150 plumbing

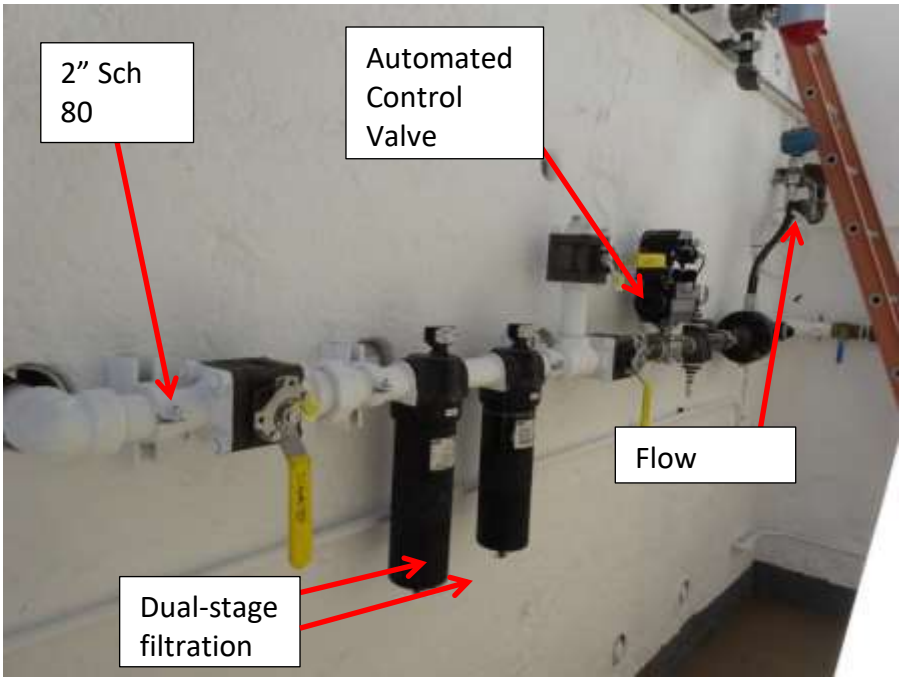

Figure 60. High pressure components

Heating chamber, SS flex hose, diverter, exhaust hose

Exhaust hose, cyclone, duct

Figure 61. Cyclone discharge subsystem

Figure 62. High-pressure compressor for AC-500 sub-system and low-pressure compressor for MOTOR-150

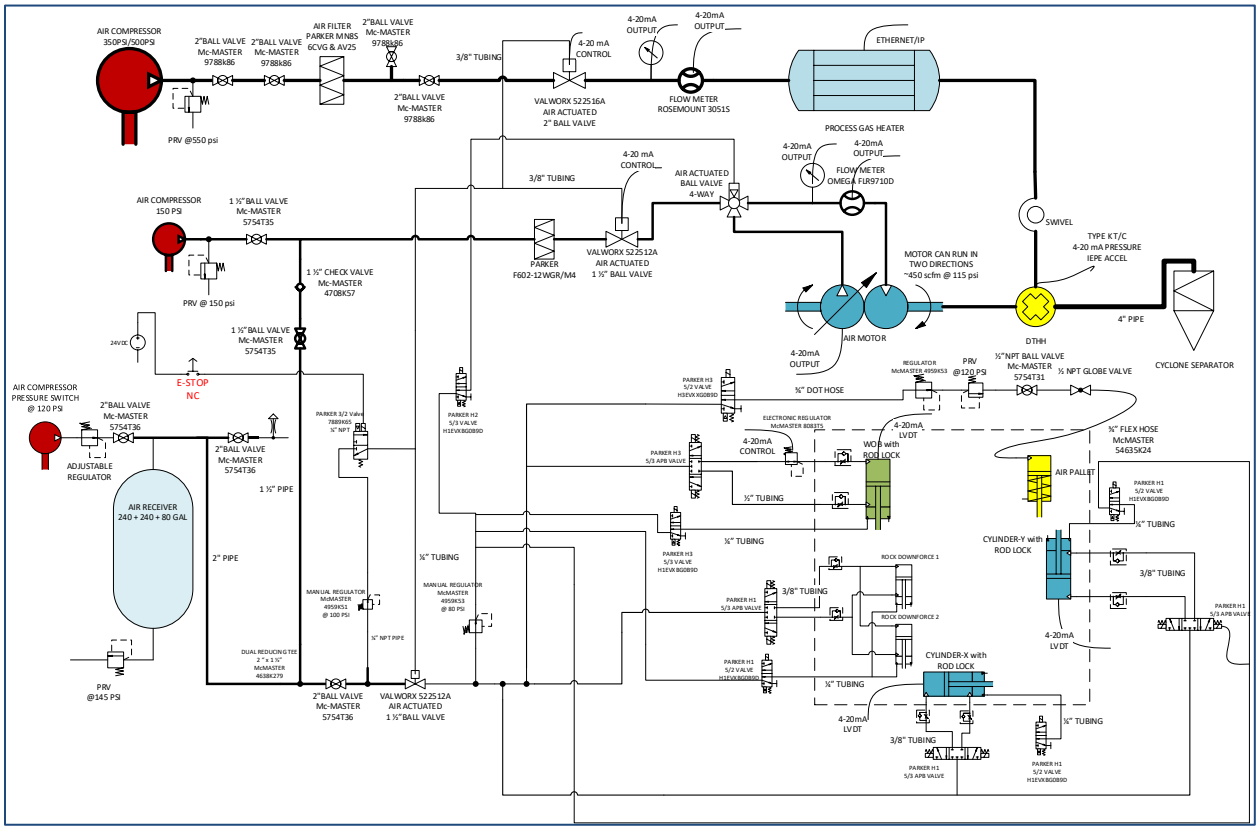

Figure 63. HOT air system schematic

4.2.3 Communication Network and Data Acquisition

The HOT facility control system relies on a local network and data acquisition (DAQ) hardware for control. An Ethernet connection is required between the actual drill facility and the control center as shown in Figure 64. The DAQ is an NI cDAQ-9188 which is an Ethernet connected

device. It will be operated with a PC or as a mobile controller via a laptop with access the DAQ for both data and control to allow for remote operation.

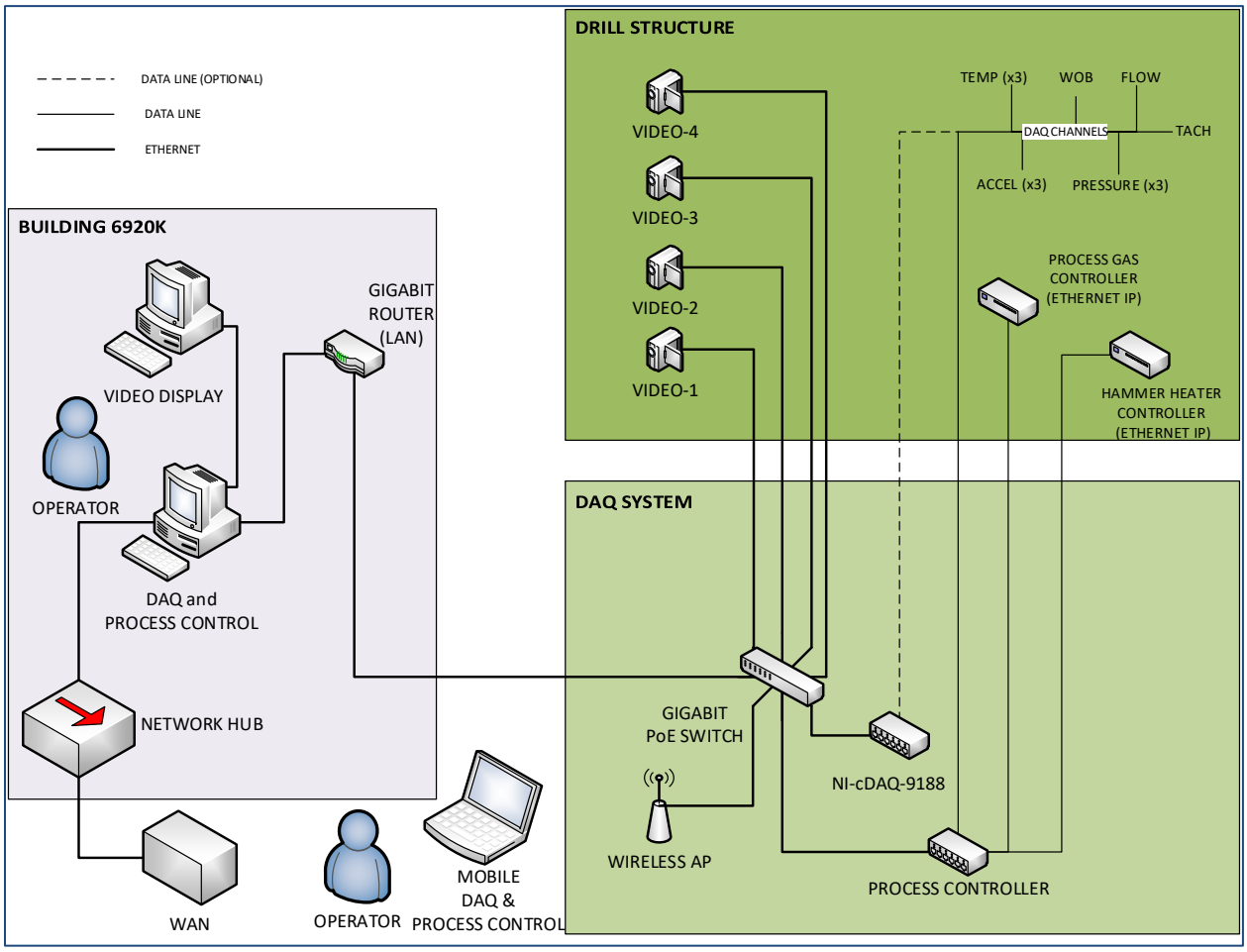

Figure 64. HOT facility network and DAQ infrastructure

4.3 Hot Cell System Design

4.3.1 Process gas heater

The process gas heater is used to simulate the temperature rise of the compressed air powering the hammer as it flows through the drill string in a geothermal environment. It is 190 kW circulation heater capable of heating the process gas up to 572°F. The heater is ASME code-stamped for 600 psi at 900°F. It can be controlled directly from the front panel or remotely via TCP/IP. It was built by Durex Industries to Sandia specifications.

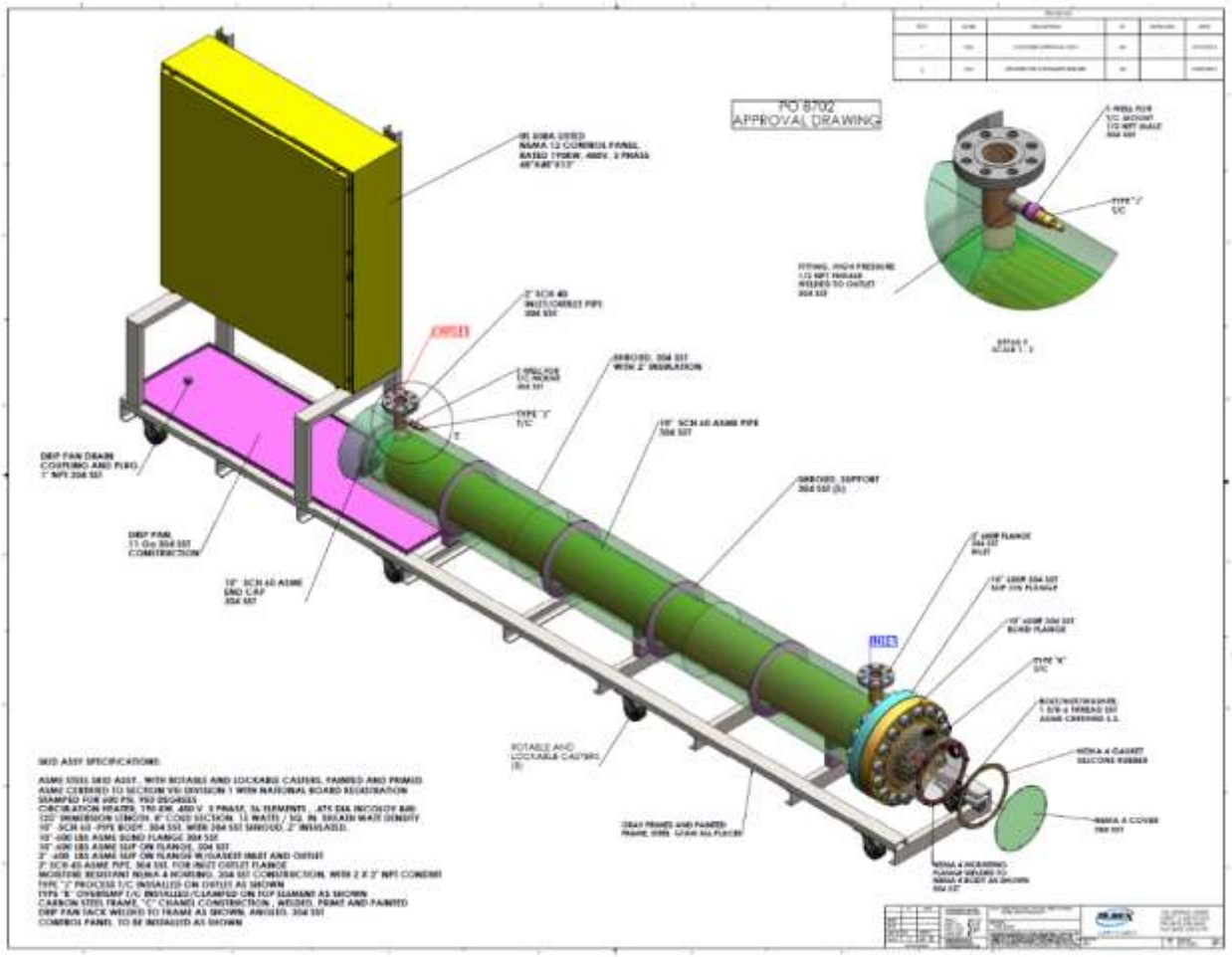

Figure 65. Process gas heater layout

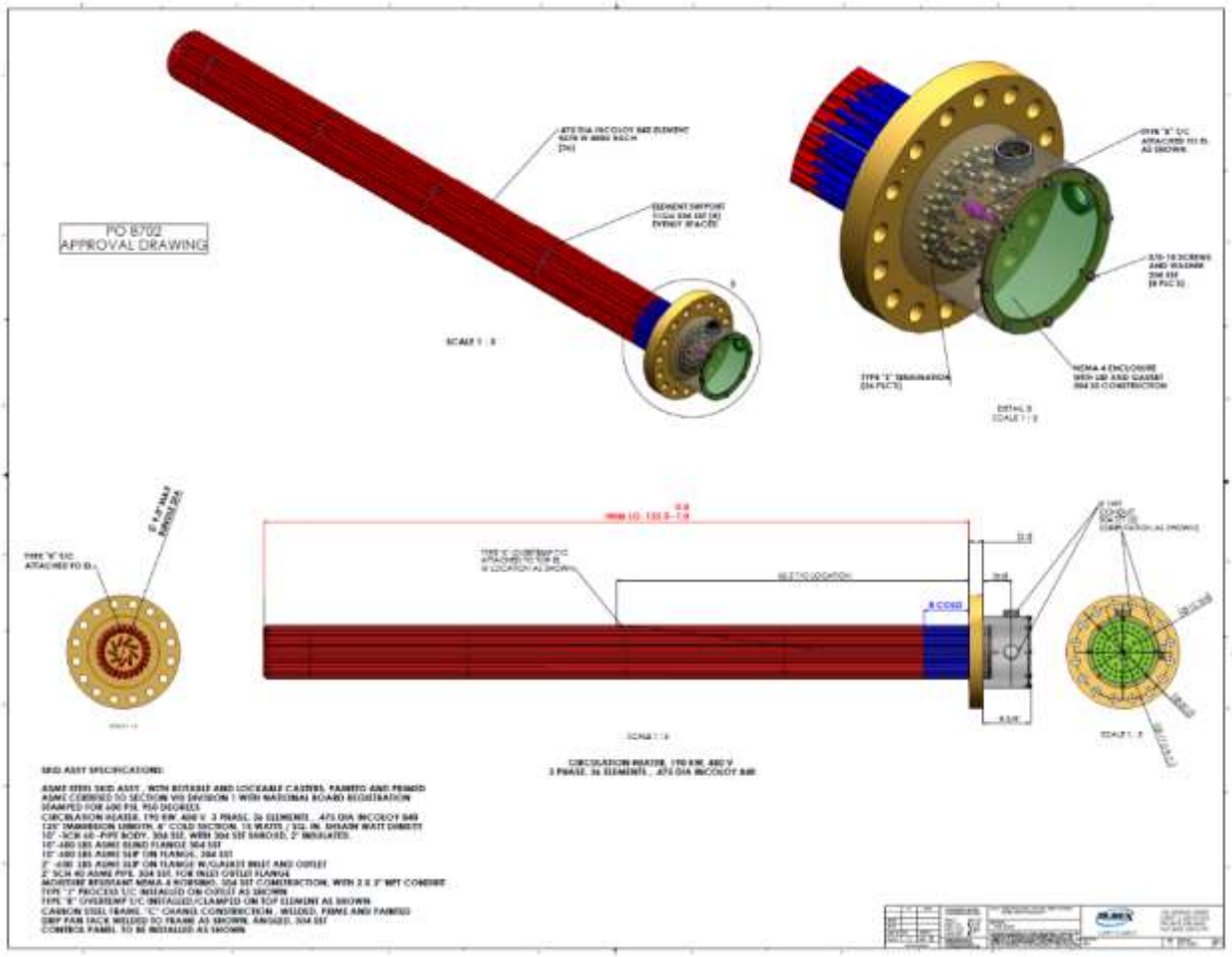

Figure 66. Process gas heater heating elements diagram

4.3.2 Hammer heater/diverter

The hammer heater/diverter is designed to serve multiple purposes in the HOT facility. First and foremost, it heats the hammer to simulate downhole temperatures in a geothermal environment. The hammer consists of six 1.5 kW band heaters surrounding a metal shell. The 9 kW heater is designed to heat the hammer to 572°F within one hour. The heater can be controlled directly on the front panel or remotely via TCP/IP.

The secondary functions of the heater/diverter are to control cuttings and prevent the rock from bouncing during drilling. Internally, the diverter has two packing gland seals designed to prevent dust from escaping during drilling. These packing glands force the cuttings through the exhaust port on the diverter. The diverter is able to generate 3000 lbf of hold-down during drilling. This force helps to create the seal between the rock and the diverter.

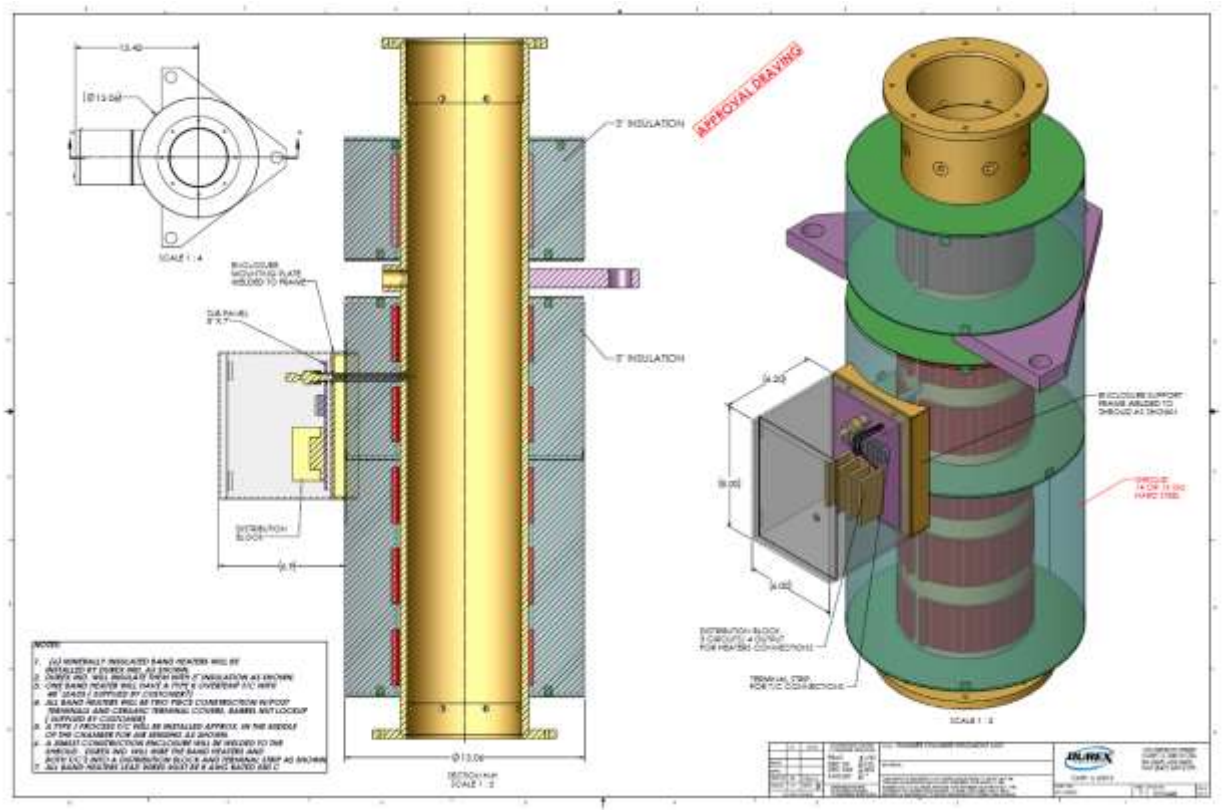

Figure 67. Heating chamber model

4.4 High Operating Temperature (HOT) Facility system design

The design for the HOT facility was developed based on the requirements provided in Section 4.1. Portions of the facility were modeled after the Atlas Copco test cell in Roanoke, Virginia.

4.4.1 Drill structure

The primary component in the HOT facility is the drill structure. The drill structure is a multi-level welded steel frame designed to support the conveyor mast, drill head, sample rock, and auxiliary equipment. The bottom level houses the rock positioning system and consist of a structural steel frame and a mast. The upper levels provide maintenance access and mounting supports for the mast which can transmit up to 10,000 lbf of drilling loads and 3000 ft-lbf of torque. It has also been engineered to handle the environmental wind and ground loads expected at the site. Design and construction details for the drill structure are provided in the Appendix.

Figure 68. HOT test cell drill structure solid model

Figure 69. HOT test cell drill structure frame as built

4.4.2 Mast

The mast provides a means of conveying the drill head during drilling. The mast is constructed from an 8" square box beam with welded angles to provide a sliding surface for the motor carriage. The mast is attached to the drill structure via bolted outriggers. A carriage on one side of the mast is attached to the pneumatic actuator. A carriage on the opposite side is attached to the drill head. Forces are transferred between the carriages through a double-stranded chain that wraps around the mast (Figure 70-Figure 71).

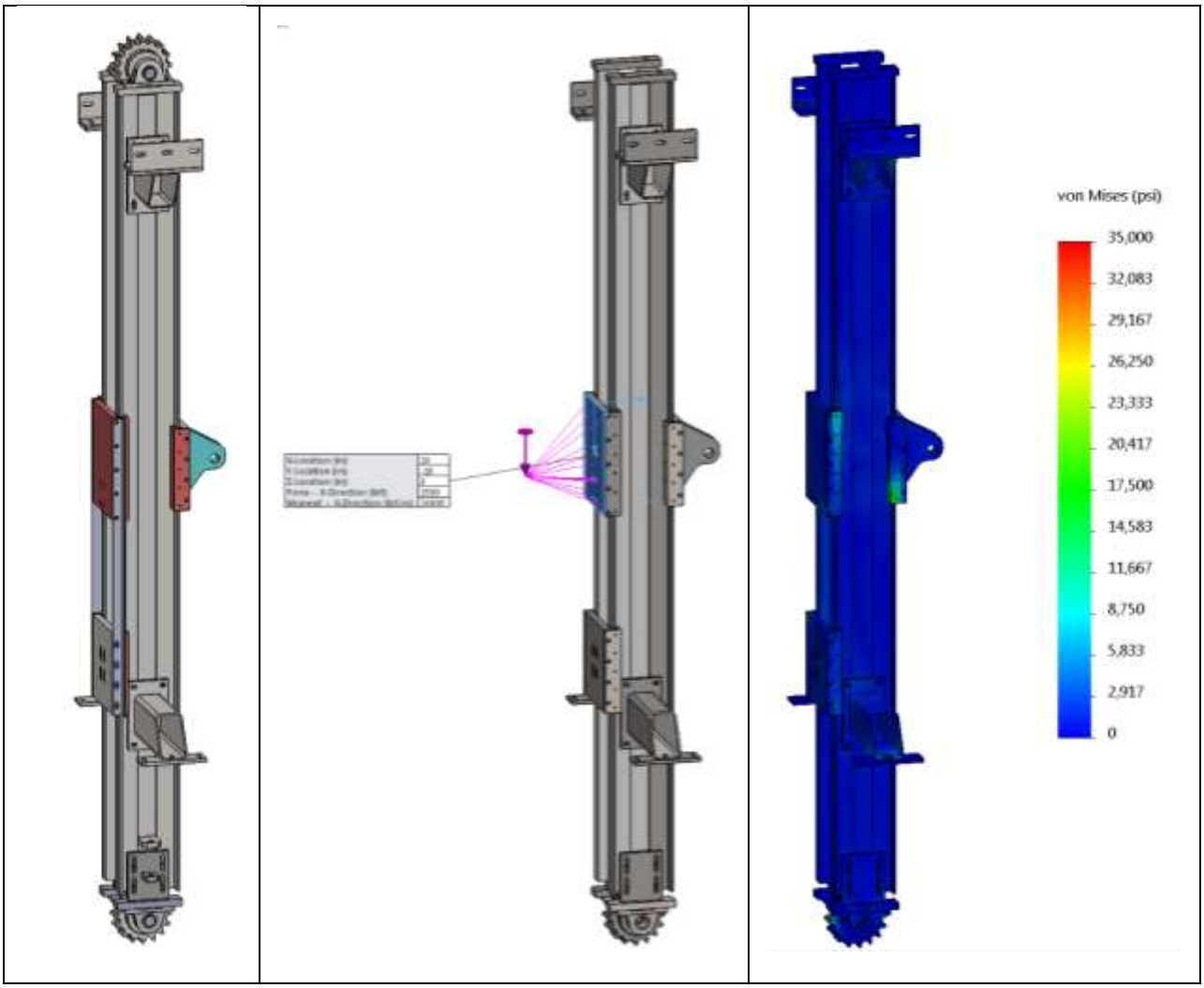

Figure 70. Mast design and stress analysis

Figure 71. Mast as built

4.4.3 Air motor

Rotation is required to properly operate a DTH percussive hammer. Rotation advances the bit buttons to new material in the rock allowing for new material to be impacted during the drilling process. An Atlas Copco DHR-56A pneumatic motor was selected to provide the rotation during drilling for the HOT cell. The motor was chosen based on torque and speed characteristics (3000 lbf-ft up to 60 RPM). It has an internal central passage that allows process gas or fluid to be fed to the tool.

Figure 72. Atlas Copco DHR-56A pneumatic motor

4.4.4 Jointed feed pipe

A typical method of making the high-pressure air connection would be to use a flex hose. However, flex hoses that are capable of operating at the conditions needed for the HOT facility have a bend radius on the order of 25ft. For a drill head with a 60 in. stroke, this proved to be a non-workable solution.

Feeding high-temperature process gas to the hammer required developing a custom feed line. This feed line was designed using Advanced Thermal Systems (ATS) Thermal Pak flexible ball joints which are normally used to absorb displacements in steam systems. These joints are designed for service conditions up to 1000psi @ 750°F[2]. The ball joints are used to create an engineered linkage that articulates as the drill head moves up and down (Figure 73).

[2] http://www.advancedthermal.net/ballJoints.html

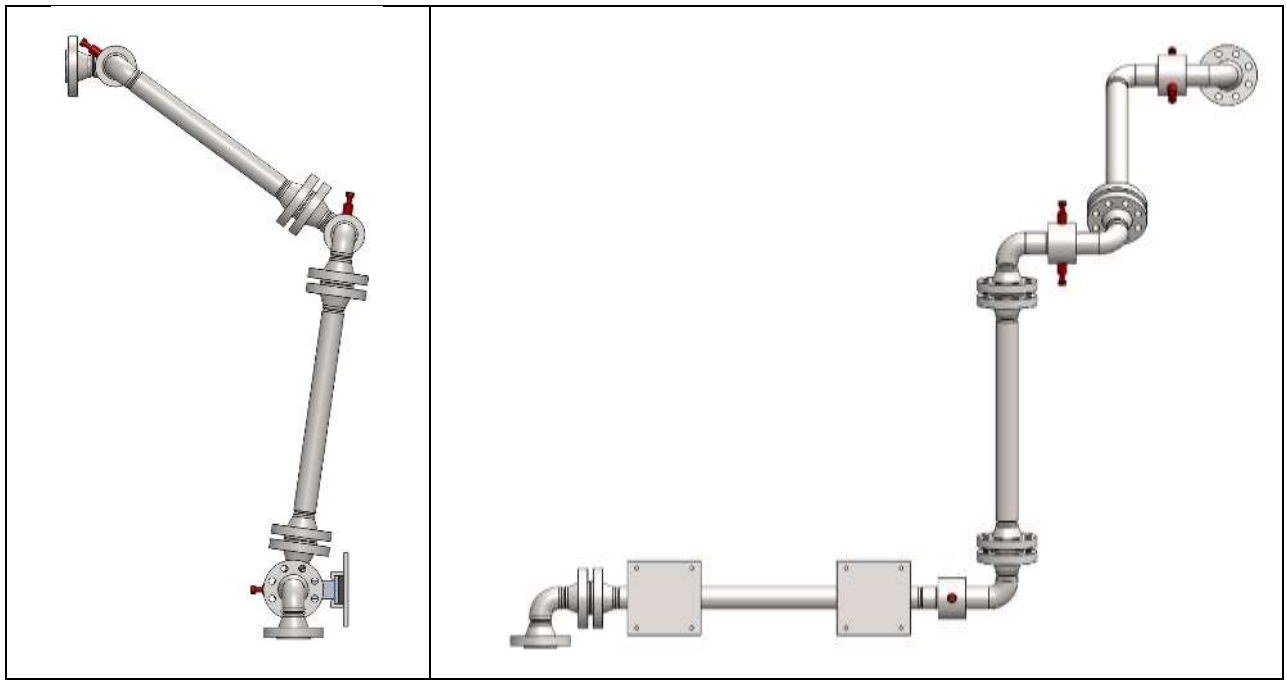

Figure 73. Feed pipe for hot process gas

4.4.5 High-temperature swivel

Process air for the hammer is designed to flow through the motor. However, for the high-temperature testing, the hot process gas can damage the internal motor components. In order to protect those components, a high-temperature swivel was devised to allow hot process gas to bypass the motor. The swivel was designed and built by Scott Rotary Seals to Sandia specifications. The swivel uses PTFE lip seals on the rotary shaft. Internal passages allow the process gas to flow to the DTH. The swivel is instrumented with a thermocouple and pressure transducer to measure process gas temperature and pressure. Prior to delivery, the swivels were pressure tested per API Spec 8C Section 9.9.2.

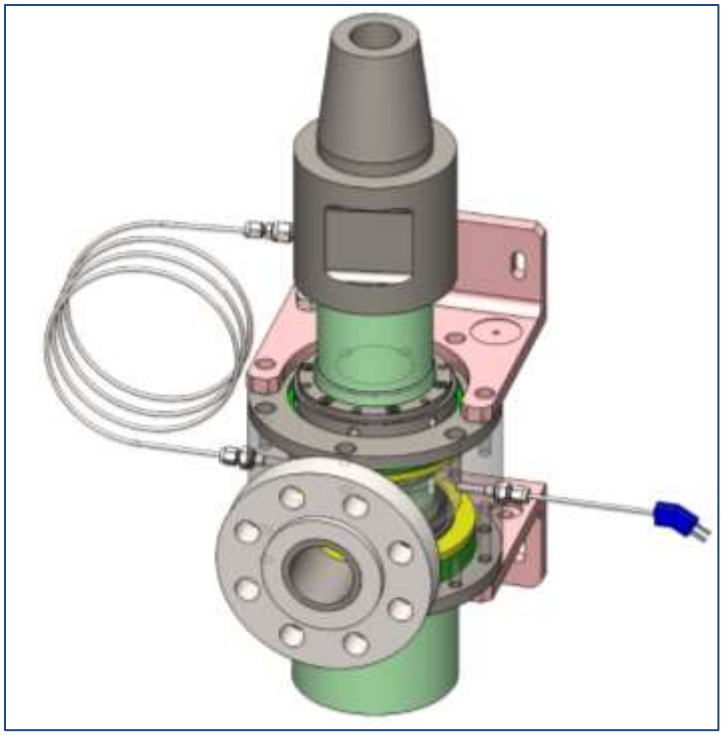

Figure 74. High-temperature swivel with thermocouple and pressure transducer

4.4.6 Rock positioning

Rock samples used for testing are approximately 4’x4’x4’ cubed and weigh approximately 10,600 lbf. Consistently locating the block under the drill head is important in an effort to maximize the footage drilled in each block.

A rock positioning system was developed to allow precise control of the rock position under the drill head (Figure 75). The system uses pneumatic actuators along with position feedback to move the rock along two axes. A single actuator, coupled to a cable and pulley system, is used for each axis. The actuators work in conjunction with an air pallet (Figure 76) to locate the rock in the drill structure within +/- 0.5 in.

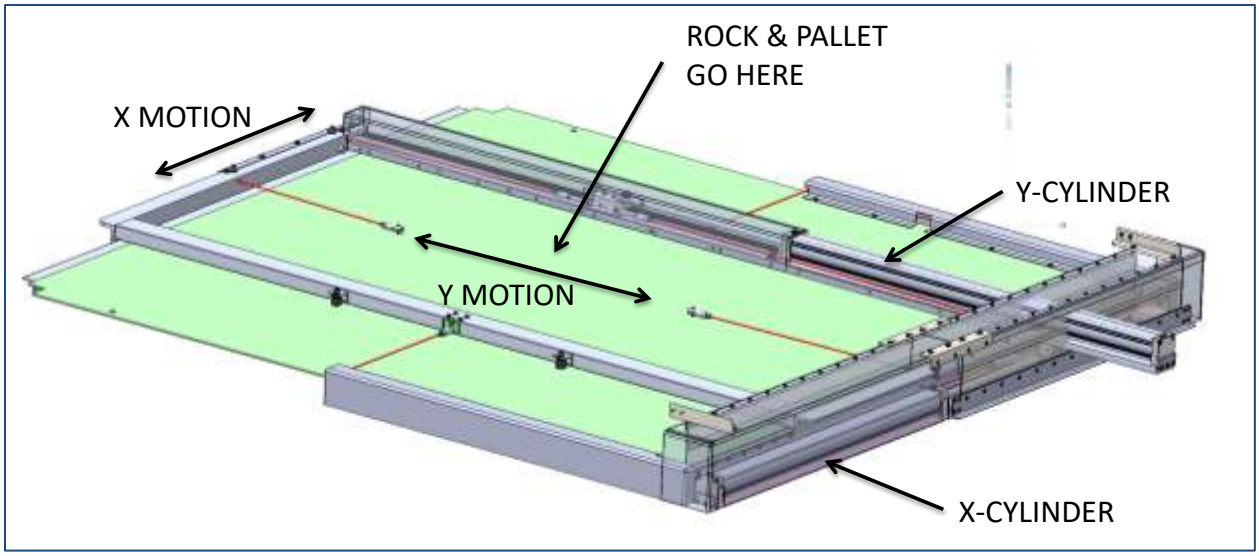

Figure 75. Rock positioning system

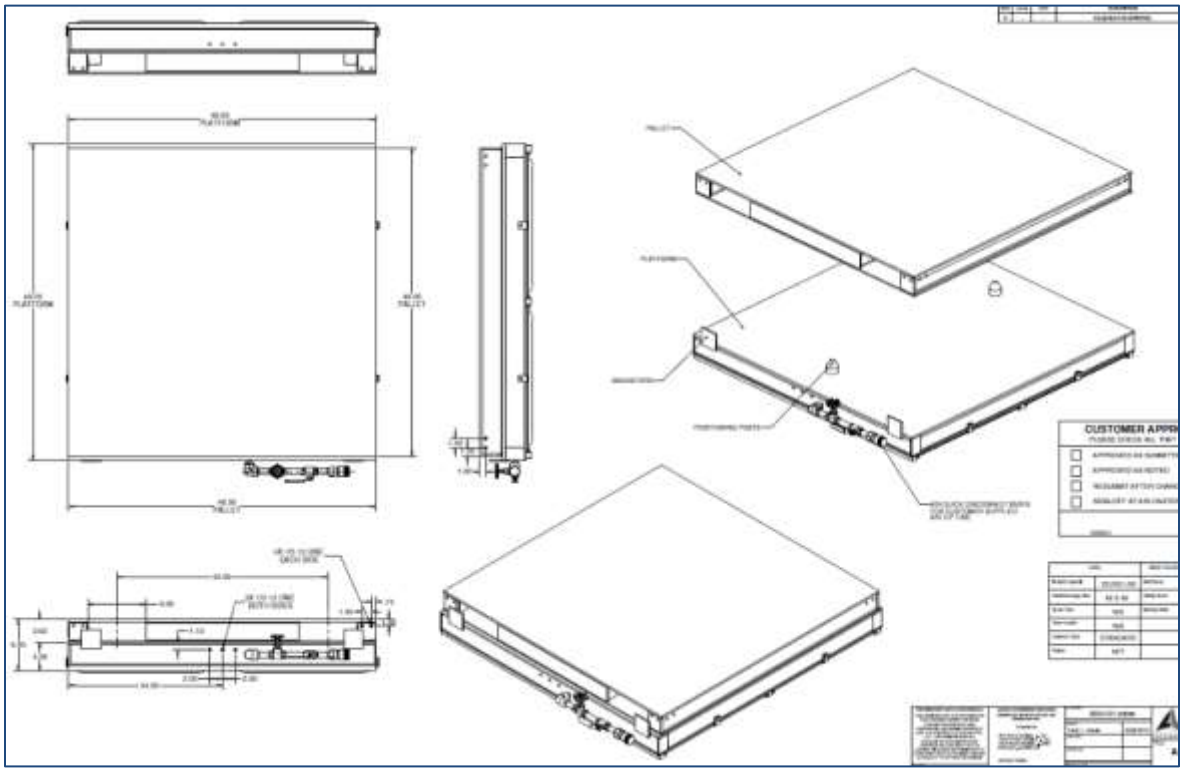

Figure 76. Air Caster air pallet used to position the rock

The overall design and layout of the facility is shown in Figure 77. The facility as built is shown in Figure 78 and Figure 79.

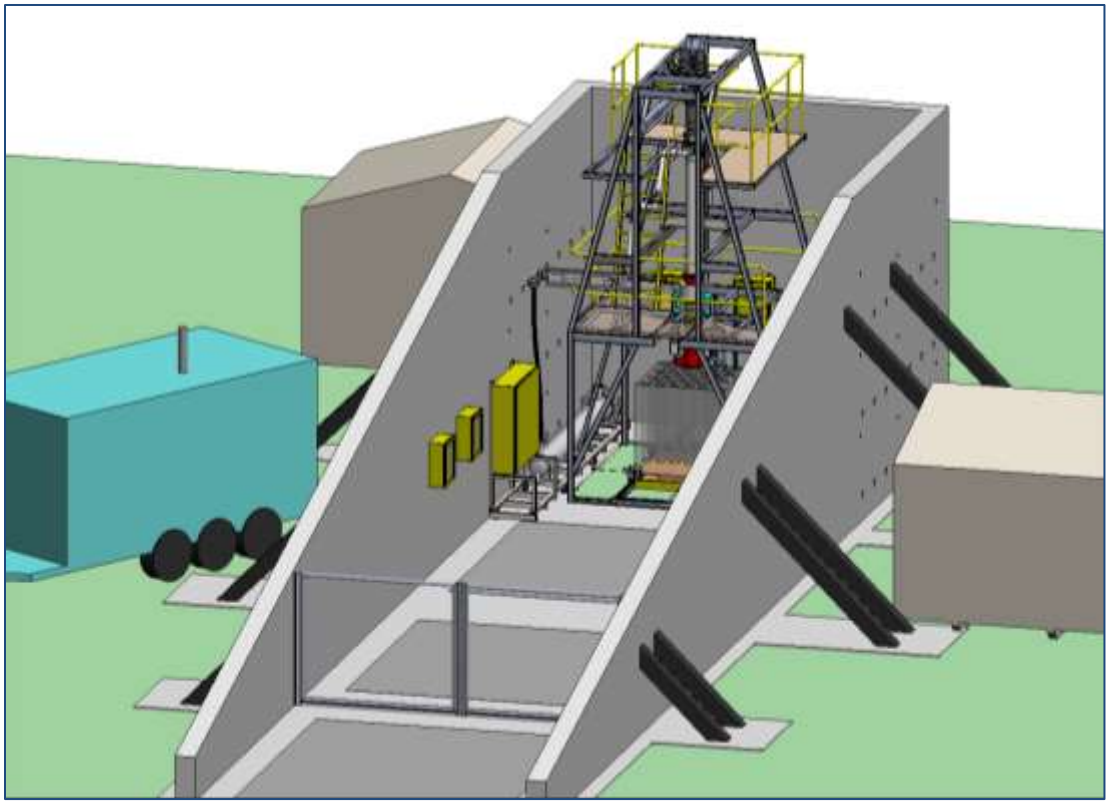

Figure 77. HOT test facility as designed

Figure 78. HOT test facility as built

Figure 79. Interior of HOT facility

4.4.7 Rock cuttings collection

Rock cuttings and silica dust are produced from the testing. All of the exhaust from the drilling is sent through a cyclone separator. The larger cuttings fall out into a barrel and the remaining dust is channeled through an exhaust duct. Water spray within the exhaust duct is used to knock down the remaining dust.

A gravity-fed water tank is used to supply water to a water pump. The pump is feeds a series of nozzles housed within the exhaust duct. The water from them is captured in a water trough and pumped back into the supply tank.

The system is configured per the schematic shown in Figure 80. The nozzle sprayer pump is gravity-fed via the main supply tank. Water flows through the pump into the nozzles and is recovered in the catch tank. Water in the catch tank is returned to the water tank with an effluent pump and filtered prior to entering the main tank. The volume flow rate of the effluent pump is 27 gpm at 15 ft of head which is approximately the same flow rate as the

supply. Two drain valves are in place to allow for winterization and draining the system when needed.

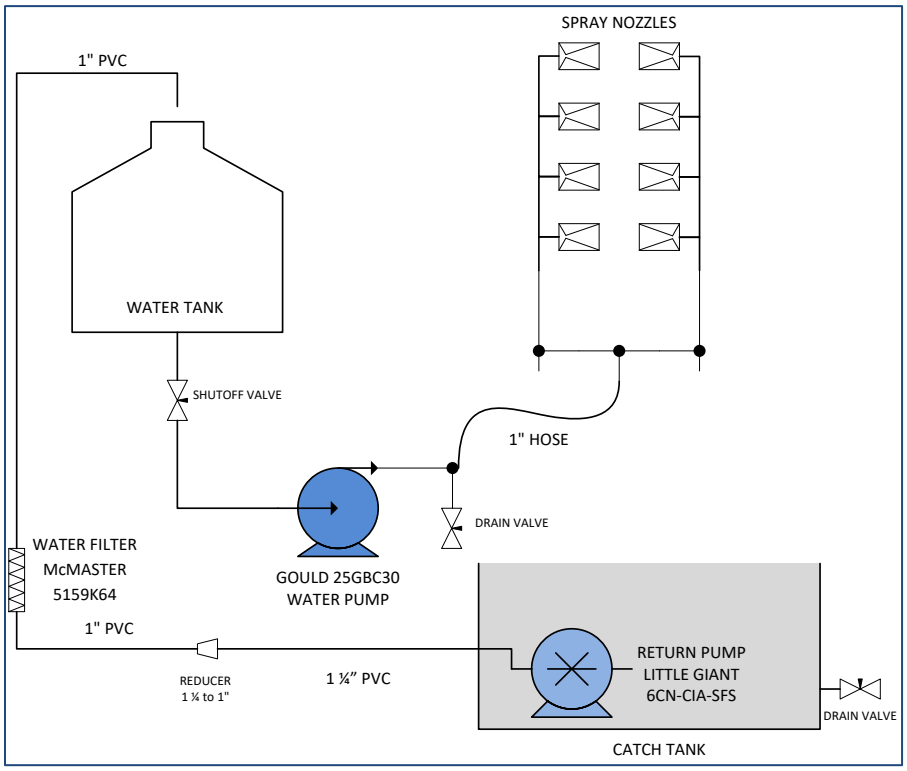

Figure 80. Wash-down system schematic

Figure 81. Dust washdown system

4.5 HOT facility control system

One of the primary drivers for the system design was limiting personnel exposure to potential hazards. The system had to be operated remotely in order to do that. Utilizing the local network infrastructure described in Section 4.2.3 allowed both video and data to be routed to a remote control center.

Cameras mounted throughout the facility provide a full view of the operation without personnel being located within the HOT facility (Figure 82).

Figure 82. HOT facility camera views

The control interface was developed using National Instruments LabView. The controller provides the operator with real-time feedback on all the measured operating parameters. The operator has control on WOB, hammer pressure, and motor speed. Each of these parameters has closed-loop PID control to maintain the set points as conditions change. The heating chamber and the process gas heater are also controlled through the user interface. There is also an optional *AutoDrill* functionality that controls the operating parameters without user intervention (Figure 83). These added features allow for more consistent and repeatable data collection. They also allow the operator to focus on monitoring the measured process parameters rather than rudimentary control of the process parameters.

Figure 83. HOT control panel screen capture

This page intentionally left blank.

5. SUMMARY

Phase I of the Advanced Percussive Drilling Technology was focused on demonstrating the feasibility of a high-temperature hammer. The primary goal of Phase I activities was to develop a proof of concept hammer validating a TRL 2/3 level. The results from Phase I activities proved to be quite promising. An elastomer-free, polymer-free hammer was designed and built from standard materials. Computational modeling of the hammer performance was used to define the timing ports for the hammer. Leak paths and other issues were identified and resolved, and the prototype was tested in the Atlas-Copco test cell. Performance levels were comparable to conventional hammers.

The initial material selection for the high-temperature piston lacked sufficient surface hardness. Although the hammer performance was in line with the low-temperature prototype, the excessive wear on the piston sliding surfaces was deemed unacceptable. The testing with the high-temperature piston, was not however a total loss. The wear patterns that developed on the softer piston material proved to be beneficial in identifying areas and geometries that were experiencing high contact forces.

Modifications to the piston geometry and material selection proved to be effective. The coating wear rate on the struck end of the piston was higher than the other sliding surfaces. The wear on the mid-section and far end of the piston reached a steady wear pattern. The multi-layer solid lubricant architecture was effective under the extreme conditions encountered during testing. The performance of the hammer over the approximately 200 feet of drilling remained consistent.

The goal of drilling at 100 ft/hr was achieved at moderate operating pressures for the hammer. This is encouraging in knowing there is additional rate of penetration gains to be made by operating with higher supply pressures.

Although the primary focus of the project was developing a percussive hammer capable of operating at high-temperatures seen in a geothermal environment, a significant portion of Phase II was dedicated to developing the elevated temperature test capability.

The development of the HOT test facility was an exercise in both design and system integration. The extreme conditions required specialized solutions for drill actuation, plumbing, and operator safety. Successful deployment and integration of multiple sub-systems was required to meet the project objectives of testing at 300°C (572°F).

This page intentionally left blank.

6. REFERENCES

1. Glowka, D.A., Recommendations of the workshop on advanced geothermal drilling systems, in Other Information: PBD: Dec 1997. 1997. p. Medium: P; Size: 53 p.
2. Polsky, Y., Louis Capuanao Jr., John Finger, Michael Huh, Steve Knudson, A.J. Chip Mansure, David Raymond, Robert Swanson, Enhanced Geothermal Systems (EGS) Well Construction Technology Evaluation Report. SANDIA REPORT, 2008(SAND2008-7866).
3. Su, J.-C., et al., Advanced Percussive Drilling Technology for Geothermal Exploration and Development Phase I Report, in SAND Report. 2013, Sandia National Labs.

7. APPENDIX A: MATERIAL HEAT TREATMENTS

Material	Condition/heat treat	Supplier	Test temp	Mechanical testing				
				Tension	Fatigue	Wear	Charpy	Hardness trace
Casing								
18Ni(T-250)	1500F, 1hr, AC+900F, 3 hr		300C	x	x		x	
18Ni (250)	1500F, 1hr, AC+900F, 3 hr		300C	x	x		x	
Aermet 100	1625F 1h, VC-100F 1h, air warm 900F 5h		300C	x	x		x	
Air distributor/bit bearing								
17-4	H1150		300C	x	x		x	
15-5	H1100		300C	x	x		x	
18Ni (200)	CVM 1500F, 1hr, AC+900F, 3 hr		300C	x	x		x	
18Ni (T-250)	1700F 1hr, AC +1500F 1 hr, AC+990F 6 h		300C	x	x		x	
Piston								
15-5	H1025		300C	x	x		x	
18Ni (200)	CVM 1500F, 1hr, AC+900F, 3 hr		300C	Same materials as air distributor/bit bearing				
18Ni (T-250)	1700F 1hr, AC +1500F 1 hr, AC+990F 6 h		300C					
[1]If room temperature fatigue crack growth data is available in literature these fatigue tests will not be run.								

8. APPENDIX B: ELECTRICAL INSTALLATION DETAILS

480/277V Panelboard @ Test Site 500A
Description Motor hp kVA Multiplier kVA Amps Notes
Hot Cell 160.0 1.25 200.0 240.7 1
120/208V Panelboard 38.3 1.00 38.3 46.1
.
Future Growth @25% 59.6
Total kVA Demand 198.3 297.9
Total Sizing Amps at 480/277 volts 358.4 2
Notes:
1. Assumed load per information provided by SNL.
2. Panelboard is sufficiently sized for new load.
SUMMARY
480/277V Panelboard near 6920F 200A
Description Motor hp kVA Multiplier kVA Amps Notes
Bauer I230 Air Compressor 30.0 1.25 37.5 45.1 1
Future Growth @25% 9.4
Total kVA Demand 30.0 46.9
Total Sizing Amps at 480/277 volts 56.4 2
Notes:
1. Assumed load per information provided by SNL.
2. Panelboard is sufficiently sized for new load.
SUMMARY
208/120V Panelboard @ Test Site 150A
Description Motor hp kVA Multiplier kVA Amps Notes
Carrier Heat Pump 20.0 1.25 25.0 120.2 1
Exhaust Fans 1.5 1.25 1.9 15.6 1
Lighting 1.0 1.25 1.3 10.4 1
DAQ/Computers 2.0 1.25 2.5 20.8 2
Future Growth @ 25% 7.7
Total kVA Demand 24.5 38.3
Total Sizing Amps at 208/120 volts 106.3 2
Notes:
1. Assumed load per information provided by SNL.
2. Panelboard is sufficiently sized for new load.

9. APPENDIX C: AIR MANIFOLD SOLENOID CONFIGURATION

Table 5. Air manifold solenoid pins

Address	D-sub wire	NI Pin
1	Black	1
2	Brown/White	2
3	Brown	3
4	Red/White	4
5	Red	5
6	Orange/White	6
7	Orange	7
8	Green/White	8
9	Yellow	11
10	Blue/White	12
11	Green	13
12	Purple/White	14
13	Blue	15
14	Red/Black	16
15	Purple	17
16	Orange/Black	18
17	Gray	20
18	Yellow/Black	21
19	White	22
20	Green/Black	23
21	Pink	24
22	Gray/Black	25
23	Lt Green	26
24	Pink/Black	27
Power	Black/White	Red

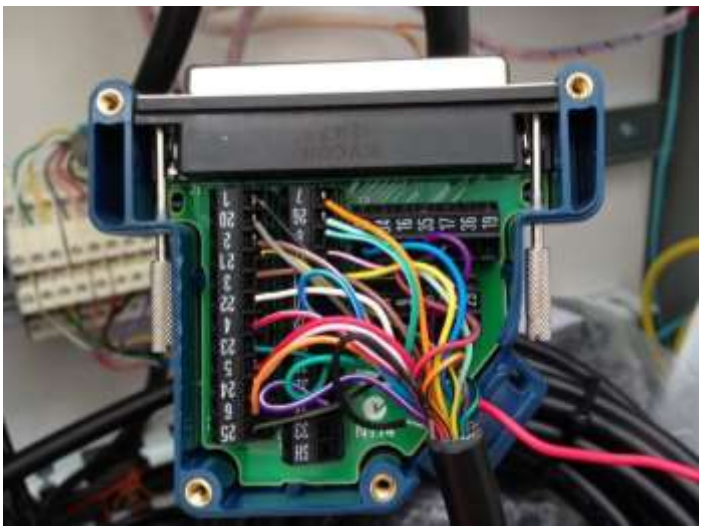

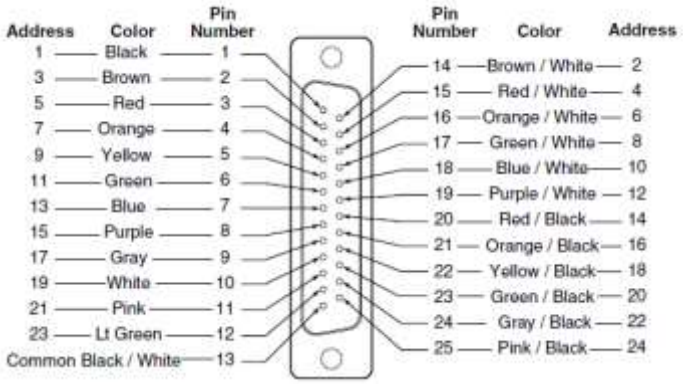
Address
Color
Pin Number
1 Black 1
3 Brown 2
5 Red 3
7 Orange 4
9 Yellow 5
11 Green 6
13 Blue 7
15 Purple 8
17 Gray 9
19 White 10
21 Pink 11
23 Lt Green 12
Common Black / White 13
Pin Number
Color
Address
14 Brown / White 2
15 Red / White 4
16 Orange / White 6
17 Green / White 8
18 Blue / White 10
19 Purple / White 12
20 Red / Black 14
21 Orange / Black 16
22 Yellow / Black 18
23 Green / Black 20
24 Gray / Black 22
25 Pink / Black 24

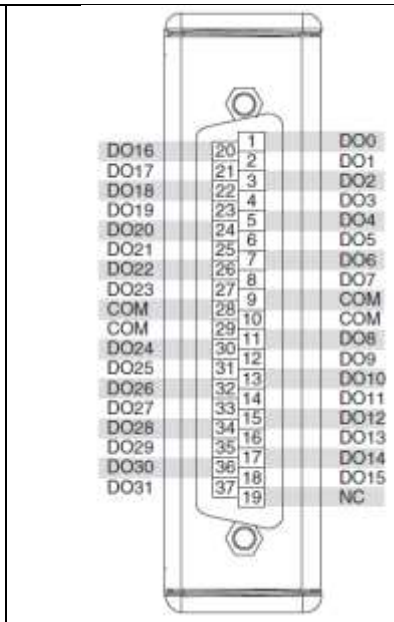
DO16 20 1 DO0
DO17 21 2 DO1
DO18 22 3 DO2
DO19 23 4 DO3
DO20 24 5 DO4
DO21 25 6 DO5
DO22 26 7 DO6
DO23 27 8 DO7
COM 28 9 COM
COM 29 10 COM
DO24 30 11 DO8
DO25 31 12 DO9
DO26 32 13 DO10
DO27 33 14 DO11
DO28 34 15 DO12
DO29 35 16 DO13
DO30 36 17 DO14
DO31 37 18 DO15
19 NC

10. APPENDIX D: HOT DATA ACQUISITION I/O CONFIGURATION

Table 6. HOT data acquisition I/O

I/O	Component	I/O	Quantity
Input/Output	Process gas heater temperature controller	RS-485/Modbus or Ethernet IP	1
Input/Output	Hammer heater temperature controller	RS-485/Modbus or Ethernet IP	1
Input	Hammer accelerometer	IEPE	3
Input	Thermocouple	Type K or J	3
Input	Pressure transducer	4-20 mA	3
Input	Motor RPM tachometer	4-20 mA	1
Input	Flow meter	4-20 mA	1
Output	Process gas heater air actuated ball valve	4-20 mA	1
Output	Motor air actuated ball valve	4-20 mA	1
Output	Motor direction control	24V DC	1
Output	Rod locks	24V DC	4
Output	Directional control valves	24V DC	4
Output	Electronic regulators	4-20 mA	3
Ouput	Solenoid valve for air pallet	24V DC	1
Input	X-cylinder position LVDT	4-20 mA	1
Input	Y-cylinder position LVDT	4-20 mA	1
Input	WOB cylinder position LVDT	4-20 mA	1
Input	Motor pressure	4-20 mA	1
Input	Motor flow	4-20 mA	1
Input	WOB extend pressure	4-20 mA	1
Input	WOB retract pressure	4-20 mA	1
Input	WOB load cell	4-20 mA	1

11. APPENDIX E: HEATER CONTROL PANELS

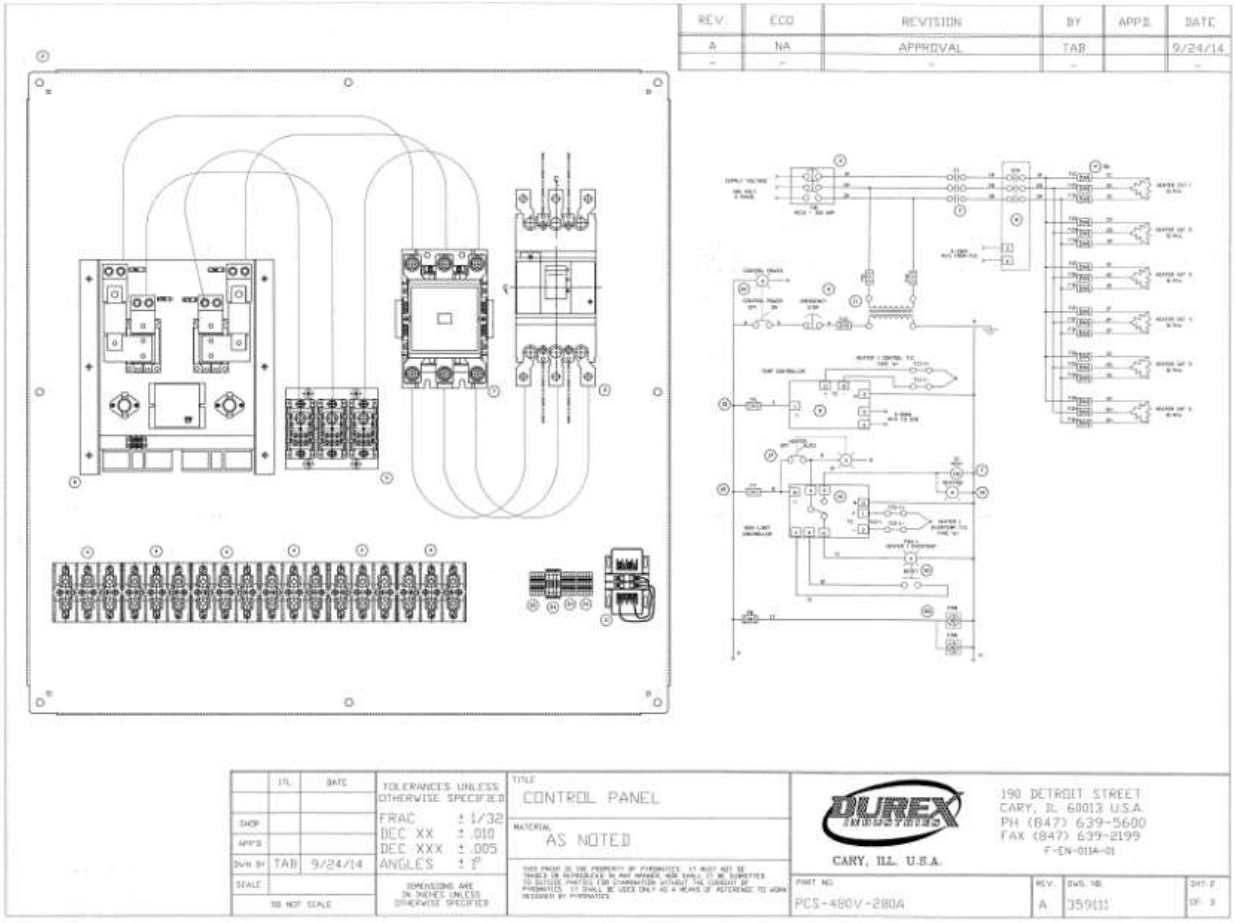

Figure 84. Process gas heater control panel schematic

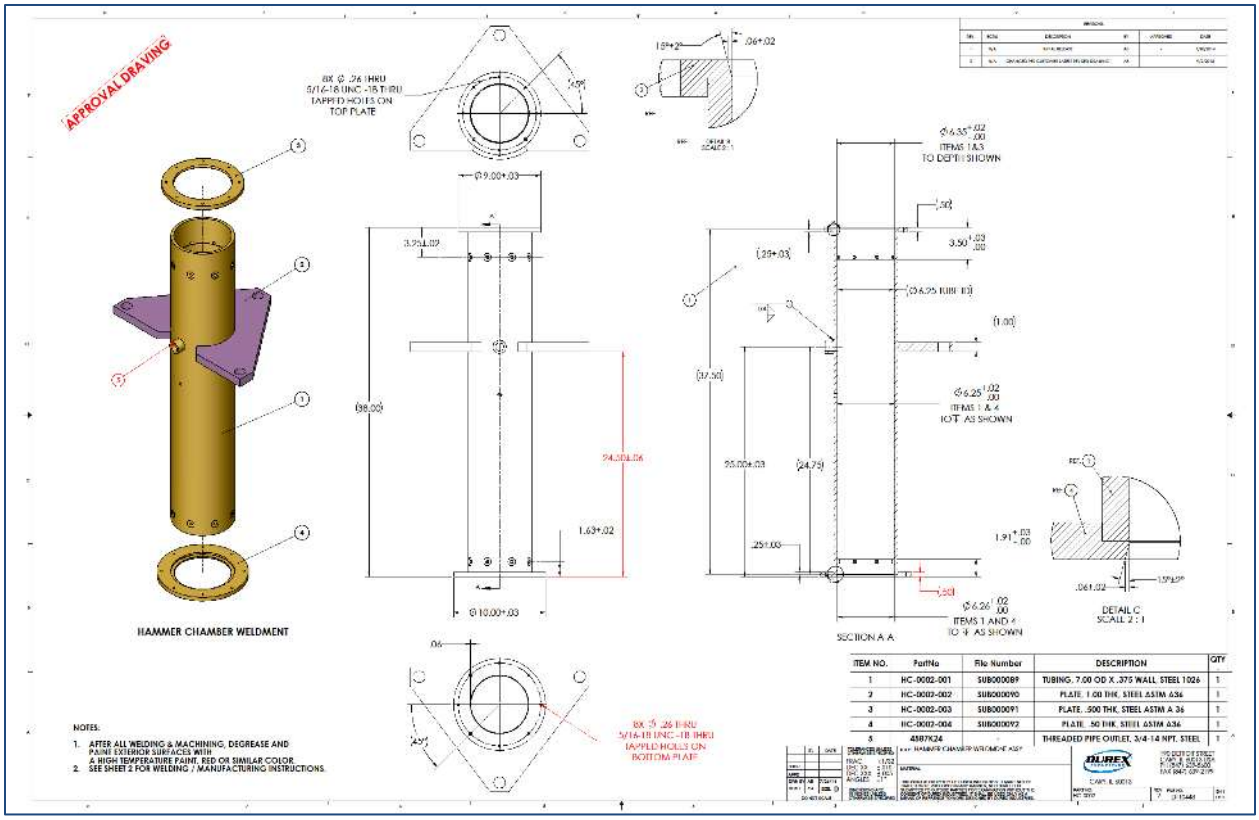

Figure 85. Heating chamber/diverter manufacturing drawing

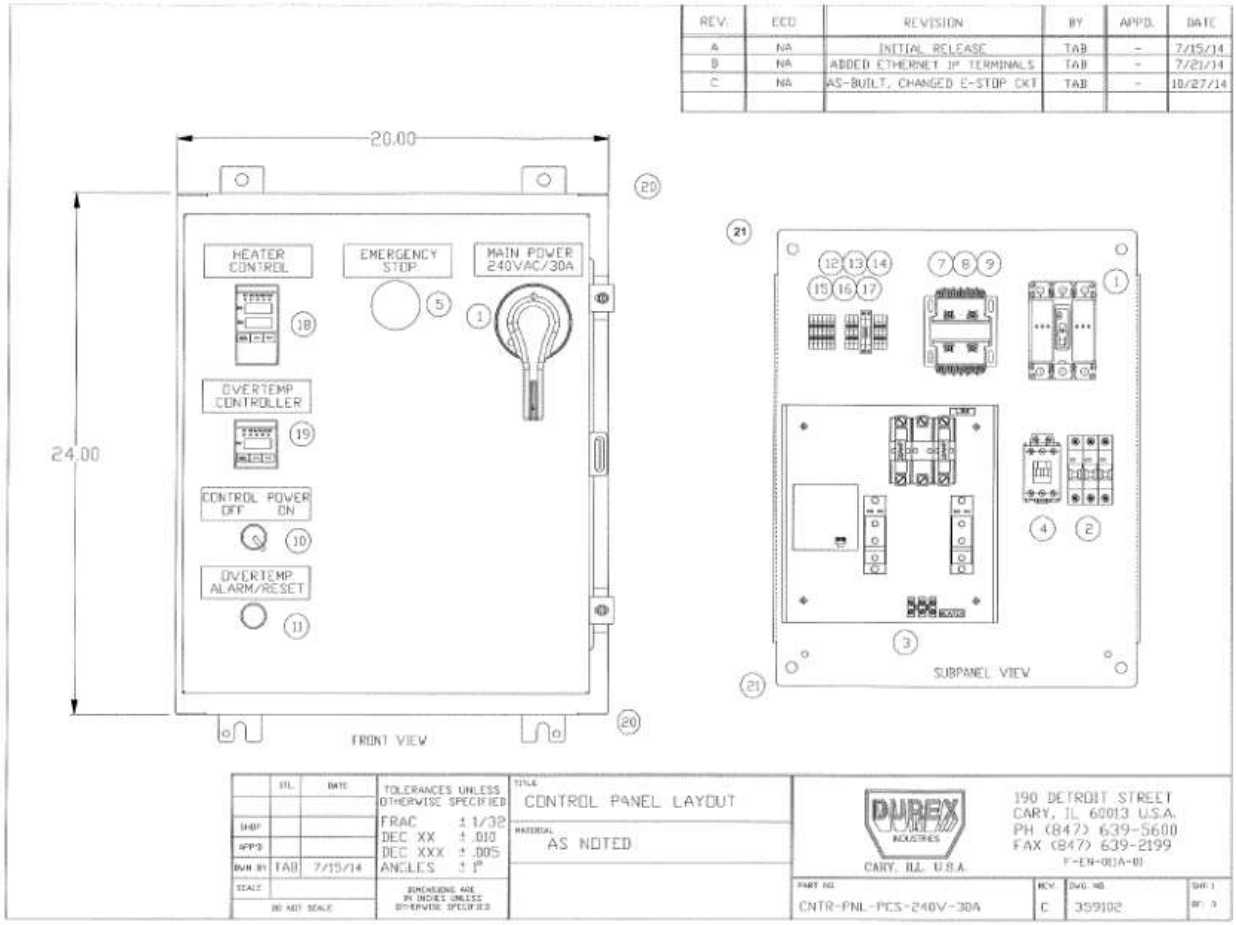

Figure 86. Heater/diverter control panel

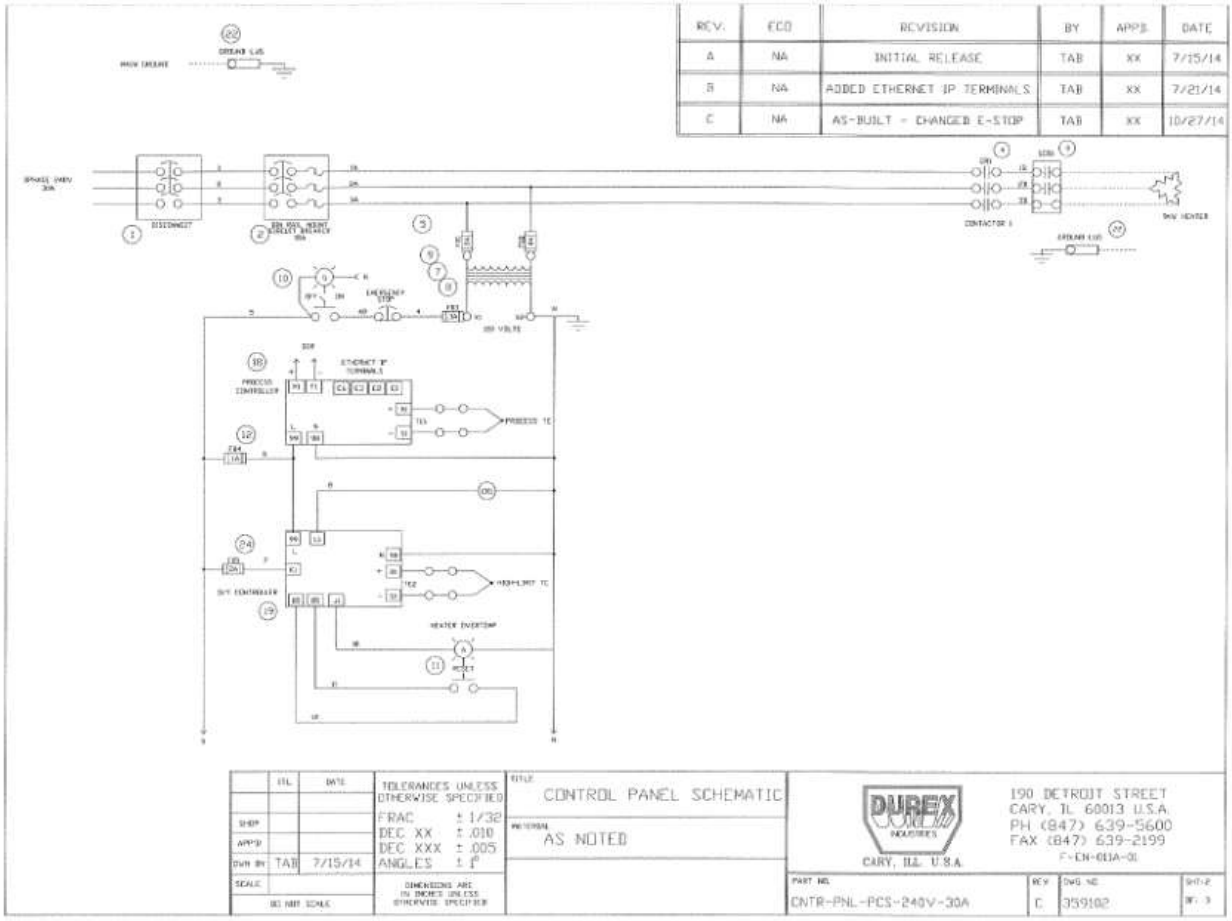

Figure 87. Heater/diverter control panel

12. DISTRIBUTION

1 Dale Wolfer
Atlas-Copco Secoroc LLC
7500 Shadwell Drive
Roanoke, Virginia 24019

1 Paul Campbell
Atlas-Copco Secoroc LLC
7500 Shadwell Drive
Roanoke, Virginia 24019

1 Ron Boyd
Atlas Copco Secoroc LLC
13278 Lincoln Way West, P.O. Box 271
Ft. Loudon, PA 17224 USA

1	MS0889	Somuri V. Prasad	01818
1	MS1033	Jiann-Cherng Su	06916
1	MS1033	David W. Raymond	06916
1	MS1033	Douglas A. Blankenship	06916
1	MS0899	Technical Library	9536 (electronic copy)
1	MS0161	Legal Technology Transfer Center	11500


Sandia National Laboratories